Membrane Type 1-Matrix Metalloproteinase Mediates Degradation of the Low-density Lipoprotein Receptor Family Members

by

Ziyang Zhang

A thesis submitted in partial fulfillment of the requirements for the degree of

Master of Science

Medical Sciences - Pediatrics

University of Alberta

Abstract

The low-density lipoprotein receptor (LDLR) family includes 13 transmembrane protein members sharing a conserved structure and common repeats. Their importance has been shown in a variety of physiological and pathophysiological events including lipid metabolism, nervous system development and maintenance, bone homeostasis and cancer progression. Cell surface LDLR family members are regulated by metalloproteinases-mediated ectodomain shedding. Membrane type 1-matrix metalloproteinase (MT1-MMP) is a key player in extracellular matrix remodelling and has been reported to cleave LDLR, low-density lipoprotein receptor-related protein 1 (LRP1) and LRP4. To study the effect of MT1-MMP on other LDLR family members, MT1-MMP and LDLR family members were co-overexpressed by transient transfection in the human hepatoma-derived Huh7 cell line. Herein, we found that MT1-MMP is able to mediate the shedding of all screened LDLR family members, including LRP3, LRP4, LRP5, LRP6, LRP8, LRP10, LRP11, and LRP12. The proteolytic activity of MT1-MMP is required for the shedding except for LRP10. In the cases of LRP3 and LRP11, the C-terminal fragments of the receptors were detected in cells after the MT1-MMP-mediated cleavage. The biological importance of MT1-MMP-mediated shedding of LDLR family members is unknown, which requires further investigation.

In addition, we investigated the combinative effect of targeting MT1-MMP with statin treatment in raising LDLR levels. Statin monotherapy can only achieve a ~50% cholesterol-lowering effect and is accompanied by dose-dependent adverse effects such as increased onset risk of type 2 diabetes. Thus, combination therapy with statin and a nonstatin cholesterol-lowering medication is recommended to enhance cholesterol-lowering outcomes and reduce

statin-associated adverse effects. In HepG2 cells, MT1-MMP knockdown can additionally increase LDLR expression levels in the presence of statin treatment. We also studied hepatic MT1-MMP depletion combined with statin treatment in mice.

Preface

This thesis is an original work by Ziyang Zhang. All animal procedures received research ethics approval from the University of Alberta's Animal Care and Use Committee with protocol AUP00000456.

Acknowledgements

I am indebted to my supervisor Dr. Dawei Zhang for his support in the research undertaken to write this thesis. I want to express my gratitude to the supervisory committee members, Dr. Richard Lehner and Dr. Maria Febbraio, for their time and feedback. Thank you to all current and former lab members: Hongmei Gu, Dr. Yishi Shen, Maggie Wang, Bonnie Wang, Suha Jarad, Yasmine Jaffar, Govind Gill, Yin May Pyone, Dr. Peter Amadi, Dr. Usman Sabir, Aaron Getachew, Garrett Chen, Wanda Huang, Moattar Latif.

Table of Contents

List of Figures

List of Abbreviation

ADAM	A disintegrin and metalloproteinase
ALT	Alanine transaminase
ANOVA	Analysis of variance
ApoE	Apolipoprotein E
APP	β-amyloid precursor protein
BCA	Bicinchoninic acid
BMSC	Bone marrow stromal cells
BSA	Bovine serum albumin
CAT	Catalytic domain
CO_2	Carbon dioxide
CQ	Chloroquine
CT	Cytoplasmic tail
CTF	C-terminal fragment
CUB	C1r/C1s, Uegf, Bmp1
CVD	Cardiovascular disease
DAPI	4′,6-diamidino-2-phenylindole
DAPT	*N*-[*N*-(3,5-Difluorophenacetyl)-L-alanyl]-*S*-phenylglycine *t*-butyl ester
DMEM	Dulbecco's Modified Eagle Medium
DMSO	Dimethylsulfoxide
DNA	Deoxyribonucleic acid
dNTP	Deoxynucleotide triphosphate

ECD	Ectodomain
ECM	Extracellular matrix
EDTA	Ethylenediaminetetraacetic acid
EGF	Epidermal growth factor
ER	Endoplasmic reticulum
FBS	Fetal bovine serum
FDA	U.S. Food and Drug Administration
GAPDH	Glyceraldehyde 3-phosphate dehydrogenase
GPT	Glutamic pyruvic transaminase
HCl	Hydrochloride
HDL	High-density lipoprotein
HEK	Human Embryonic Kidney
HMG-CoA	β-Hydroxy β-methylglutaryl-CoA
HMGCR	HMG-CoA reductase
HoFH	Homozygous familial hypercholesterolemia
HPX	Hemopexin-like repeats
ICD	Intracellular domain
IDOL	Inducible degrader of the LDLR
IP	Immunoprecipitation
LB	Lysogeny broth
LDL	Low-density lipoprotein
LDLR	Low-density lipoprotein receptor

LKO	Liver knockout
LRP	Low-density lipoprotein receptor related protein
LRP-DIT	Lipoprotein receptor related protein-deleted in tumors
MANEC	Motif at N terminus with eight cysteines
MHC	Major histocompatibility complex
MMP	Matrix metalloproteinase
MTP	Microsomal triglyceride transfer protein
MT1-MMP	Membrane type 1-matrix metalloproteinase
MuSK	Muscle-specific kinase
NC	Negative control
NMJ	Neuromuscular junction
NPC1L1	Niemann-Pick C1-like protein 1
NPXY	Asn-Pro-X-Tyr
OPDM	Oculopharyngodistal myopathy
PBS	Phosphate buffered saline
PBST	Phosphate Buffered Saline with Tween 20
PCR	Polymerase chain reaction
PCSK9	Proprotein convertase subtilisin/kexin type 9
PEI	Polyethylenimine
PI3K	Phosphoinositide 3-kinase
PKD	Polycystic kidney disease
qRT-PCR	Quantitative reverse transcription polymerase chain reaction

RIPA buffer	Radioimmunoprecipitation assay buffer
RNA	Ribonucleic acid
SAMS	Statin-associated muscle symptoms
SDS	Sodium dodecyl sulfate
SDS-PAGE	Sodium dodecyl-sulfate polyacrylamide gel electrophoresis
SREBP2	Sterol regulatory element-binding protein 2
TAPI	TNF protease inhibitor
TFR	Transferrin receptor
TGN	*trans*-Golgi network
TIMP	Tissue inhibitor of metalloproteinases
TM	Transmembrane domain
UPS	Ubiquitin proteasome system
VLDL	Very low density-lipoprotein
VLDLR	Very low density-lipoprotein receptor
WT	Wild-type
YWTD	Tyr-Trp-Thr-Asp

Chapter 1

Introduction

1.1 LDLR family

LDLR family is a set of receptor proteins involved in the endocytosis of a variety of ligands that have structural or evolutionary homology with the founding member – low-density lipoprotein receptor (LDLR) [1]. The LDLR family is an ancient class of cell membrane surface proteins with 13 members discovered up to date. Most LDLR family members are named by low-density lipoprotein receptor-related protein (LRP), including LDLR, LRP1, LRP1B, LRP2/Megalin, LRP3, LRP4, LRP5, LRP6, LRP8/ApoER2, LRP10, LRP11, LRP12 and VLDLR. LDLR family members are evolutionarily conserved transmembrane proteins and share similar structures and motifs (**Fig. 1.1**).

All LDLR family members are type I membrane proteins with N-terminal extracellular domains and C-terminal intracellular cytoplasmic tails [2]. As a hallmark, all LDLR family members have shared LDLR class A repeats which are known to be responsible for ligand binding [3,4]. There are seven core members of the LDLR family that are structurally closer. They have more conserved ligand-binding domains including N-terminal LDLR class A repeats with shared YWTD beta-propeller domains and epidermal growth factor-like domains which are responsible for the pH-dependent dissociation of ligands in the endosome [5]. The intracellular domains of the seven core members share another common feature that each of them at least has one NPXY (Asn-Pro-X-Tyr) or NPXY-like motif which functions in intracellular protein interaction, signal transduction and endocytosis [6,7]. LRP5 and LRP6 are two distant members of LDLR family; structurally, their N-terminuses are not LDLR class A repeats but YWTD beta-propeller domains and epidermal growth factor-like domains. Also, the distant members

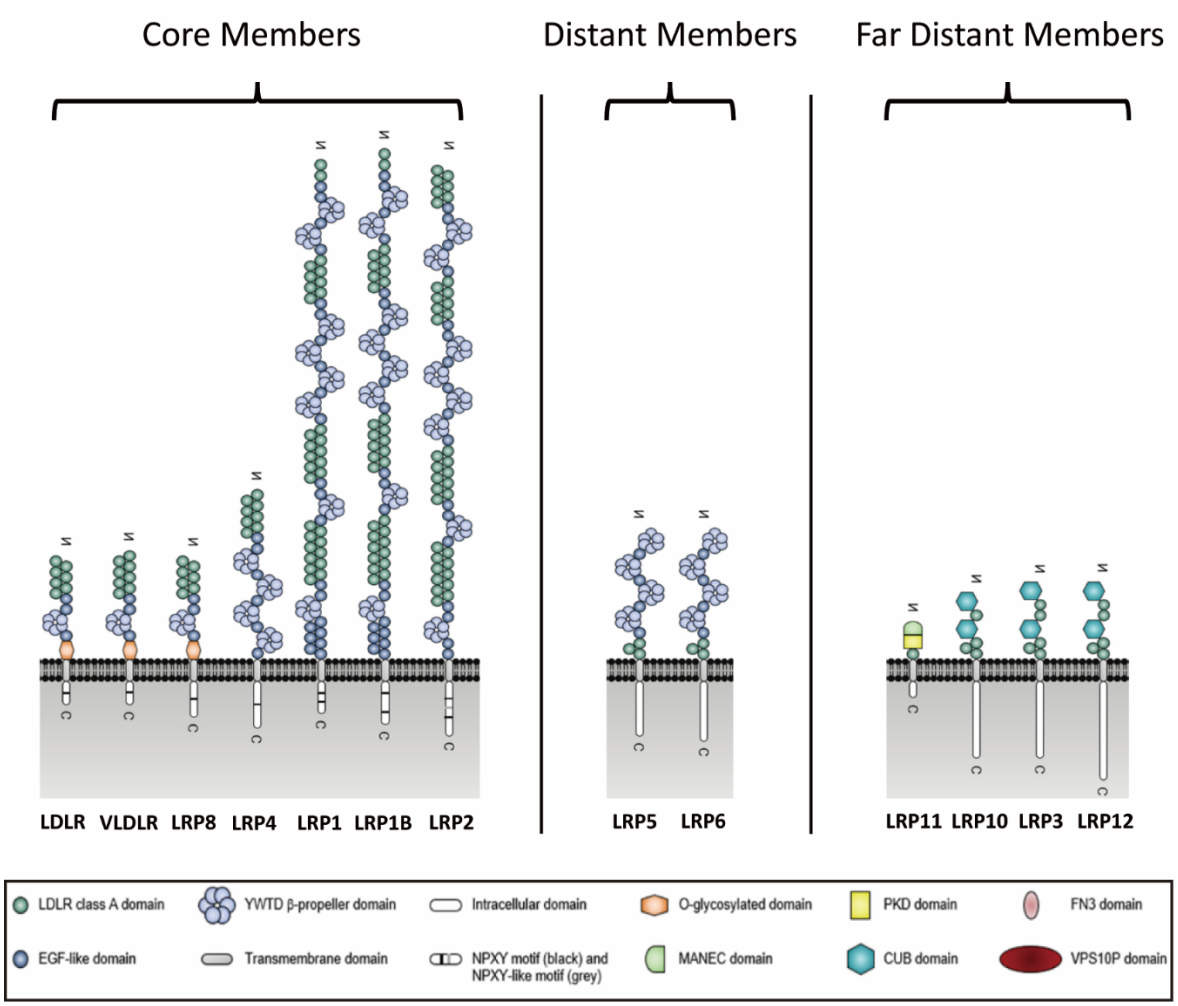

Figure 1. 1. Schematic diagram of low-density lipoprotein receptor (LDLR) family. All LDLR family members are single-spanning transmembrane receptors with shared LDLR class A domain responsible for the ligands binding. LDLR closely related members also have similar YWTD beta-propeller and epidermal growth factor-like domains. Schematic is modified from Principe et al. 2021 [8].

lack the NPXY motifs in their intracellular cytoplasmic tails. For the far distant members, they are structurally more distinct from the LDLR. They only harbour the LDLR class A repeats as an identity of the LDLR family. The far distant members have their unique structure domains. A new N-terminal CUB domain (for complement C1r/C1s, Uegf, Bmp1) connected to LDLR class A repeats is a shared structure among LRP3, LRP10 and LRP12. LRP11 itself has MANEC (motif at N terminus with eight cysteines) and PKD (polycystic kidney disease) domains that do not share with other LDLR family members [9].

The LDLR family was initially thought to be only involved in lipid metabolism as the receptors of lipoprotein particles but with more extensive studies and new member discoveries, the LDLR family are now known to have in multiple physiological and pathophysiological roles in biology [10]. Emerging evidence suggests that the potential functions of the LDLR family members should not be neglected.

1.1.1 LDLR

LDLR is the fundamental member of the LDLR family, which Brown and Goldstein first discovered in the study of familial hypercholesterolemia in 1973 [11]. The most prominent function of LDLR is its ability to take up cholesterol-rich LDL particles from the circulation system, regulating lipid homeostasis [12].

Mature LDLR is a transmembrane protein with a molecular mass of ~160 kDa [13]. LDLR is initially synthesized as a ~120 kDa immature precursor in the rough endoplasmic reticulum (ER). After that, the precursor LDLR is transported to the Golgi apparatus for post-translational modifications in which the majority is glycosylation. Insufficient glycosylation dramatically reduces the binding capacity of LDLR to ligands [14,15]. The mature LDLR is then guided to the cell surface waiting for ligand binding.

LDLR is ubiquitously expressed in human and the hepatic LDLR is the protein primarily responsible for the clearance of cholesterol from circulation [16]. LDLR primarily interacts with cholesterol-rich LDL, β-VLDL and chylomicron remnants through the binding of

apolipoprotein B and E on the surface of these lipoprotein particles, respectively [4]. Structurally, the LDLR class A repeats are responsible for ligand recognition and binding. As repeats 3-7 are important for LDL binding and repeat 5 is required for both LDL and VLDL binding [17,18]. After the binding of LDLR and its LDL ligand, the receptor-ligand complex is then internalized into cells through clathrin-mediated endocytosis [19,20]. After endocytosis, the clathrin-coated endocytic vesicles are delivered to the lysosome for degradation. The pH change in the endosome stimulates the conformation change of LDLR which releases the bound LDL [21]. After the dissociation of LDL and LDLR in the endosome, the LDL particles are delivered to the lysosome for degradation. On the other hand, LDLR undergoes a recycling pathway back to the cell surface [22].

Loss-of-function mutations in LDLR result in familial hypercholesterolaemia (FH) which is characterized by inherited abnormally elevated serum levels of LDL-cholesterol from birth [23]. FH is a common genetic disorder. Heterozygous FH affects roughly 1 in 220 individuals globally [24]. Autosomal dominant mutations in LDLR impair the function of LDLR removing cholesterol from circulation, and the elevated cholesterol increases the risk of atherosclerosis and other cardiovascular diseases. Severe homozygous FH patients not only have marked premature and progressive atherosclerosis but also extensive xanthomas [25]. The role of LDLR is relatively onefold in biology that regulates lipid homeostasis but its importance to the normal physiology of organisms cannot be underestimated.

1.1.2 LPR1

LRP1 is one of the earliest discovered members of LDLR family [26]. One feature of LRP1 is its

molecular mass of ~600 kDa large containing two subunits of a ~515 kDa α-chain and a ~85 kDa β-chain [27]. The ~600 kDa LRP1 precursor is cleaved by furin-like endoproteases in the trans-Golgi complex to generate the α- and β-chains and form mature LRP1. The β-chain is a type I transmembrane protein and it is non-covalently associated with the extracellular α-chain which is responsible for ligand binding. Surprisingly, LRP1 is capable of interacting and binding more than 100 ligands which range from lipoproteins and proteases to toxins and viruses [28].

LRP1 is also ubiquitously expressed in a variety of tissues. Unlike LDLR where the hepatic LDLR plays the majority role in regulating lipid homeostasis, LRP1 due to its a broad range of ligands plays multiple roles involving various biological processes [29]. Like LDLR, LRP1 is also involved in lipid metabolism through endocytosis of lipoprotein particles but it is restricted to ApoE-containing lipoproteins, such as β-VLDL and chylomicron remnants [30,31]. Global deletion of *Lrp1* in mice results in embryonic lethality, revealing that LRP1 plays essential roles in embryo development [32]. As LRP1 interacts with multiple extracellular matrix proteinases and proteinase inhibitors, it is not surprising that LRP1 is also involved in angiogenesis [33]. Another major role of LRP1 is regulating multiple cell signalling, which either through a direct ligand-binding event and endocytosis or indirectly serves as a co-receptor for some proteins [29].

LRP1 has been extensively studied in several common diseases. In Alzheimer's disease, LRP1 is one major receptor mediating the clearance of amyloid β (Aβ) whose accumulation is believed to be the reason for neurodegeneration [34]. In tumors, LRP1 can promote cell migration and invasion through interacting with extracellular matrix proteinases (MMP-2 and MMP-9)

and stimulate cell proliferation by regulating multiple signaling pathways [35]. In cardiovascular disease, LRP1 has shown its importance in vasculature integrity [36], lipid metabolism [37] and inflammation regulation [38]. Due to the large ligand pool of LRP1, it is not surprising for its multi-faceted role in a variety of physiological and pathological events.

1.1.3 LRP1B

LRP1B is a member of LDLR family which shares highly conserved mRNA (86%) and amino acid sequences (52%) with LRP1 [10]. LRP1B is also a large receptor as LRP1 that LRP1B is constituted by a ~520 kDa α-chain and a ~90 kDa β-chain. Two subunits are non-covalently connected to form the mature LRP1B whose molecular mass is as large as ~600 kDa. Due to the high structural homology between LRP1B and LRP1, LRP1B shares a pool of ligands overlapped with LRP1 which also suggests that they may have similar biological roles [39,40]. However, a kinetic study revealed that the internalization rate of LRP1B is much slower than LRP1, and its endocytosis takes more than a 15-folder of time [39]. In the cases of β-amyloid precursor protein (APP) endocytic trafficking, LRP1 and LRP1B can both bind and internalize APP, but the endocytosis rate difference results in different physiological effects [41]. The rapid endocytosis rate of LRP1 causes a higher level of Aβ since more APP is internalized and processed into Aβ in unit time [42]. On the other hand, the slowly internalized LRP1B reduces Aβ production by inhibiting APP endocytosis [43]. It is believed that there is a competition between LRP1 and LRP1B on ligand endocytosis.

LRP1B was originally named LRP-DIT (lipoprotein receptor related protein-deleted in tumors)

since it was first discovered as a frequently inactivated LRP in non-small cell lung cancer [44]. This first discovery also implies the importance of LRP1B in tumors and led to a focus on LRP1B studies in cancer research. Mutations of LRP1B have been discovered in a variety of cancers which not only increases susceptibility to certain cancers but also is associated with poor survival outcomes of cancers [45-48]. For this reason, LRP1B is generally believed as a tumor suppressor. Molecular biology studies have shown evidence that the downregulation of LRP1B would promote the growth and migration of cancer cells through multiple signaling pathways [49-51]. LRP1B as a highly conserved protein of LRP1 exhibits some shared features with LRP1 but also shows distinct functions in disease development and progression.

1.1.4 LRP2

LRP2, as known as megalin, is the last large member in the LDLR family with a molecular mass of ~600 kDa [52]. Unlike LRP1 and LRP1B, the LRP2 precursor does not need furin cleavage and exists as a mono-molecular on the cell surface after maturation [53].

Similar to LRP1, due to the large and complex structure of LRP2, it can bind and internalize a large number of ligands usually with the assistance of cubilin as a dual-receptor complex [54]. Distinct from LRP1, the expression pattern of LRP2 is restricted to the apical surfaces of epithelial cells in several organs [55]. The location of LRP2 implies its main function as a receptor to absorb macromolecules from the lumen of organs. The LRP2-deficient mice have holoprosencephaly, a defective forebrain development, which is due to the insufficient endocytic uptake of essential nutrients in the post-gastrulation stage [55].

A critical role of LRP2 is its reabsorption of tubular proteins and molecules from primary urine that are filtered through the glomerular barrier [56]. A set of LRP2 reabsorbed molecules are vitamins including vitamins A, B_{12} and D [57]. Mice with LRP2 depletion in kidney showed a disruption in reabsorption of 25-(OH) vitamin D3 from the primary urine and exhibited vitamin D deficiency and bone defects [58,59]. LRP2 also mediates the uptake of hormones and signaling proteins from tubular filtrate [60]. The absence of LRP2 in mice resulted in a 4-fold increased level of parathyroid hormone fragments in urine [61]. Impaired sexual maturation was also observed in both male and female mice lacking LRP2 [62]. The reabsorption function of LRP2 ensures the homeostasis of multiple essential molecules and proteins.

LRP2 was first identified as a major antigen in the rat model for immune-mediated nephritis [63]. LRP2 is also most abundant in the kidney [64]. Since that, LRP2 started to be revealed for its importance in multiple renal diseases including diabetes- and obesity-induced nephropathy [56]. One shared feature of these renal diseases is the impaired renal reabsorption of proteins due to the loss of LRP2 [60]. In nephrotoxin-induced acute kidney injury, the reabsorption function of LRP2 has conflicted effects [65]. On one side, LRP2 mediates the uptake of proteins that have renoprotective functions such as neutrophil gelatinase-associated lipocalin and survivin [66,67]. On the other side, some nephrotoxins are also the ligands of LRP2, the binding and internalization of nephrotoxins extend their retention in body [68]. LRP2, like the other large members in LDLR family, is multifunctional due to its large ligand pool but restricted by its limited tissue distribution.

1.1.5 LRP3

LRP3 is a ~105 kDa LDLR family member ubiquitously expressed in multiple organs [69]. It was discovered in 1998 by screening the amino acid sequence homology of LDLR family in the cDNA library of rat liver. Ligand binding experiment showed that LRP3 is not a receptor of Apo-E and may not participate in lipoprotein metabolism [69]. Although LRP3 has been discovered for more than 20 years, there are still not many studies on it.

In brain, just like some of the LDLR family members (e.g. LRP1 and LRP8), it was also found that LRP3 compromises β-amyloid precursor protein levels which is regulated by LRP8/reelin signaling [70]. It again highlights the importance of LDLR family in the development and progress of Alzheimer's disease.

Recently, emerging publications suggested a new function of LRP3 in regulating stem cell differentiation. *LRP3* expression is highly elevated in human bone marrow stromal cells (hBMSC) with a higher degree of mineralization [71]. Based on functional and gene expression assays, it is speculated that LRP3 may determine the differentiation fate of BMSC into either osteoblasts or adipocytes as a molecular switch. Reduction of the level of LRP3 would promote hBMSC adipogenesis and suppress osteogenesis [71]. Meanwhile, it was discovered that during the chondrogenesis of rat bone marrow stromal cells (rBMSC) the level of LRP3 was markedly increased [72]. Manipulating LRP3 expression could effectively control the chondrogenesis of rBMSC. In mice, genetically engineered LRP3 deficiency and diet-induced LRP3 downregulation both promoted cartilage degeneration and osteoarthritis progression [73]. As a barely-studied LDLR family member, we still know very little about the function of LRP3 but

its importance in cartilage health is a promising start.

1.1.6 LRP4

LRP4 is a ~250 kDa LDLR family member with a similar molecular mass as LRP5 and LRP6 and ubiquitously expressed in various tissues [74,75]. In 1998, a group of scientists identified LRP4 through motif-trap screening based on epidermal growth factor-like motif which is a shared structure in LDLR family [76].

LRP4 deficiency in mice resulted in abnormal embryological development of the apical ectodermal ridge to form limb buds [77]. It is also found that LRP4 inhibits the Wnt/β-catenin signaling which is important in limb development and could be the reason for the development abnormality [78]. LRP4 is a receptor of multiple Wnt proteins but also some Wnt/β-catenin signaling inhibitors [79,80]. It is speculated that the Wnt/β-catenin signaling inhibition is achieved by either a competing of Wnt with LRP5/6 or an enrichment of LRP5/6 inhibitor proteins through LRP4-ligand interactions [81]. Wnt/β-catenin signaling is also tightly related to the bone-mass homeostasis which explains the common association of mutations in LRP4 with bone disorders [82,83].

Besides the regulatory function of LRP4 in the Wnt signaling, researchers more focus on the importance of LRP4 in the neuromuscular junction (NMJ) formation and maintenance [84]. LRP4 was also independently discovered by a different research group as a synaptic LDL receptor-related protein due to its enrichment in postsynaptic density fraction [85,86]. This finding also

suggested the potential role of LRP4 in the synapse. Mice with specific LRP4 mutants showed a defective NMJ formation which is similar to the phenotypes in agrin and muscle-specific kinase (MuSK) deficient mice [87-89]. The importance of agrin and MuSK in NMJ formation was discovered earlier than LRP4, but researchers also proved that agrin does not directly bind to MuSK [90]. The appearance of the critical of LRP4 in NMJ formation suggested that LRP4 could be the bridge between agrin and MuSK. Further studies confirmed the role of LRP4 as the coreceptor of agrin with MuSK whose activation is critical for the pre- and postsynaptic differentiation in NMJ [91,92]. Structurally, LRP4 and MuSK are first assembled together and then with the additional agrin binding to LRP4 [93]. Two agrin-LRP4-MuSK complexes further bind together and promote MuSK activation for downstream signaling. Due to this finding, LRP4 is now a popular target in NMJ studies. Besides the role of LRP4 in NMJ formation, new evidence also suggests that LRP4 may be involved in the central synapse development in brain [94].

1.1.7 LRP5 and LRP6

LRP5 and LRP6 belong to the LDLR family with close molecular masses at ~250 kDa and are ubiquitously expressed in both embryonic and adult tissues [95,96]. LRP5 and LRP6 were identified at almost the same time in 1998 through the cDNA library screening [97,98]. Structurally, LRP5 and LRP6 shared ~71% identity in amino acid sequence. The high homology between LRP5 and LRP6 points out their analogous functions. Similar to the other LDLR family members, LRP5 and LRP6 have a shared ligand pool which includes ApoE and may involve in lipoprotein metabolism [99,100].

The most prominent role of LRP5 and LRP6 is as the essential co-receptor of Wnt ligands and activates the Wnt/β-catenin signaling [101]. Wnt signaling is critical for normal cell proliferation and differentiation during embryogenesis and adult tissue homeostasis [102]. In mice with mutant LRP6, there is a development defective phenotype which is also exhibited in mice with the mutant Wnt ligand, suggesting that Wnt signals are disrupted with mutant LRP6 [103]. The following studies proved that the entire Wnt receptor complex is composed of a member of the Frizzled (Fzd) family and LRP5/6 [81,104]. With the Wnt activation, Fzd and LRP5/6 heterodimer activates the release of β-catenin to translocate to the nucleus as a transcriptional factor to activate the expression of Wnt target genes.

Besides the physiological role of Wnt/β-catenin signaling in regulating embryonic development and tissue homeostasis, its pathological role in tumor development and progression is more attractive [105]. The lost control of Wnt/β-catenin signaling has been observed in multiple cancers as the overactivated Wnt/β-catenin signaling maintains the stemness of cancer cells and also stimulates the growth of cancer cells [105,106]. Modulation of LRP5 and LRP6 is considered as a therapeutic strategy targeting the Wnt/β-catenin signaling [107].

Mutations in LRP5 and LRP6 also lead to the discovery of the role of Wnt/β-catenin signaling in bone homeostasis [108]. Abnormal high bone mass in human is commonly associated with mutations in the first β-propeller domain of LRP5 and LRP6 as well as increased Wnt/β-catenin signaling [109,110]. Mutant LRP5 and LRP6 impair the normal inhibitory control of Wnt/β-catenin signaling by sclerostin and thus result in an overactivated Wnt/β-catenin signaling to enhance osteoblast proliferation and maturation. The regulation role of LRP5 and LRP6 as a bone mass

determiner also guides the therapeutic studies on utilizing the LRP5 and LRP6 activation to recover osteoporosis [111].

LRP5 and LRP6 are also involved in many other diseases including coronary artery disease and Alzheimer's disease [112]. The compensatory roles of LRP5 and LRP6 may mask the biological importance of them when only one of them is defective, suggesting that there may be more important functions of LRP5 and LRP6 underestimated or undiscovered [113].

1.1.8 VLDLR and LRP8

VLDLR and LRP8 are two structural similar members in the LDLR family with molecular masses at ~130 kDa. There is a ~50% homology between VLDLR and LRP8 in amino acid sequence [114]. However, the O-linked glycosylation domain in LRP8 is more than twice in size of that in VLDLR which results in a slighty larger molecular mass of LRP8. Like most LDLR family members, VLDLR and LRP8 are able to bind and mediate endocytosis of ApoE-rich β-VLDL [115] [114]. Of note, VLDLR can even bind with high affinity to lipid-free ApoE isoforms [116].

VLDLR is ubiquitously expressed in almost all tissues, but the expression of LRP8 is mainly restricted in brain and testis [114,117]. Besides that, neither protein is expressed in the liver (the main organ for lipid metabolism) under normal physiological conditions. It suggests that VLDLR and LRP8 are not involved in the liver-mediated clearance of VLDL and chylomicron remnants. Mice with a global deficiency in VLDLR or LRP8 do not exhibit any apparent

change in plasma lipids [118,119]. However, a later study proved the role of VLDLR in peripheral uptake of VLDL triglycerides through manipulating VLDLR levels in LDLR-deficient mice with high-fat food challenge [120]. Significant reduction in adipose tissue mass is also a feature of VLDLR-deficient mice. The significant levels of VLDLR and LRP8 in brain suggest the function of them in the transportation of cholesterol from astrocytes to neurons via ApoE which is necessary for synapse formation [121]. Subcellularly, VLDLR is mainly disturbed in non-lipid raft regions of the plasma membrane but LRP8 is mainly located in the lipid rafts [122].

Reelin signaling is essential in neural development and maintenance by regulating the proper migration of neurons [116]. In *Vldlr* and *Lrp8* double knockdown mice, neuronal migration disturbed neuropathology was observed, which recapitulated the phenotype of mice with defective Reelin signaling [123]. In vitro study also approved the interactions between the cytoplasmic tail of VLDLR or LRP8 and disabled-1 which is a key component in Reelin pathway initiation. Further molecular biology studies then showed that VLDLR and LRP8 are the two exclusive receptors of Reelin in nervous system [116]. VLDLR or LRP8 single knockdown mice do not exhibit dramatic neuronal migration defects which suggests a compensatory relationship between VLDLR and LRP8 [123]. In human, homozygous deletion of VLDLR leads to cerebellar hypoplasia due to an impaired Reelin pathway [124].

The ApoE isoform ApoE4 has been identified as the strongest genetic risk factor for Alzheimer's disease [125]. People who carry two alleles of APOE4 have an increased chance to get Alzheimer's disease by eight- to twelvefold [126]. As two ApoE receptors in brain, it is not surprising that VLDLR and LRP8 also play critical roles in the development and progression of Alzheimer's disease [127]. ApoE4 has been found to impair LRP8 recycling which sequentially

affects its availability on cell surface [128]. As β-amyloid precursor protein is the ligand of LRP8, the reduction of cell surface LRP8 increases the production of cytotoxic amyloid β [129]. VLDLR- and LRP8-Reelin signaling also has a protective role in Alzheimer's diseases by enhancing synaptic plasticity [130]. Competition between AopE4, one of the strongest competitors, and Reelin could be a reason for disturbed the VLDLR- and LRP8-Reelin signaling pathway in Alzheimer's disease [131].

1.1.9 LRP10

LRP10 is a far distant member of LDLR family with a molecular mass at ~100 kDa [132]. Structurally, LRP10 is closer to the LRP3 and LRP12 as they are the only three members in the LDLR family containing the CUB domains which facilitate the ligand binding [8,52]. LRP10 can be widely detected in most organs with high expression levels in the liver, kidney, lung and heart but low levels in the brain [132]. LRP10 can mediate the uptake of ApoE-enriched β-VLDL which suggests that ApoE is a ligand of LRP10.

Unlike other LDLR family members located on the cell surface, LRP10 is mainly disturbed in the *trans*-Golgi network (TGN) and endosomes with a clathrin-mediated cycling [133]. The cytoplasmic tail of LRP10 is the key domain responsible for its intracellular trafficking. Calnuc is the protein found to ensure the correct sorting of LRP10 from TGN to endosomes and it prevents the delivery of LRP10 to lysosomes [134]. Deletion of Calnuc results in the redistribution of LRP10 to late endosomes and lysosomes which enhances the degradation of LRP10. However, the detailed biological role of LRP10 during the cycling between TGN and

endosomes is still unclear.

In Alzheimer's disease, LRP10 mutation has been identified as a possible risk factor [135,136]. It was found that LRP10 binds and traps APP in the intracellular cycling between the Golgi apparatus and endosome which prevents the amyloidogenic process of APP at the cell surface [135].

Another controversial finding related to LRP10 is that it may be a causative factor of Parkinson's disease. A multiple genome-wide linkage analysis in Italian individuals has first shown *LRP10* as a causative gene of Parkinson's disease [137]. Although other replication studies on different populations cannot provide strong evidence to support the causal relation between LRP10 and Parkinson's disease, several potentially pathogenic variants of LRP10 have been discovered in the cohorts of Parkinson's disease patients [138-140]. It suggests that even though LRP10 does not directly cause Parkinson's disease, it may be still involved in the onset and progression of the disease. The mechanism of how LRP10 affects Parkinson's disease is still unknown but probably depends on LRP10-related intracellular trafficking of proteins [141].

An interesting feature of LRP10 is its stable mRNA expression in adipose tissue and LRP10 is commonly used as a reference gene in the qRT-PCR analysis [142]. It suggests that LRP10 may play an essential role in adipose tissue and its expression level is not easily disrupted.

1.1.10 LRP11

LRP11 is a ubiquitously expressed LDLR family member with a molecular mass of ~90 kDa

[64]. Structurally, LRP11 is the most distinct from other members in the LDLR family. The ectodomain of LRP11 consists of only three domains: a MANEC domain, an LDLR class A repeat, and a PKD domain [9]. The MANEC domain was first identified in the LRP11 and it commonly presents at the N terminus of membrane and extracellular proteins but the detailed function of MANEC is still unknown. Up to date, LRP11 is the least characterized member in LDLR family.

Multiple analyses on tumor transcriptome revealed that LRP11 is highly expressed in various cancers [143-145]. Silence of LRP11 can inhibit tumor cell proliferation and growth through cell cycle protein regulation [143]. Besides that, LRP11 was also found to induce PD-L1 expression through β-catenin activation which helps tumor cells for immune escape [144]. The pan-cancer analysis also illustrated that the high LRP11 level is related to the lack of immune cells around tumor [146]. Upregulation of LRP11 is also associated with poor prognosis and short overall survival time in patients with cancer [145,147]. All these findings imply that LRP11 may promote tumor growth and regulate the immune response to tumors.

Another possible function of LRP11 is its regulation role in stress responses, especially under cold stimulus [148,149]. Upregulated LRP11 levels were observed in a couple of animal models responding to cold exposure [148-150]. Meanwhile, depletion of LRP11 in HEK293 cells led to the downregulation of several genes involved in stress pathways [150].

1.1.11 LRP12

LRP12 is the last member classified to the human LDLR family so far. The molecular mass of LRP12 is around 100 kDa. LRP12 is structurally similar to LRP3 and LRP10 that they all share a CUB domain linked with LDLR class A repeats [151]. LRP12 is most abundant in heart and skeletal muscle and also expressed in other organs but not the liver or kidney [152].

When *LRP12* was first identified, it was classified as a tumor suppressor gene whose expression is downregulated in multiple tumor cell lines [152]. Hypermethylation of the *LRP12* gene is commonly observed in cancer and is related to chemotherapy resistance [153,154]. One recent study revealed that LRP12 is able to mediate cell migration as an endogenous transmembrane inactivator of integrins which are principal receptors to bind the extracellular matrix [155]. It may partially explain the role of LRP12 as a tumor suppressor in preventing the malignancy of tumor cells.

Expression of LRP12 is also critical for normal brain development [156]. Restricted expression of LRP12 in a transient population of future neocortical cells ensured the correct positioning and differentiation of neurons [157]. Mice with LRP12 deficiency had an abnormality in cortical development as aberrant neuron lamination [156]. Decreased expression is observed in schizophrenia and may also result in seizures [156,158]. Special LRP12 mutation with noncoding CGG repeat expansions is a causative factor in the movement disorder oculopharyngodistal myopathy (OPDM) [159]. The exact pathogenesis mechanism on how CGG repeats in LRP12 result in OPDM is unclear but this particular mutation is highly present in OPDM patients in certain areas [160].

1.2 Degradation of LDLR family members

1.2.1 Intracellular degradation

LDLR degradation has been exclusively studied due to its importance in lipid metabolism and cardiovascular diseases. LDLR binds LDL and then the complex is internalized via clathrin-mediated endocytosis [19]. In endosomes, LDL dissociates from LDLR due to the conformation change of LDLR responding to the acidic environment [21]. The majority of LDLR is recycled back to the cell surface while a small portion of LDLR failed to dissociate and join the degradation with LDL in lysosomes [161]. Proprotein convertase subtilisin/kexin type-9 (PCSK9) is a protein binding to the epidermal growth factor-like domain in LDLR and induces the lysosomal degradation of LDLR through impairing the recycling of LDLR [162]. Alternatively, the inducible degrader of the LDLR (IDOL) promotes the ubiquitylation of the C-terminal tail of LDLR which triggers the internalization and lysosomal degradation of LDLR [163].

LRP1 binds ligands and delivers them to lysosomes for degradation in a similar way as LDLR [164]. However, unlike LDLR, the ubiquitin proteasome system (UPS) is the major pathway for LRP1 degradation [165]. HepG2 cells treated with proteasomal inhibitors have a significant increase in the LRP1 level. Under specific conditions, LRP1 can also be proteolytically degraded through the lysosomal system [166,167]. Similar to LRP1, LRP2 also mainly undergoes UPS for its intracellular degradation [168].

The other core members of LDLR family including VLDLR and LRP8 have been proved to undergo intracellular lysosomal degradation for their turnovers [169]. For the distant members, LRP5 and LRP6, the lysosomal pathway is also their major way of intracellular degradation

[170,171]. Due to the highly conserved structure among the LDLR family, the other less studied members are also likely degraded through the lysosomal pathway. A possible reason for the proteasomal degradation of LRP1 and LRP2 could be due to their large molecular mass which distinguishes them (including LRP1B) from the rest of LDLR family members.

1.2.2 Extracellular shedding

Besides the intracellular degradation, as cell surface proteins, LDLR family members also undergo ectodomain shedding by sheddases. Sheddases are a group of membrane surface proteases which mediates the ectodomain cleavage of cell surface proteins [172]. An additional following cleavage by γ-secretase commonly occurs to further degrade the cell surface proteins [173].

Members of the matrix metalloproteinase (MMP) family or ADAM (a disintegrin and metalloproteinase) family are the common sheddases responsible for extracellular ectodomain shedding. In the LDLR family, some of the members have been reported to be proteolytically processed by the sheddases on the plasma cell surface. Members in the MMP family are able to cleave LDLR [174], VLDLR [175], LRP1 [176], LRP2 [177]and LRP4 [75]. ADAM family is also reported to shed the LDLR family members including LDLR [178], VLDLR [179], LRP1 [180],LRP1B [181], LRP4 [182], LRP5/6[183], LRP8 [184]. After the LDLR family member is cleaved by a sheddase, the full-length receptor turns into a soluble ectodomain (ECD) part and a membrane-anchored C-terminal fragment (CTF). The ectodomain shedding is generally followed by a γ-secretase cleavage which further cleaves the CTF of LDLR family members into a soluble intracellular

domain (ICD). The ECD and CTF or ICD are the final products of the LDLR shedding which sometimes may partially preserve the function of original full-length receptor or may gain new functions [185].

Both intracellular degradation and extracellular shedding of the LDLR family members are post-transcriptional regulation methods of cells to downregulate the levels of LDLR family members which implies their importance in controlling the physiological and pathophysiological functions of the LDLR family.

1.3 Membrane type 1-matrix metalloproteinase (MT1-MMP)

MT1-MMP, a Zn-containing endopeptidase, belongs to the family of MMPs and is one of the six human membrane-bound matrix metalloproteinases [186]. Humans have 23 MMP members identified so far, and most of them are secreted proteins. MT1-MMP is the first MMP discovered as a transmembrane protein on the cell surface and is highly overexpressed in malignant tumor tissues [187]. MT1-MMP can be detected in various tissues with high expression in adipose tissue, skin and lung [64]. MT1-MMP is synthesized as a zymogen and requires enzymes, such as furin, to cleave its prodomain for activation [188-190]. Activated MT1-MMP is then trafficked to the cell membrane surface along the tubulin cytoskeleton [191]. Besides cell surface, MT1-MMP can also be found in subcellular regions including the cytoplasm, caveolae, Golgi apparatus and nucleus [192].

1.3.1 Structure of MT1-MMP

Structurally, MT1-MMP consists of a signal peptide, a prodomain, a conserved catalytic domain that includes a conserved zinc-binding motif, a hemopexin-like domain linked to the catalytic domain by a flexible hinge region, a stalk region linking the transmembrane domain, and the intracellular C-terminal cytoplasmic tail (**Fig. 1.2**) [193,194].

MT1-MMP is synthesized as a zymogen and its prodomain at the N-terminus masks the proteolytic activity of MT1-MMP. In the Golgi apparatus, the autoinhibitory prodomain is released by furin cleavage and also degraded by MMPs (including MT1-MMP autocatalysis) to fully liberate the activity of MT1-MMP [195]. The structurally homological catalytic domain is responsible for the proteolytic activity of all MMPs. The conserved catalytic domain can be found in all members of MMPs and ADAMs which is characterized by a 3-histidine zinc(II)-binding motif [196]. Mutations in the catalytic domain affect the proteolytic activity of MT1-MMP. A single mutation of converting glutamic acid (E240) to alanine (E240A) in the catalytic domain of MT1-MMP causes the loss of proteolytic activity [197,198]. MT-loop is a small flexible exosite region in the catalytic domain, and its deletion does not affect the proteolytic activity of the catalytic domain [199]. However, MT-loop is important for some substrate recognition [200,201]. The deletion of the MT-loop impairs the interaction between MT1-MMP and cell adhesion complexes, then further disrupts the association between MT1-MMP and substrates [200]. In MT1-MMP, the hemopexin-like domain is necessary for its homodimerization and interaction with some substrates [202]. In the case of MT1-MMP-mediated CD44 shedding, the hemopexin-like domain is required for CD44 binding and relocation to lamellipodia followed

by sequential CD44 cleavage by MT1-MMP [203,204]. MT1-MMP is a glycoprotein which is O-glycosylated in the hinge region [205]. The glycosylation of MT1-MMP modulates the activity of MT1-MMP by broadening its substrate profile. For example, activation of MMP2 requires the proper glycosylation of MT1-MMP which is important for the recruitment of substrates [205]. The transmembrane domain of MT1-MMP is not only critical for its membrane anchoring but also important for the dimerization of MT1-MMP as a dimer interface [206]. The deletion of the C-terminal cytoplasmic tail (CT) affects the distribution of MT1-MMP on the cell surface and endocytosis [192]. The cell surface MT1-MMP undergoes rapid turnover by cytoplasmic tail-dependent endocytosis [207,208]. There is evidence showing that the lack of the C-terminal cytoplasmic tail causes aberrant accumulation of MT1-MMP in the caveolae [209]. The CT-deleted MT1-MMP exhibits a slower internalization rate and the clathrin-mediated endocytosis is blocked which suggests that the CT is essential for the clathrin-mediated endocytosis but not caveolae-dependent endocytosis [208].

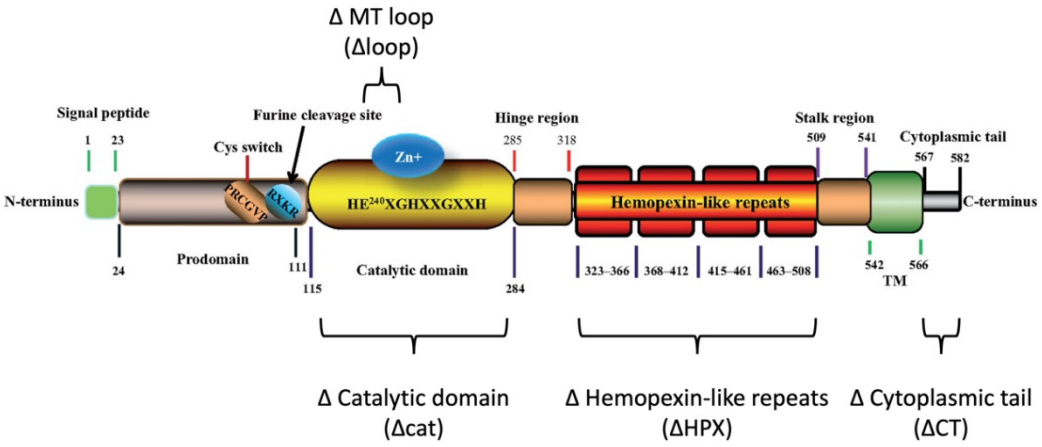

Figure 1. 2. Schematic diagram of the MT1-MMP structure. MT1-MMP is composed of several domains including an N-terminal signal peptide, prodomain, catalytic domain (cat) which also contains an eight-amino acid MT-loop, hinge region, hemopexin-like repeats (HPX), stalk region, transmembrane domain (TM) and C-terminal cytoplasmic tail (CT). Schematic is modified from Xia et al. 2021 [193].

1.3.2 Physiological and pathophysiological function of MT1-MMP

MT1-MMP is essential for normal embryo development. The global deletion of MT1-MMP results in early postnatal death of mice, mostly due to wasting and cachexia [210]. A few survivors have severe development issues, including dwarfism, craniofacial abnormalities, and the absence of sexual maturation. It is found that MT1-MMP is important for extracellular matrix remodeling during embryogenesis, angiogenesis and vascularization in multiple organs including the lung, cartilage, skeletal muscle and brain [211-213]. MT1-MMP is important for diverse biological processes such as tissue remodelling and wound healing [214,215]. MT1-MMP remodels the extracellular matrix by directly cleaving extracellular matrix proteins (e.g. collagens and fibronectin) or activating other extracellular matrix-remodelling proteins (e.g. proMMP2) [216]. MT1-MMP plays important roles in cell migration due to its ability to remodel extracellular matrix and regulate cell motility, growth and adhesion [203,217-219]. MT1-MMP is enriched in invadopodia through which cells degrade extracellular matrix and migrate [220]. MT1-MMP also modulates inflammation through PI3K-delta activation in a proteolytic activity-independent manner in macrophages [221]. The expression levels of MT1-MMP are upregulated in atherosclerotic plaques and multiple pathogen infections where inflammation is a critical part of immune response [222-224]. The signalling function of MT1-MMP is in a proteolysis-independent mechanism through the C-terminal cytoplasmic tail [225,226]. For example, a single mutation in the C-terminal cytoplasmic (Y573D) impairs the MT1-MMP-induced Erk1/2 and Akt signalling [227].

MT1-MMP is closely related to several common diseases [192,193,228]. The expression levels of

MT1-MMP are elevated in multiple cancers [229]. In clinic, the expression of MT1-MMP is positively and negatively related to the progression and prognosis of cancers, respectively [230-233]. It was found that MT1-MMP is involved in cancer development through different mechanisms [234,235]. The ECM remodelling ability of MT1-MMP facilitates cancer cell migration, invasion and metastasis by giving cancer cells more space to grow [236]. The cleavage of cell membrane surface proteins by MT1-MMP can also promote cancer development. MT1-MMP was found to cleave EphA2 on the cell surface, which further triggers the EphA2 oncogenic signalling and promotes tumour progression [237]. In addition, MT1-MMP can help tumour cells evade the immune response by cleaving MHC class I chain-related molecule A which recruits natural killer cells [238]. Interestingly, MT1-MMP is also related to virus infection, which facilitates the cell entry of SARS-CoV-2 [239]. In the lungs of patients and mice with SARS-CoV-2 infection, the MT1-MMP expression levels were found to be increased [240,241]. MT1-MMP is closely associated with cardiovascular diseases for its ability to regulate blood cholesterol level, blood sugar level and body weight, which are all risk factors for cardiovascular diseases, by proteolytical cleavage of multiple cell membrane surface receptors [174,242-245]. The expression of MT1-MMP in the atherosclerotic plaques also makes the plaques more vulnerable to rupture and increases the chance of stroke [222]. Recent evidence has shown that MT1-MMP may also relate to Alzheimer's disease [227]. MT1-MMP is able to cleave and degrade soluble and fibrillar amyloid beta-protein, whose aggregation is the hallmark of Alzheimer's disease, and its degradation may alleviate Alzheimer's disease [246-248]. Furthermore, MT1-MMP is highly expressed in arthritic joints, and its inhibition reduces cartilage degradation which highlights the importance of MT1-MMP homeostasis in bone disorders [249-

[251]. Mice with global MT1-MMP deficiency develop severe arthritis [210].

1.3.3 Connections between MT1-MMP and LDLR family

The interaction between MT1-MMP and LDLR family has first been shown in the case of LPR1 that MT1-MMP is able to cleave LRP1 in multiple malignant cell lines [176]. This could partially explain the fact that in some cancers LRP1 levels are downregulated [252]. Recent studies revealed more cellular physiological and pathophysiological functions of MT1-MMP-mediated LRP1 shedding including vascular smooth muscle dedifferentiation, osteoarthritis and drug uptake through the blood-brain tumour barrier [253-255]. Our lab also first proved that MT1-MMP mediates the ectodomain shedding of hepatic LDLR to regulate plasma cholesterol level and the development of atherosclerosis [174]. Both findings imply that MT1-MMP could have vital effects on LRP1 and LDLR similar proteins – the LDLR family members. Meanwhile, knockdown of hepatic MT1-MMP in mice has no effect on the shedding of hepatic LRP1 which suggests that the proteolytical impact on LDLR family members could be in a cell-type and tissue-specific manner [174].

LDLR family members also have a regulation role in matrix metalloproteinases. Some metalloproteinases and their inhibitors are the ligands for LDLR family members including LRP1 and LRP2 [185]. LRP1 is able to endocytose MMP2, MMP9 and MMP13, as well as the tissue inhibitor of metalloproteinases (TIMP) family members [256]. TIMPs are endogenous protease inhibitors to the MMPs including MT1-MMP. LRP1-mediated endocytosis of TIMPs indirectly mediates the activity of MT1-MMP. Besides LRP1, LRP2 is also responsible for the

endocytosis clearance of MMP9 [257]. The signalling function of LDLR family members may also regulate the expression of MMPs [185]. There is evidence showing that LRP5 and LRP6-induced Wnt/beta-catenin cascade upregulates the expression of multiple MMPs including MMP2, MMP3, MMP7, MMP9, MMP13 and MMP14 [258,259].

1.4 Statin

1.4.1 Cardiovascular diseases and cholesterol as a risk factor

Cardiovascular diseases (CVDs) are the global leading cause of death in the current society which are responsible for 31.8% of all deaths annually and the total number of deaths caused by CVDs is still climbing [260]. Besides the impact of CVDs on mortality, the disability caused by CVDs affects more people and reduces their life qualities [261]. Globally, the prevalent cases of total cardiovascular diseases are 523 million in 2019 which affects around 7% of the total population [261]. In the case of CVDs, the years lived with disability is 34.4 million in 2019 which is doubled compared to the number in 1990 [261]. CVDs are a group of disorders that affect heart and blood vessel. Common CVDs include ischemic heart disease and stroke. Ischemic heart disease and stroke are caused by decreased blood supply to part of heart or brain and atherosclerosis is the common cause for arteries narrowing and blockage due to the buildup of plaque inside the artery walls [262]. There are several modifiable risk factors that can reduce the risk of CVDs and among them, hypercholesterolemia is the major factor for developing CVDs [263]. Serum total cholesterol and LDL-cholesterol are associated with the CVD mortality that the pooled hazard ratio for total cholesterol was 1.27 and for LDL-cholesterol was 1.21 by

comparing the mortalities between the highest level with the lowest level categories of cholesterol levels [263]. For people under 50 years old, 30-year mortality caused by CVDs increases by 9% for each 10 mg/dL increase in total cholesterol levels [264]. Under high circulating LDL-cholesterol conditions, the excess cholesterol is deposited in the artery walls which forms plaques and narrows arteries [265]. Premature atherosclerosis is the underlying cause of increased risks in CVDs like ischemic heart disease and stroke.

1.4.2 Statin as a cholesterol-lowering drug

In circulation, most of cholesterol exists as cholesterol esters carried by low-density lipoprotein (LDL) particles [266]. High levels of LDL-cholesterol increase the risk of atherosclerosis and thus lowering LDL-cholesterol is a primary therapeutic target in clinic to reduce the risk of cardiovascular diseases. Physiological clearance of LDL-cholesterol is primarily through hepatic uptake of cholesterol-enriched LDL particles by LDLR. Hence, regulating the LDLR-mediated clearance of LDL is a pharmacological goal.

Statin is the main prescribed medicine in the management of circulating LDL-cholesterol levels [267]. A large part of cholesterol in body is from *de novo* cholesterol synthesis in the liver where cholesterol is synthesized from acetyl coenzyme A [268]. Statins are 3-hydroxy-3-methylgutaryl coenzyme A reductase (HMGCR) inhibitors which block the rate-limiting step of *de novo* cholesterol synthesis. With statin treatments, intracellular cholesterol level is reduced due to inhibition of *de novo* cholesterol synthesis, which activates the sterol regulatory element binding protein 2 (SREBP2) to upregulate the expression of LDLR [12]. Upregulated hepatic

LDLR then increases clearance of LDL-cholesterol from circulation. Since the first commercial statin was approved in 1987, statins have been prescribed for decades to lower circulating cholesterol levels and reduce the risk of CVDs. Lowering 2-3 mmol/L of circulating LDL cholesterol by statin treatments is able to successfully reduce the risk of CVDs by 40-50% [269].

1.4.3 Statin combination therapy

Statin monotherapy is able to reduce the circulating LDL-cholesterol levels by more than 50% with high-intensity statins [267]. However, statin monotherapy sometimes is not sufficient for certain patients, especially those with homozygous familial hypercholesterolemia (HoFH) [270]. A key feature of patients with HoFH is the severely impaired LDLR activity due to mutations hence they very poorly respond to statins. Therefore, it is recommended to combine statin therapy with additional medications for reducing LDL-cholesterol in HoFH patients.

The two most common combined medicines are PCSK9 inhibitors and ezetimibe. PCSK9 targets LDLR and promotes the lysosomal degradation of LDLR which subsequently increases the LDL-C levels [271]. PCSK9 and LDLR are both transcriptionally upregulated by SREBP2 which is activated by statins. Hence, statin therapy also increases the lysosomal degradation of LDLR triggering by PCSK9, and using PCSK9 inhibitors can further increase hepatic LDLR levels. By combining PCSK9 inhibitors, it can achieve an incremental 50% LDL-cholesterol reduction from statin therapy alone.

The major source of cholesterol is from the *de-novo* cholesterol synthesis in the liver but dietary

cholesterol is also introduced into circulation [266]. Ezetimibe reduces the absorption of dietary cholesterol and reabsorption of hepatically excreted biliary cholesterol from small intestine by blocking the sterol transporter Niemann-Pick C1-like protein 1 (NPC1L1) [272]. Reductions in cholesterol absorption and delivery to the liver trigger the upregulation of hepatic LDLR expression and enhance the LDL-cholesterol clearance from the blood. Thus, ezetimibe is used to treat hypercholesterolemia when patients have an intolerance to statins [273]. The potency of ezetimibe is relatively low compared to statins and PCSK9 inhibitors. Ezetimibe can only reduce LDL-cholesterol by around 13-20% but it is critical to hypercholesteremia patients [272].

Since the efficiencies of statins and PCSK9 inhibitors largely rely on the remaining LDLR activities, medicines regulating LDL-cholesterol through alternative pathways are also applied in HoFH patients [270]. Microsomal triglyceride transfer protein (MTP) inhibitors are a typical type of drug for HoFH patients who have no remaining LDLR activity. MTP inhibitors impair the production of VLDL particles and chylomicrons to reduce circulating LDL-cholesterol levels in the blood [274]. This action is independent of LDLR which helps reduce about half of the LDL-cholesterol levels in HoFH patients [270]. However, the accumulation of lipids in the hepatocytes and enterocytes is the main side effect which leads to liver damages and gastrointestinal symptoms.

1.5 Rationale, Hypothesis and Aim of thesis

LDLR family is a group of multifunctional transmembrane receptors involved in different but important physiological and pathophysiological processes including lipid metabolism [3], bone

homeostasis [275], nervous system development and maintenance [7], cancer progression [276] etc. Metalloproteinases are closely associated with and regulate the LDLR family members through ectodomain shedding [185]. MT1-MMP is a transmembrane matrix metalloproteinase ubiquitously expressed in humans with a prominent role in remodelling the extracellular matrix [186]. It has been reported that MT1-MMP sheds and regulates the cell surface LDLR, LRP1 and LRP4 which subsequently affects the functions involving these LDLR family members [174,176,277]. Due to the structural similarity among the LDLR family members, it is very likely that MT1-MMP also mediates the ectodomain shedding of other LDLR family members. Through investigating the effects of MT1-MMP on the LDLR family, we may reveal how MT1-MMP regulates LDLR family related biological processes and find out new roles of some poorly studied members. We hypothesize that MT1-MMP sheds all LDLR family members.

MT1-MMP has been shown to promote hepatic LDLR shedding, and its deletion can reduce plasma LDL-cholesterol levels [174], suggesting that hepatic MT1-MMP inhibition could be a potential treatment for reducing LDL-cholesterol levels. The gold standard treatment for hypercholesterolemia is statin [267]. However, unfortunately, the maximal effect of high-intensity statins only reduces around 50% of LDL-cholesterol which is not sufficiently in patients with high baseline of LDL-cholesterol [278]. Furthermore, statins have dose-dependent adverse effects including higher risk of developing type 2 diabetes [279]. By using hepatic MT1-MMP inhibition with lower dose of statin as a combined therapy, it is possible to achieve the same LDL-cholesterol lowering effect as high-intensity statin treatment. We propose that MT1-MMP inhibition has an additive effect on lowering LDL-cholesterol levels when combined with the statin treatment.

Taken together, our research aims are:

1. **To investigate the effects of MT1-MMP on the LDLR family members.**

2. **To investigate the possibility of inhibiting MT1-MMP as a combined treatment for statin therapy.**

Chapter 2

Materials and Methods

2.1 Plasmid

2.1.1 Site-directed mutagenesis

Recombinant plasmids carrying genes of interest were applied in cultured cell transfection. Plasmids containing cDNA of different LDLR family members (LRP3: NM_002333, LRP4: NM_002334, LRP5: NM_002335, LRP6: NM_002336, LRP8: NM_017522, LRP 10: NM_014045, LRP11: NM_032832 and LRP12: NM_013437) with a DDK-tag at the C-terminus were purchased from Origene. The plasmid containing cDNA of the full-length human MT1-MMP (NM_004995) with an HA-tag between Asp115 and Glu116 was a kind gift from Dr. Weiss (University of Michigan) and used as the template to generate the mutant forms of MT1-MMP. Plasmids containing domain-deleted MT1-MMP variants (ΔHPX, ΔMT-loop, Δcat, ΔCT) were generated as described previously [201]. The plasmid containing catalytically inactive MT1-MMP mutant (E240A) was generated as described [174]. Mutagenesis was performed using QuikChange Lightning site-directed mutagenesis kit (Agilent Technologies) following the manufacturer's instruction. The presence of the desired mutation and the integrity of cDNA were confirmed by DNA sequencing.

2.1.2 Transformation

Two ng of each plasmid was transformed into 50 μL of DH5-α competent cells using the heat shock method. Briefly, the plasmid / DH5-α mixture was first incubated on ice for 30 minutes, followed by a 45-second heat shock in a 42 ℃ water bath and returned on ice. Transformed cells were then recovered in prewarmed 0.5 ml NZY+ broth (Fisher BioReagents) at 37 ℃ with shaking at 225 rpm for 1 hour. After, recovered cells were plated on lysogeny broth (LB) agar

supplemented with appropriate antibiotics (ampicillin or kanamycin) allowing for an overnight growth in a moist 37 ℃ incubator for selection.

2.1.3 Amplification and purification

Successfully transformed DH5-α cells were first grown in 3 mL LB broth supplemented with appropriate antibiotics (100 μg/mL of ampicillin or 50 μg/mL of kanamycin) at 37 ℃ with shaking at 225 rpm for 8 hours. After, enriched bacteria suspension was inoculated (1:1,000, v/v) into a large-scale (50 mL or 250 mL) LB broth supplemented with appropriate antibiotics and grew at the same conditions overnight. For cell harvest, LB culture with enriched bacterial cells was centrifuged at 4,000 x g for 10 minutes at room temperature. Cell pellets collected after centrifugation were then subjected to plasmid DNA extraction and purification using either GeneJET Plasmid Midiprep Kit (Thermo Scientific) or PureLink™ HiPure Plasmid Maxiprep Kit (Invitrogen) according to the manufacturer's instructions. Purified plasmid DNA was measured using the Nanodrop spectrophotometer (Nanoview Plus, GE) and stored at -80 ℃ until further use.

2.2 Cell Culture

2.2.1 Cultured cell lines and conditions

Huh7 (Human hepatocellular carcinoma cell line) and HepG2 (human hepatoblastoma cell line) cells were applied in the study. All cell culture experiments were carried out under aseptic conditions in class II, type A2 biosafety cabinets. Both cell lines were cultured and maintained in DMEM–high glucose (Sigma, cat# D6429) supplemented with 10% (v/v) FBS (Sigma, cat#

F1051) at 37 ℃ in a humidified incubator with a constant 5% CO_2 supply. Cryopreserved cells in a standard freezing medium (10% DMSO and 10% FBS in DMEM, v/v) and stored in liquid nitrogen were thawed and cultured in 10 mL DMEM + 10% FBS in a 100 mm culture dish. The growth medium was changed every 2-3 days and cells were passaged once they reached an 80-90% confluence observed under an inverted microscope. Cells with passage number under 25 were applied to experiments. For cell passaging, briefly, cultured cells were washed with PBS and dissociated by adding 1 mL 0.05% trypsin (Cytiva). Trypsinization was stopped by adding 10 mL DMEM + 10% FBS, and cells were resuspended. For HepG2 cells, during resuspension, additional cell resuspension by pipetting through a p200 tip attached to a 10 mL serological pipette was required for sufficient cell dissociation. Suspended cells were then counted and subjected to experimental seeding or new culture dishes with fresh medium for continuous maintenance. For experiments, Huh7 cells were seeded at a density of 1.5×10^5 cells/mL for 1 mL in each well of a 12-well plate or seeded at a density of 2×10^5 cells/mL for 2 mL in each well of a 6-well plate. HepG2 cells were seeded at a density of 2×10^5 cells/mL for 1 mL in each well of a 12-well plate or seeded at a density of 2.5×10^5 cells/mL for 2 mL in each well of a 6-well plate.

2.2.2 Transfection

2.2.2.1 Polyethylenimine (PEI) Transfection

Huh7 cells were transiently transfected 24 hours after seeding. 1.2 μg or 2.5 μg of total plasmid DNA was transfected into Huh7 cells cultured in each well of 12-well plates or 6-well plates, respectively. 1.2 μg or 2.5 μg of plasmid DNA was diluted in 50 μL or 125 μL of

Gibco™ Opti-MEM™ I reduced serum medium (Life Technologies), respectively. Polyethylenimine (PEI, 25 kDa branched), with a ratio of 1:3 (DNA:PEI, w/w), was diluted in the same amount of Opti-MEM™ I reduced serum medium as plasmid DNA. Diluted total plasmid DNA and diluted PEI were then mixed by pipetting and incubated for 15 minutes at room temperature. After incubation, plasmid DNA/PEI mixture in Opti-MEM™ I reduced serum medium was added drop by drop to cells followed by gentle mixing. 4 hours after culturing with plasmid DNA/PEI mixture, the culture medium was replaced by fresh 10 mL DMEM + 10% FBS.

2.2.2.2 RNAiMAX Transfection

HepG2 cells were transiently transfected by siRNA (synthesized by IDT) using Lipofectamin™ RNAiMAX Transfection Reagent (Invitrogen). 2 μL of 10 μM siRNA dissolved in Nuclease-Free Duplex Buffer (IDT) was diluted in 125 μL of Gibco™ Opti-MEM™ I reduced serum medium. 7 μL RNAiMAX was also diluted in 125 μL of Opti-MEM™ I reduced serum medium. Diluted siRNA and RNAiMAX were then mixed by pipetting and incubated for 15 minutes at room temperature. After incubation, HepG2 cells were seeded on the siRNA/RNAiMAX mixture as a standard reverse transfection followed by gentle mixing.

Negative control DsiRNA: IDT, cat# 51-01-14

MMP14 DsiRNA: 5′-UCUGGCUAAAAGGAAUCUAAUCUTG-3′; 5′-CAAGAUUAGAUUCCUUUUAGCCAGAAA -3′

2.2.3 Compounds treatment

2.2.3.1 MG132 and chloroquine

48 hours after transfection, 1 μL of 10 mM proteasome inhibitor MG132 (Sigma) dissolved in DMSO or 1 μL of 10 mM lysosome inhibitor chloroquine (Sigma) dissolved in water was added to 1 mL culture medium in each well of 12-well plates with gentle mixing to generate a final concentration of 10 μM of each compound. After an 8-hour incubation in the same cultured condition, cells were collected and then subjected to further processes.

2.2.3.2 DAPT

32 hours after transfection, 2 μL of 10 mM a γ-secretase inhibitor, DAPT (Sigma), dissolved in DMSO was added to 2 mL culture medium in each well of 6-well plates with gentle mixing to generate a final concentration of 10 μM. After a 16-hour incubation in the same cultured condition, cells were collected and then subjected to further processes.

2.2.3.2 Lovastatin

Different concentrations of lovastatin (Acros Organics) stock dissolved in DMSO were prepared freshly through a serial dilution from a 100 mM lovastatin suspension. 24 hours after cell seeding, 2 μL of 1,000X lovastatin stock dissolved in DMSO and 2 μL of 5 mg/mL mevalonate aqueous solution were added to 2 mL culture medium in each well of 6-well plates with gentle and sufficient mixing. After an additional 24-hour incubation in the same cultured condition, cells were collected and then subjected to further processes.

2.3 Animal

2.3.1 Ethics and animal care

All animal studies were conducted in accordance with the Canadian Council on Animal Care Guidelines and Policies with approval from the Animal Care and Use Committee: (Biosciences, Health Sciences or Livestock) for the University of Alberta.

Mmp14^{Flox} and *Mmp14*^{LKO} mice in C57BL/6J backgrounds were applied in this study and generated as described before [174]. Briefly, the Cre-*lox* system was used to delete the mouse *Mmp14* gene. Homozygous *cre* transgenic Alb-cre mice (The Jackson Laboratory) were mated and bred to *Mmp14*^{Flox} mice to generate conditional hepatocyte-specific MT1-MMP knockout (*Mmp14*^{LKO}) mice.

All mice were housed and bred in the Health Sciences Laboratory Animal Services at the University of Alberta. Mice were housed in a number of 1 to 5 per cage with a climate-controlled environment and a 12-hour light/dark cycle. Mice were allowed to access water and diet *ad libitum*. Mice were fed a regular chow diet containing 20% protein and 4.5% fat (LabDiet, 5053).

2.3.2 Lovastatin administration

Lovastatin administration was achieved by adding lovastatin (Acros Organics) powder to a powered diet and feeding mice *ad libitum*.

Mmp14^{Flox} and *Mmp14*^{LKO} mice were fed a powdered western-type diet containing 0.15% cholesterol, 20% protein, 21% fat and 50% carbohydrate (Research Diets, D12079B) for 10

days. After, mice were fed the same powdered western-type diet supplemented with or without 0.2% (w/w) lovastatin for additional 10 days. Blood was collected before and after the special 10-day feeding. Plasma was separated by centrifugation at 2,000 x g for 20 minutes at 4 ℃. Tissues were collected from euthanized mice at the endpoint. All plasma and tissues were stored at -80 ℃.

2.4 mRNA quantification

2.4.1 Total RNA isolation

Total RNA was extracted from cultured cells using PureLink^{TM} RNA Mini Kit (Invitrogen) according to the manufacturer's instructions. Briefly, cells in each well were lysed in 300 μL of lysis buffer supplemented with 1% β-mercaptoethanol and passing through a 21-G needle 5 times. The same amount of 70% ethanol was then added. The mixture was transfer to a spin cartridge to collect total RNA. Solvent and impurities were eluted by centrifugation at 12,000 x g for 30 seconds. The column was then washed with Wash Buffer I and Wash Buffer II. After, bound RNA was eluted using 30 μL of Nuclease-Free water and quantified using the NanoDrop spectrophotometer (Nanoview Plus, GE). RNA was stored at -80 ℃. All buffers were included in the RNA isolation kit.

2.4.2 cDNA synthesis

cDNA was synthesized from the total RNA extracted from either cultured cells or animal tissues using the High-Capacity cDNA Reverse Transcription Kit (Life Technologies) according to the manufacturer's instructions. 2 μg of total RNA dissolved in Nuclease-Free

water was mixed with 2 μL 10X RT Buffer, 2 μL 10X RT Random Primers, 0.8 μL 25X dNTP Mix and 1 μL MultiScribe™ Reverse Transcriptase and topped up to 20 μL by adding Nuclease-Free water. All reagents were provided in the kit. The polymerase chain reaction was carried out with a thermal cycler (C1000, BioRad) under the following condition: 25 ℃ for 10 min, 37 ℃ for 120 min, and 85 ℃ for 5 min. cDNA products were stored at -20 ℃.

2.4.3 Real-time qRT-PCR

Quantitative real-time reverse transcription PCR (qRT-PCR) was performed to quantify the mRNA levels of targeted genes on a StepOnePlus™ Real-Time PCR System (Life Technologies) using SYBR® Green PCR Master Mix (Life Technologies). The standard curve was generated by using cDNA samples from pooling the control groups with a dilution series: 3.9X, 15.6X, 62.5X and 250X. All cDNA samples were diluted by a factor of 100:7. Reaction mixture was prepared by mixing the following components: 2X SYBR® Green PCR Master Mix (10 μL), forward primer (2 μL of 10 μM stock), reverse primer (2 μL of 10 μM stock), ddH_2O (4 μL) and diluted cDNA standards or samples (2 μL). The polymerase chain reaction was carried out under the following condition: 95℃ for 120 seconds, 40 cycles of 95 ℃ for 15 seconds and 60 ℃ for 60 seconds. A melting curve analysis was also carried out for the quantitative identification of PCR products. Primers for human *GAPDH*, *MMP14, SREBP2,* and *LDLR* were designed by PrimerQuest Real-Time PCR Design Tool and synthesized by IDT, Inc..

Primers:

Human

GAPDH-Forward: 5′-GGTGTGAACCATGAGAAGTATGA-3′

GAPDH-Reverse: 5′-GAGTCCTTCCACGATACCAAAG-3′

MMP14-Forward: 5′-TGCCTACCGACAAGATTGATG-3′

MMP14-Reverse: 5′-ATCCCTTCCCAGACTTTGATG-3′

SREBP2-Forward: 5′-TTCCTGTGCCTCTCCTTTAAC-3′

SREBP2-Reverse: 5′-TCATCCAGTCAAACCAGCC-3′

LDLR-Forward: 5′-TTCACTCCATCTCAAGCATCG-3′

LDLR-Reverse: 5′-ACTGAAAATGGCTTCGTTGATG-3′

2.5 Protein quantification

2.5.1 Protein extraction from cultured cells

2.5.1.1 Whole-cell lysate

Cultured cells were scraped and resuspended in PBS. Cells were then pelleted by centrifugation at 7,000 rpm for 7 minutes at 4 ℃. The cell pellets were lysed in lysis buffer (1% Triton X-100, 150 mM NaCl, and 50 mM Tris-HCl at pH 7.4) supplemented with cOmplete^{TM}, EDTA-free protease inhibitor cocktail (Roche) for 30 minutes on ice and vortexed intermittently every 10 minutes. Cell debris was removed by centrifuging at 14,000 rpm for 10 minutes at 4 ℃. The supernatant was collected as the whole-cell lysate and stored at -80 ℃.

2.5.1.1 Cytosol and membrane fractions

Cultured cells were scraped and resuspended in PBS. Cells were then pelleted by centrifugation

at 7000 rpm for 7 minutes at 4 ℃. The cell pellets were resuspended in a non-detergent lysis buffer (150 mM NaCl, 50 mM Tris-HCl and at pH 7.4) supplemented with cOmplete™, EDTA-free protease inhibitor cocktail (Roche) and lyzed by passing through a 27-G needle syringe 15 times and incubated on ice for 20 minutes. After, homogenized samples were centrifugated at 1,000 x g for 10 minutes at 4 ℃ to remove unbroken cells and cell debris. The supernatant was collected and centrifugated at 20,000 x g for 20 minutes at 4 ℃ to separate the cytosol fraction (supernatant) and membrane fraction (pellet). Membrane fraction pellets were washed twice by resuspending in the same volume of ddH_2O and spinning at 20,000 x g for 20 minutes at 4 ℃. Washed pellets were then lyzed in an appropriate amount of lysis buffer (1% Triton X-100, 150 mM NaCl and 50 mM Tris-HCl at pH 7.4).

2.5.2 Protein extraction from animal tissues

100 mg of mouse tissue sample was first washed in 1 mL of ice-cold PBS and centrifugated at 2500 rpm for 5 minutes at 4 ℃ to remove soluble impurities. Washed tissue was homogenized sufficiently in 1 mL of RIPA buffer (1% NP-40, 1% sodium deoxycholate, 0.1% SDS, 150 mM NaCl and 25 mM Tris-HCl at pH 8.0) supplemented with cOmplete™, EDTA-free protease inhibitor cocktail (Roche) by using a Power Gen 500 Homogenizer (Fisher Scientific). Homogenized tissue was then incubated on ice for 30 min with intermittent vortex every 10 min. After, the sample was centrifugated at 20,000 x g for 15 minutes at 4 ℃ and the supernatant was collected as tissue lysate and stored at -80 ℃.

2.5.3 Protein quantification

Protein concentrations of whole-cell lysate, cytosol fraction, membrane fraction and tissue lysate were determined using a bicinchoninic acid assay (BCA) with Pierce™ BCA Protein Assay Reagent A and B (Thermo Scientific). Basically, reagents A and B were mixed at a ratio of 50:1 to generate a working solution. A series of different concentrations of bovine serum albumin (BSA) solution were prepared as standards. 4 μL of standards or samples was added to a 96-well plate, followed by the addition of 200 μL of the working solution. Sample mixtures were incubated at 37 ℃ for 30 minutes. Absorbance was read at 562 nm using a SPECTRAmax™ 250 Microplate Spectrophotometer (Molecular Devices).

2.5.4 Immunoprecipitation

Whole-cell lysate with the same amount of total proteins (~500 μg) was incubated with 2 μL of mouse anti-HA antibody (Proteintech) or mouse anti-DDK antibody (OriGene) for 2 hours with rotating at 4 °C. After, 25 μL of prewashed 50% slurry Protein G Sepharose™ 4 Fast Flow (GE Healthcare) was added to the mixture for incubation overnight with rotating at 4 °C. The immunoprecipitated proteins on the protein G beads were washed three times in lysis buffer and then eluted by adding 2X Laemmli sample buffer with a 5-minute heating at 85 °C. Eluted immunoprecipitated proteins were stored at -20 °C.

2.5.5 Immunoblotting

The same amount of whole-cell or tissue lysate was subject to SDS-PAGE and immunoblotting. Samples were prepared by adding 4X Laemmli sample buffer (0.2 M Tris-HCl at pH 6.8, 8%

SDS, 40% glycerol, 0.08% bromophenol blue and 4% β-mercaptoethanol) to lysate, followed by a 5-minute heating at 85 °C for sufficient protein denaturation. Proteins in samples were then separated by appropriate percentage of SDS-PAGE under the following running conditions: constant 80 V for 30 minutes followed by a constant 120 V till the elution of tracking dye in running buffer (25 mM Tris, 192 mM glycine and 0.1% SDS). Separated proteins in acrylamide gels were then transferred to 0.2 μm nitrocellulose membranes (Cytiva) using a wet tank transfer system under the following conditions: constant 0.4 A for 90 minutes in transfer buffer (25 mM Tris-HCl and 192 mM glycine). After transfer, membranes were blocked in 5% skimmed milk in PBST (0.2% Tween-20 in PBS) for 30 minutes at room temperature. Membranes were then incubated with appropriate antibodies in PBST with 0.2% sodium azide overnight with gentle shaking at 4 °C. Following antibodies were applied in this study: rabbit anti-DDK (OriGene), rabbit anti-MT1-MMP (Abcam), mouse anti-TFR (BD Bioscience), Rabbit anti-HA Dylight^{TM} 800 conjugated (Rockland), mouse anti-HA (Proteintech), rabbit anti-ubiquitin (Proteintech), rabbit anti-Na^+/K^+-ATPase, mouse anti-GAPDH, mouse anti-DDK (Proteintech), rabbit anti-LDLR (Abcam) and rabbit anti-mouse LDLR. Secondary antibodies (IRDye®680 or IRDye®800-labeled goat anti-mouse or anti-rabbit IgG, Li-Cor) were used for signal detection. Membranes were incubated in 1:20,000 diluted secondary antibodies in PBST for 30 minutes at room temperature. During each step of blocking, primary antibody binding and secondary antibody binding, membranes were washed 3 times in 1x PBST for 5 minutes at room temperature. Signals on membranes were detected and quantified using an Odyssey Infrared Imaging System (Li-Cor).

2.6 Immunofluorescence

Huh7 cells were seeded on coverslips inserted into 12-well plates otherwise all the procedures and treatments were applied the same way as described above. At the endpoint of cultured cell treatments, cells were fixed in ice-cold 3% (w/v) paraformaldehyde in PBS for 5 minutes and permeabilized in methanol for 10 minutes at -20 °C. Cells were then blocked with 1% (w/v) bovine serum albumin (BSA) in PBS for 30 minutes at room temperature and incubated with rabbit anti-DDK (OriGene) and mouse anti-HA (Proteintech) antibodies in 1% (w/v) BSA in PBS overnight at 4 °C. Secondary Alexa Fluor 488-labeled goat anti-rabbit IgG (R&D Systems) and Alexa Fluor 568-labeled goat anti-mouse IgG (R&D Systems) antibodies were used for signal detection. Cell nuclei were stained with 4′,6-diamidino-2-phenylindole (DAPI). After mounting, cells were viewed and imaged by a Leica SP-5 laser scanning microscope (wavelengths used for excitation and emission, DAPI *ex*: 351 or 364 nm / *em*: 465 nm, Alexa Fluor 488 *ex*: 488 nm / *em*: 519 nm, and Alexa Fluor 568 *ex*: 543 nm / *em*: 603 nm).

2.7 Plasma clinical chemistry

2.7.1 Collection and preparation

Mouse blood was collected using heparinized micro-hematocrit capillary tubes (Fisher) or MiniCollect K3E K3EDTA (Greiner Bio-One) tubes, and then subjected to centrifugation at 2,000 x g for 20 minutes at 4 °C to isolate plasma. Plasma was then collected and stored at -80 °C.

2.7.2 Measurement of alanine transaminase (ALT)

Plasma alanine transaminase (ALT) was measured using Alanine Transaminase Colorimetric Activity Assay Kit (Cayman Chemical) according to the manufacturer's instructions. Briefly, 20 µL of positive control or plasma samples were added into a 96-well plate in technical triplicates. Next, 150 µL of Substrate and 20 µL of Cofactor were added and then incubated for 15 minutes at 37 °C. 20 µL of ALT Initiator was quickly added into each using a multi-channel pipette. The plate was then immediately measured for absorbance on a SPECTRAmax^{TM} 250 Microplate Spectrophotometer (Molecular Devices). Kinetic measurement was performed for reading under the following setting: 37 °C, 340 nm and 10 minutes with intermittent reading for every 1 min. The maximum linear reaction rate was taken and used to calculate the ALT activity from the following formula:

$$\text{ALT activity (U/mL)} = \left[\frac{\Delta A_{340}/\text{min} \times 0.21\ \text{mL}}{4.11\ \text{mM}^{-1} \times 0.02\ \text{mL}}\right] \times \text{Sample dilution}$$

Otherwise, ALT was measured using Micro Alanine Aminotransferase (ALT/GPT) Activity Assay Kit (Abbkine) according to the manufacturer's instructions. Briefly, ALT standards were prepared (0, 0.05, 0.1 0.2, 0.4, 0.8, 1 and 1.5 µmol/mL) by dilute the provided Standard in ddH_2O. In 96-well plate, 25 µL of Reagent I was first added for standard wells, test wells and control wells. Standards and plasma samples were mixed with Reagent I in standard wells and test wells and incubated at 37 °C for 30 minutes. Then, 25 µL of Reagent II was added to all wells followed by 5 µL of plasma samples to control wells. Plate was mixed and incubated at 37 °C for 20 minutes. Reagent III was then mixed to all wells and left at room temperature for 10 minutes. Plate was then read at 505 nm, the absorption differences were calculated from test

wells and control wells. ALT concentrations were then generated according to the standard curve.

2.8 Statistical analysis

All statistical analyses were conducted using GraphPad Prism 10 (Dotmatics). Significant differences between groups were assessed by Student's *t*-test or one-way ANOVA or two-way ANOVA followed by Tukey-Kramer or Dunnett multiple comparisons tests where appropriate. Values of all data were presented as mean ± S. D.. The significance was set as ns = not significant $p > 0.05$; * $p < 0.05$; ** $p < 0.01$; *** $p < 0.001$; **** $p < 0.0001$. Number of animals and replicates for each experiment are indicated in the figure legends. All experiments were repeated at least three times except where indicated.

Chapter 3

MT1-MMP-mediated degradation of LDLR family

3.1 Introduction

The low-density lipoprotein receptor (LDLR) family is a group of receptors sharing conserved domains and structural homologies with the founding member – LDLR. So far, a total of 13 proteins have been classified in the human LDLR family [280]. There are LDLR, low-density lipoprotein receptor related protein 1 (LRP1), LRP1B, LRP2, LRP3, LRP4, LRP5, LRP6, LRP8, LRP10, LRP11, LRP12, and very low-density lipoprotein receptor (VLDLR). LDLR family members can be found in almost all tissues throughout the body [64]. The intuitive role of the LDLR family is their ability to mediate lipoprotein metabolism as the cell surface receptors for different lipoprotein particles [281]. Hepatic LDLR and LRP1 are responsible for the clearance of most circulating lipoprotein particles in the blood [37]. Meanwhile, more than half of the LDLR family members have shown affinities to apolipoprotein E (apoE) which can be found in triglyceride- and cholesterol-rich lipoproteins including chylomicron remnants, VLDL, intermediate-density lipoproteins, and some HDL [132,282-284]. The presence of apoE in lipoprotein particles can promote the clearance of lipoprotein particles from the blood by receptor-mediated endocytosis [285].

In fact, the LDLR family is not only important for lipoprotein metabolism but also for other physiological and pathophysiological processes. LRP2 is abundantly expressed in absorptive epithelial cells such as in renal tubules functioning as an endocytic receptor for protein reabsorption of filtered proteins [56]. LRP4 is the co-receptor involved in the signaling pathway essential for normal neuromuscular junction formation and maintenance [84]. LRP5 and LRP6 are the famous two co-receptors of Wnt ligands and activate the canonical Wnt/β-catenin

signaling which controls cell proliferation and is frequently overactivated in human cancers [107,286]. In addition, LRP5 and LRP6 are the determinants for bone mineral density whose mutations are frequently observed in patients with abnormal bone mass [275,287,288]. In the development of the central nervous system, LRP8- and VLDLR-mediated Reelin signaling pathway is critical for proper neuron migration [289]. Moreover, the LDLR family members more or less contribute to the development and progression of cancer [276,290]. There are a few recently discovered members (i.e. LRP3, LRP10, LRP11 and LRP12) of the LDLR family whose functions have not yet been well clarified [9,69,132,152].

Membrane type 1-matrix metalloproteinase (MT1-MMP) is a type I transmembrane endopeptidase belonging to the family of matrix metalloproteinases (MMPs) [186]. The predominant role of MT1-MMP is its proteolytic activity in remodelling the extracellular matrix [291]. MT1-MMP is ubiquitously expressed in a variety of tissues along with its importance in embryogenesis and angiogenesis [210,292]. It is also not surprising that elevated MT1-MMP levels are frequently observed in tumors which facilitates tumor growth, invasion and metastasis through shaping the tumor microenvironment [293,294]. Hence, MT1-MMP has attracted a lot of research interest in areas of tissue remodelling and cancer progression [229,295].

The cell surface proteolytic activity of MT1-MMP makes it as a potent sheddase to cleave a broad spectrum of transmembrane proteins [296,297]. Recently, it was reported that MT1-MMP mediates hepatic LDLR shedding and subsequentially increases the plasma LDL-cholesterol levels [174]. Due to the structural similarities among LDLR family members and the biological importance of them, it is necessary to investigate if MT1-MMP also sheds the other LDLR members. In this study, we found that MT1-MMP is able to mediate the degradation of all

LDLR family members we tested. This work will provide fresh insight into the cellular regulation of LDLR family-related physiological and pathophysiological processes.

3.2 Results

3.2.1 MT1-MMP regulates the mature LDLR family members

MT1-MMP was found to be able to mediate the degradation of LDLR and LRP1 [174,176]. To assess the regulation role of MT1-MMP on the other LDLR family members, we used an in vitro method of transient transfection of both MT1-MMP and each of the LDLR family members in cultured Huh7 cells. Due to the reason that LDLR and LRP1 are both proteolytically cleaved by MT1-MMP [174,176], besides the wild-type MT1-MMP, a plasmid containing catalytically inactive MT1-MMP mutant E240A was also transfected. As shown in **Fig. 3.1**, we tested 8 members of the LDLR family, LRP3, LRP8, LRP11, LRP4, LRP5, LRP6, LRP10 and LRP12. All LDLR members that had a C-terminal DDK tag were detected in two forms with different molecular masses except for LRP10 (**Fig. 3.1A**, **3.1C** and **3.1E**). The upper band (indicated by "*") was the mature fully glycosylated forms of each LDLR family member, and the lower bands (indicated by "#") were their immature under glycosylated forms [15,298]. Overexpression of wild-type MT1-MMP reduced the levels of the mature form of each LDLR family member but not their immature forms. The catalytically inactive MT1-MMP-E240A did not cause a dramatic degradation of LDLR family members as wild-type MT1-MMP (**Fig. 3.1**). Unlike other LDLR family members, LRP10 was the only member detected as only one major band. Interestingly, the level of LRP10 was also reduced by both wild-type MT1-MMP and catalytically inactive MT1-MMP-E240A to the same degree at about a 50% reduction (**Fig. 3.1E** and **3.1F**).

An additional interesting result was the appearance of the C-terminal fragments (CTF) of two

LDLR family members under the overexpression of wild-type MT1-MMP (**Fig. 3.1A**). MT1-MMP-medicated LRP3 degradation resulted in two CTFs with a different molecular mass at around 75 kDa. These two bands were also observed in cells expressing LRP3 only or LRP3 with MT1-MMP-E240A, but at a much lower degree, probably due to endogenous MT1-MMP in Huh7 cells as shown in our previous study [174]. MT1-MMP-induced degradation of LRP11 also generated a ~40 kDa CTF. Degraded forms of LRP8 were also observed in **Fig. 3.1A** with the overexpression of wild-type MT1-MMP. Unlike CTFs of LRP3 and LRP11, degraded LRP8 was shown as a smeared trailing band which indicated that LRP8 was not degraded at certain specific sites by MT1-MMP. Overall, overexpression of wild-type MT1-MMP induces degradation of all mature LDLR family members tested. The catalytic activity of MT1-MMP is required for its full actions on degrading these proteins except for LRP10.

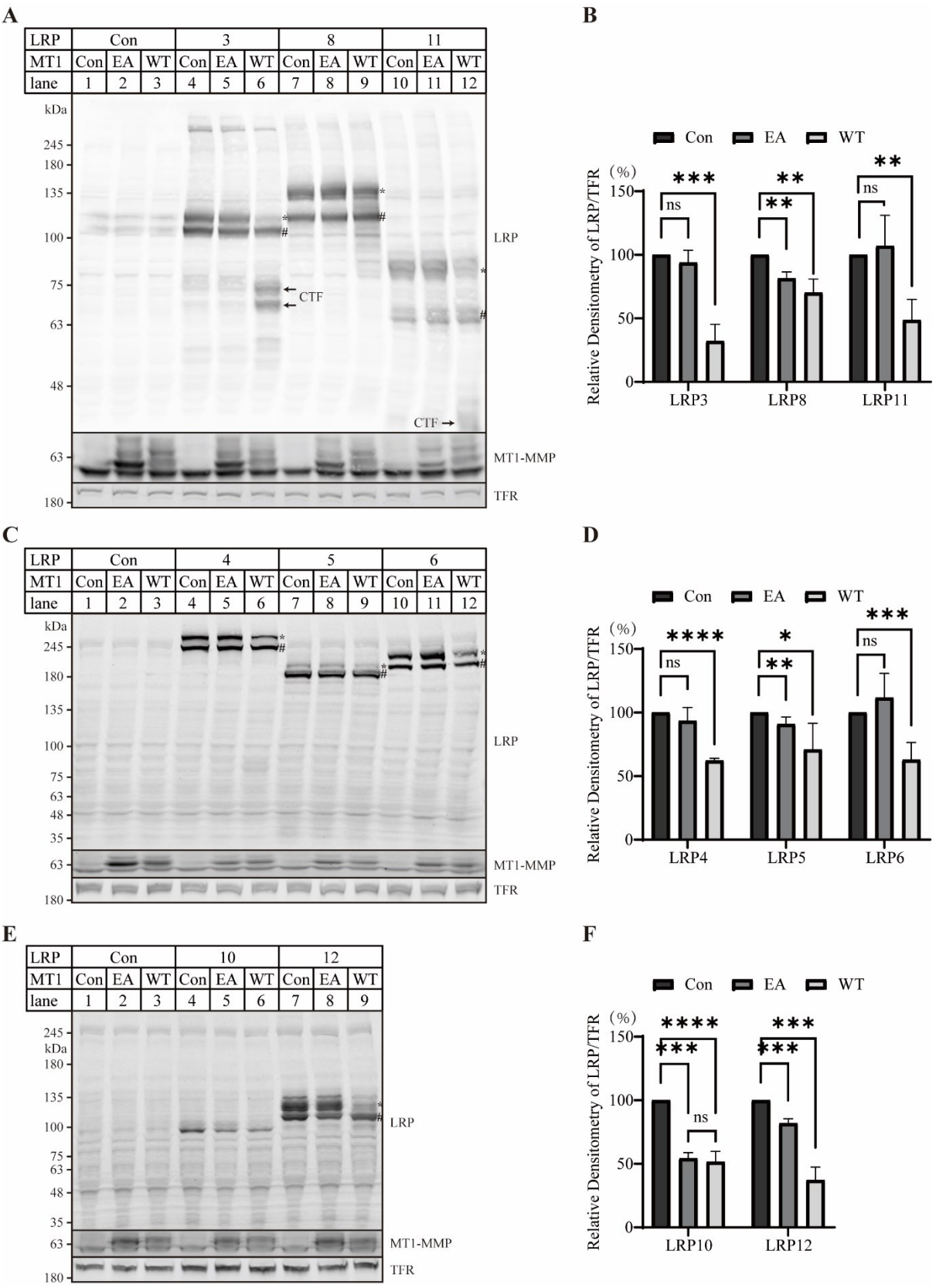
A
LRP
MT1
lane
Con
EA
WT
3
8
11
kDa
245
180
135
100
75
63
48
35
CTF
LRP
MT1-MMP
TFR
B
Con
EA
WT
Relative Densitometry of LRP/TFR
(%)
150
100
50
0
ns
***
**
LRP3
LRP8
LRP11
C
4
5
6
D
****
*
LRP4
LRP5
LRP6
E
10
12
F
LRP10
LRP12

Figure 3. 1. The effects of MT1-MMP on the LDLR family members. (**A** to **B**) **Immunoblotting and quantification of LRP3, LRP8 and LRP11 (n=3).** (**C** to **D**) **Immunoblotting and quantification of LRP4, LRP5 and LRP6 (n=5).** (**E** and **F**) **Immunoblotting and quantification of LRP10 and LRP12 (n=3).** Huh7 cells were transfected with an empty vector (**Con**), or a C-terminal DDK-tagged LRP plasmid with an empty vector, a HA-tagged catalytically inactive MT1-MMP (**EA**), or HA-tagged wild-type MT1-MMP (**WT**) as indicated for 48 hours. The same amount of whole-cell lysate was then subjected to immunoblotting. The entire membrane was first detected with a rabbit anti-DDK (OriGene) antibody, and then stripped and detected with a rabbit anti-MT1-MMP (Abcam) and a mouse anti-TFR (BD Biosciences) antibody. Representative images were shown. *, the mature form of LRP; #, immature form. CTF, the C-terminal fragment of LRP. For quantifications, the relative densitometry was the ratio of the densitometry of each LRP to TFR in the same condition. For each replicate, the percentage of relative densitometries of each LPR was normalized to the control empty vector transfection that was defined as 100%. Values of all data were mean with S. D.. Student's *t*-test was used to analyze and determine the statistical significance between groups. For LRP10 only, one way ANOVA followed by multiple comparison was applied. $n \geq 3$ for each condition; ns = not significant; *, $p < 0.05$; **, $p < 0.01$; ***, $p < 0.001$; ****, $p < 0.0001$.

3.2.2 Importance of individual MT1-MMP regions in LDLR family degradation

MT1-MMP consists of different functional domains. To investigate the mechanism of MT1-MMP-induced degradation in each LRP, we first assessed the effect of each MT1-MMP functional domain on its action on LRPs. Four different regions were selected given their essential and distinct roles in MT1-MMP functions [200,299,300]. Plasmids containing wild-type or mutant MT1-MMP, in which each functional domain was deleted as described in our previous study [201], were co-expressed with each LDLR family member in Huh7 cells (**Fig. 3.2**). Deletion of the hemopexin-like domain (ΔHPX) or the C-terminal cytoplasmic tail (ΔCT) did not significantly abolish MT1-MMP-mediated degradation of any LDLR family members tested. Removing the MT-loop (ΔLoop) in the catalytic domain resulted in a mild but not significant increase of most LDLR family members compared to wild-type MT1-MMP. In the case of LRP12, MT-loop deletion greatly impaired the LRP12 degradation by doubling the remaining mature LRP12 level (**Fig. 3.2O** and **3.2P**). The loss of the entire catalytic domain (ΔCAT) restrained MT1-MMP and increased the mature proteins of LRPs compared to wild-type MT1-MMP, as observed in our previous experiment with the catalytically inactive E240A mutant of MT1-MMP. Among all the LDLR family members, LRP10 still displayed its uniqueness that no matter which regions were removed from MT1-MMP the degradations of LRP10 were unstoppable (**Fig 3.2M** and **3.2N**). For LRP12 although ΔLoop and ΔCAT rescued a certain degree of degradation, at least half of mature LRP12 was lost. As summarised in **Fig 3.2Q**, except for LRP10, the catalytic inactivation E240A almost terminated the degradation in the LDLR family, followed by the catalytic domain-deleted MT1-MMP which also greatly impacted the degradation and the MT-loop-removed mutant which only slightly rescued the

degraded LDLR family members. ΔHPX and ΔCT were not required for the degradations of LDLR family members.

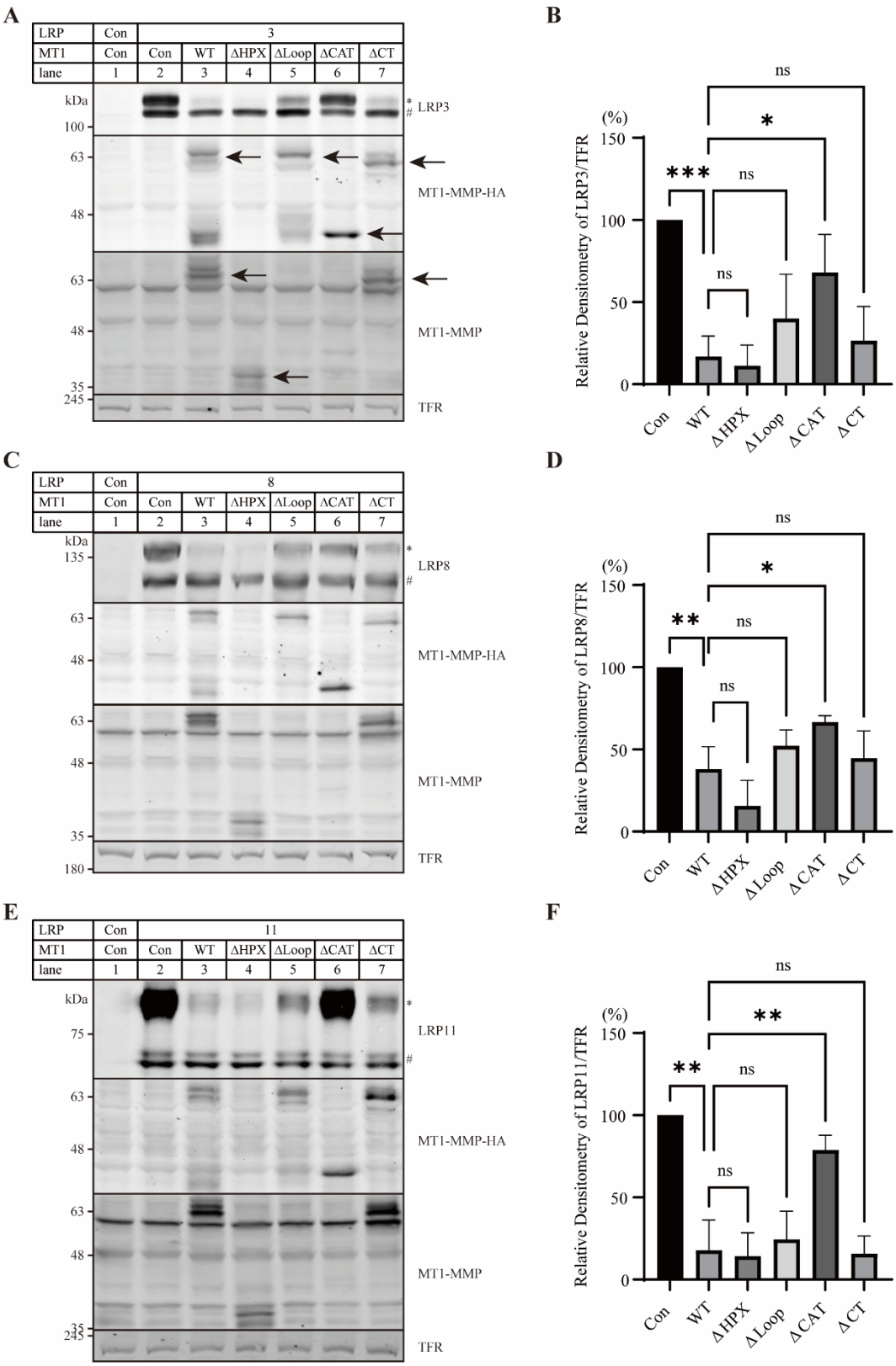
A
LRP
MT1
lane
Con
WT
ΔHPX
ΔLoop
ΔCAT
ΔCT
kDa
LRP3
MT1-MMP-HA
MT1-MMP
TFR
B
Relative Densitometry of LRP3/TFR
(%)
ns
*
***
C
LRP8
D
Relative Densitometry of LRP8/TFR
**
E
LRP11
F
Relative Densitometry of LRP11/TFR

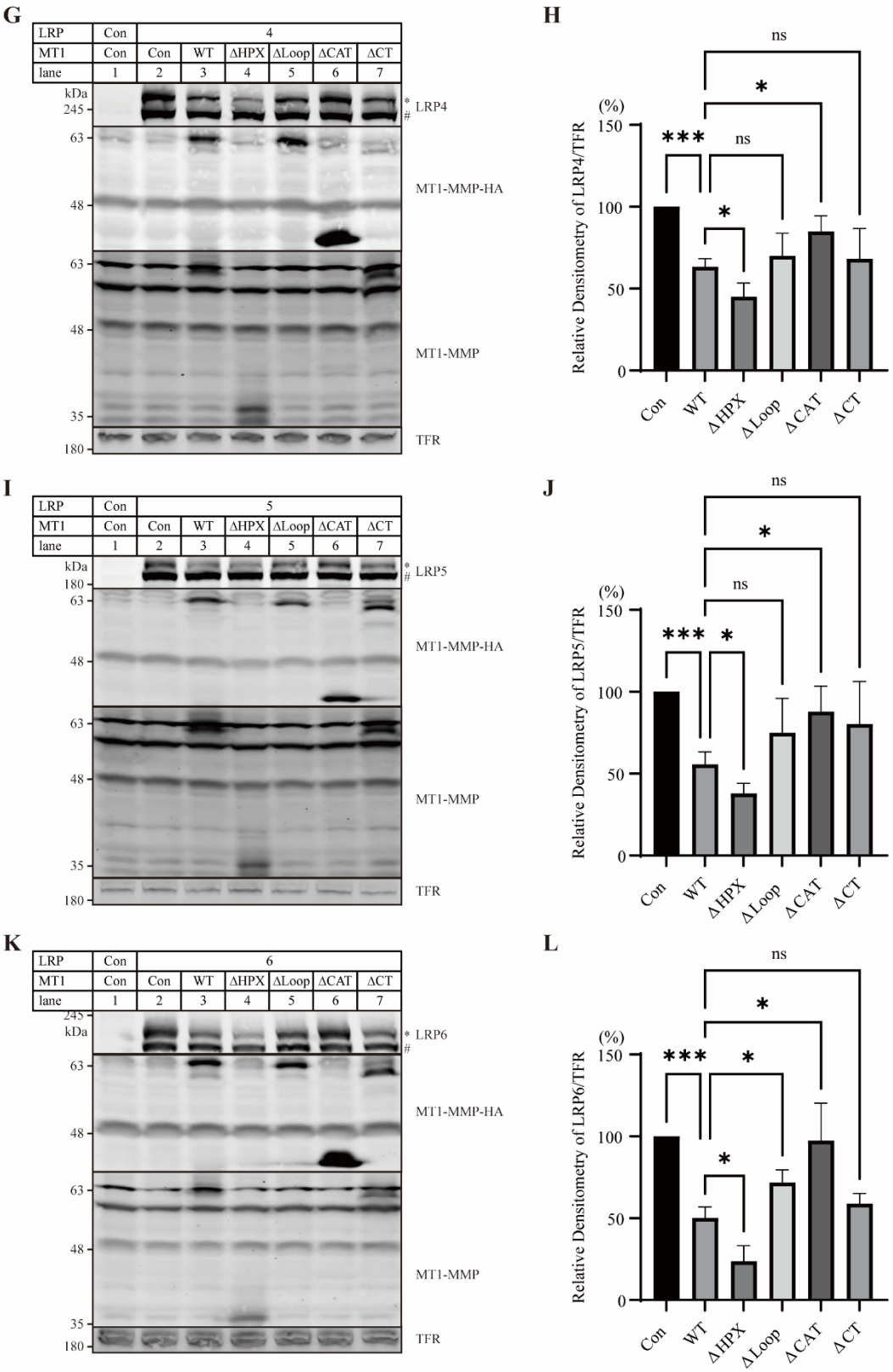

Figure 3. 2. (Continued)

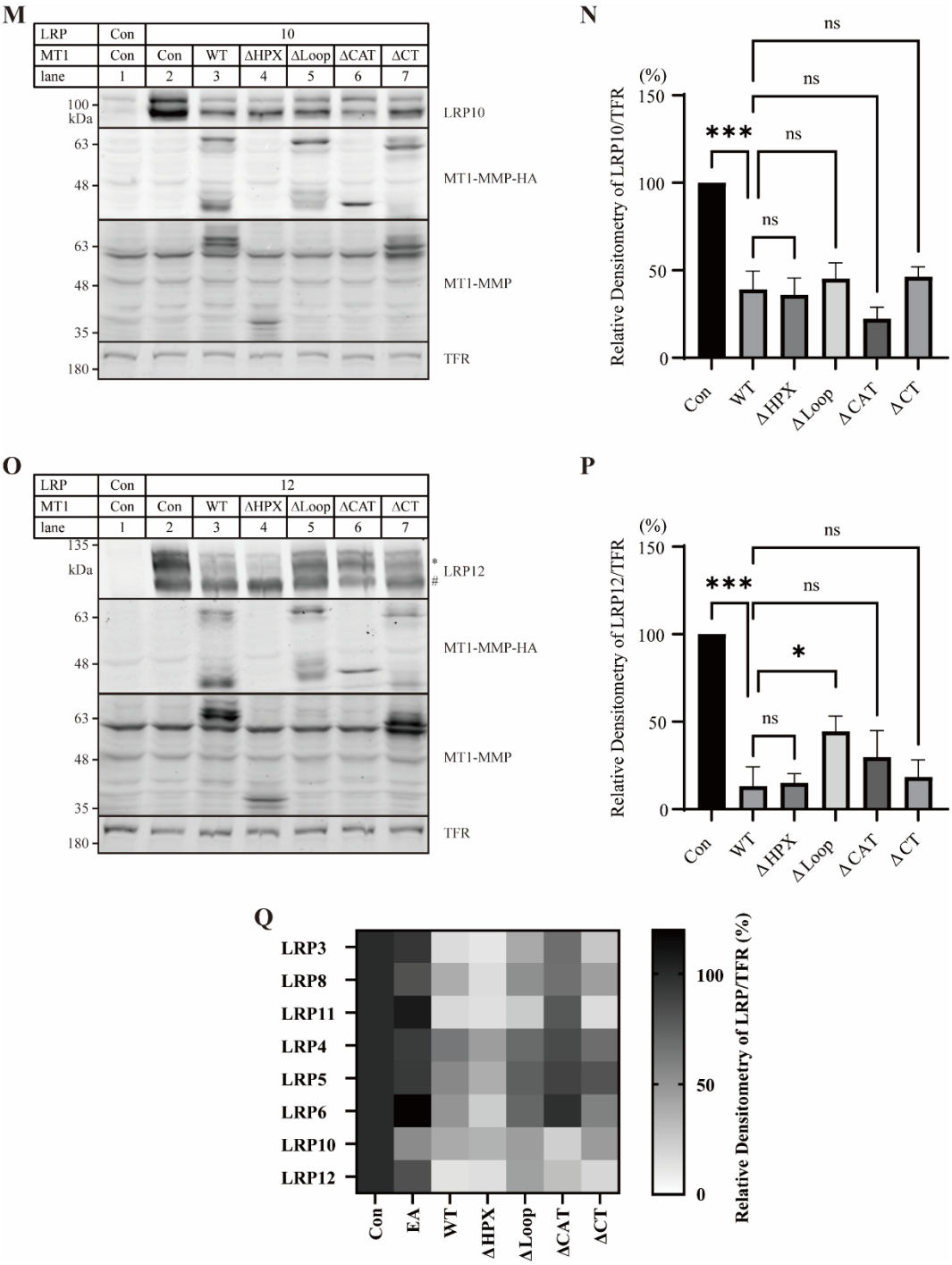

Figure 3. 2. (Continued)

Figure 3. 2. The effects of domain-deleted MT1-MMP mutants on the degradation of LDLR family members. (**A** to **P**) **Immunoblotting and quantification of each LRP with different MT1-MMP mutants.** Huh7 cells were transfected with a C-terminal DDK-tagged LDLR family member, LRP3 (**A** and **B**), LRP8 (**C** and **D**), LRP11 (**E** and **F**), LRP4 (**G** and **H**), LRP5 (**I** and **J**), LRP6 (**K** and **L**), LRP10 (**M** and **N**), or LRP12 (**O** and **P**) and empty vector (**Con**), or either HA-tagged wild-type MT1-MMP (**WT**) or mutant MT1-MMP (hemopexin domain-deleted MT1-MMP (**ΔHPX**), HA-tagged MT-loop-deleted MT1-MMP (**ΔLoop**), HA-tagged catalytic domain-deleted MT1-MMP (**ΔCAT**), or HA-tagged C-terminal cytoplasmic tail-deleted MT1-MMP (**ΔCT**)). 48 hours after transfection, cells were lysed and whole-cell lysate was subjected to immunoblotting. Proteins on immunoblots were detected by rabbit anti-DDK (OriGene), rabbit anti-HA Dylight^{TM} 800 conjugated (Rockland), mouse anti-HA (Proteintech), rabbit anti-MT1-MMP (Abcam, MT-loop epitope) and mouse anti-TFR (BD Biosciences) antibodies. On the representative immunoblot image. * and # indicated the mature and immature form of LRPs, respectively. Arrows indicated bands of each MT1-MMP mutant. For quantifications, the relative densitometry was calculated by normalizing the densitometry of each LRP to TFR in the same condition. The percentage of relative densitometry was the ratio of each LPR to the control empty vector transfection that was defined as 100%. Values of all data were mean with S. D.. Student's *t*-test was used to analyze and determine the statistical significance between groups. n = 3 for each condition; ns = not significant; *, $p < 0.05$; **, $p < 0.01$; ***, $p < 0.001$; ****, $p < 0.0001$. (**Q**) **Heat map summary of the effects of MT1-MMP mutants on the degradation of LDLR family members.** Mean values of the relative densitometry of each LRP/TFR with different MT1-MMP mutants from **Figure 3. 1** and **Figure 3. 2** were plotted as a heat map. Darkness indicated the percentage of each LRP remained.

3.2.3 Proteasome- and lysosome-independent MT1-MMP-mediated degradation of LRPs

Next, we tested whether the two most common protein degradation pathways, proteasome and lysosome-mediated protein degradation, were involved in MT1-MMP's action on the LDLR family members. A proteasome inhibitor, MG132, or a lysosome inhibitor, chloroquine, was applied to Huh7 cells co-expressing wild-type MT1-MMP and one of LDLR family members. As shown in **Fig. 3.3G**, treatment of MG132 and chloroquine increased the levels of ubiquitinated proteins and LDLR, respectively, indicating effective inhibition of the two pathways by their respective inhibitors. However, treatment of either MG132 or chloroquine did not significantly affect MT1-MMP-induced degradation of all LRPs tested. Thus, MT1-MMP regulates the level of LRPs primarily in a proteasome- and lysosome-independent pathway.

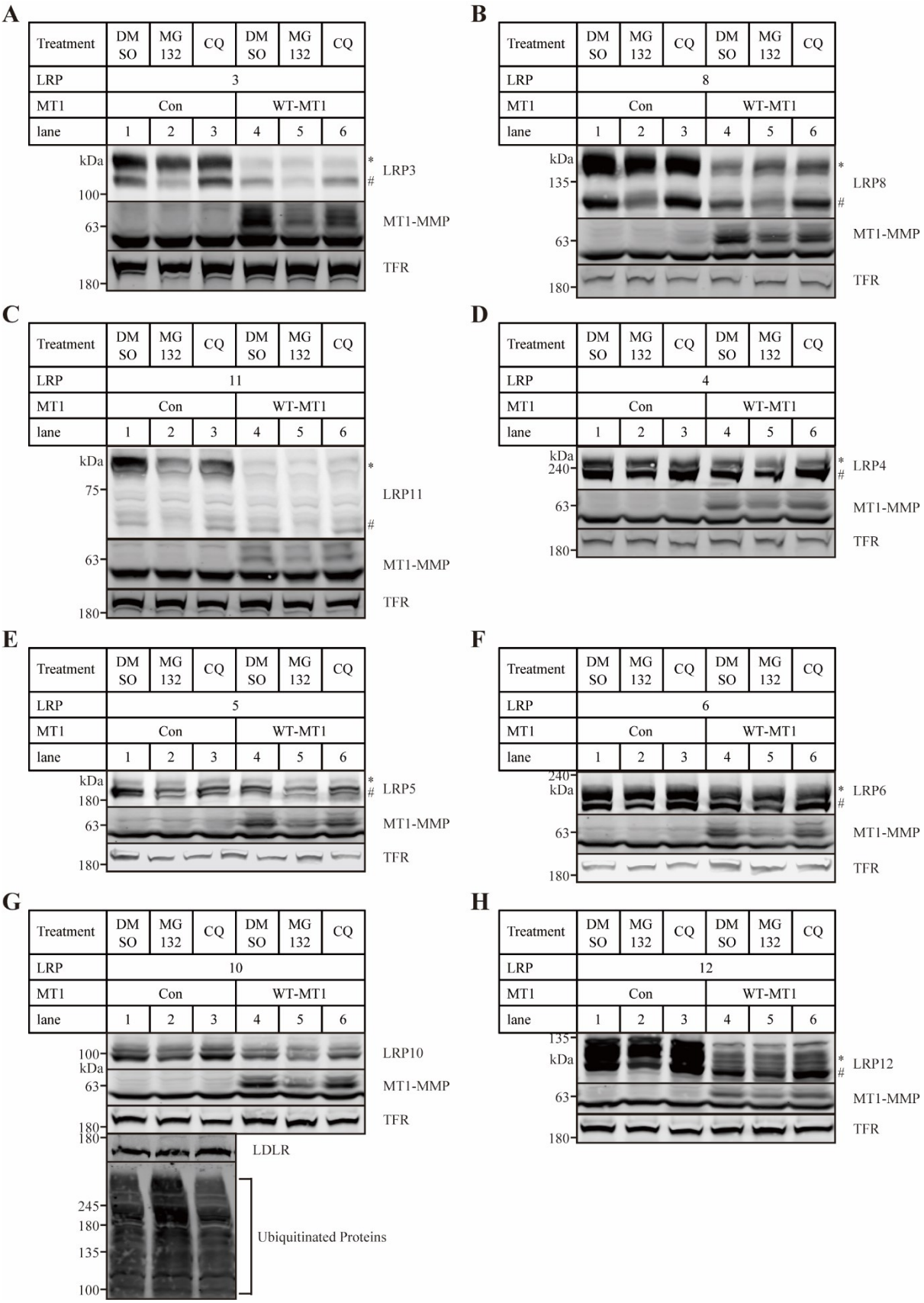
A
Treatment
DMSO
MG132
CQ
DMSO
MG132
CQ
LRP
3
MT1
Con
WT-MT1
lane
1
2
3
4
5
6
kDa
100
63
180
*
#
LRP3
MT1-MMP
TFR
B
LRP
8
135
LRP8
C
LRP
11
75
LRP11
D
LRP
4
240
LRP4
E
LRP
5
LRP5
F
LRP
6
LRP6
G
LRP
10
LRP10
LDLR
245
135
Ubiquitinated Proteins
H
LRP
12
LRP12

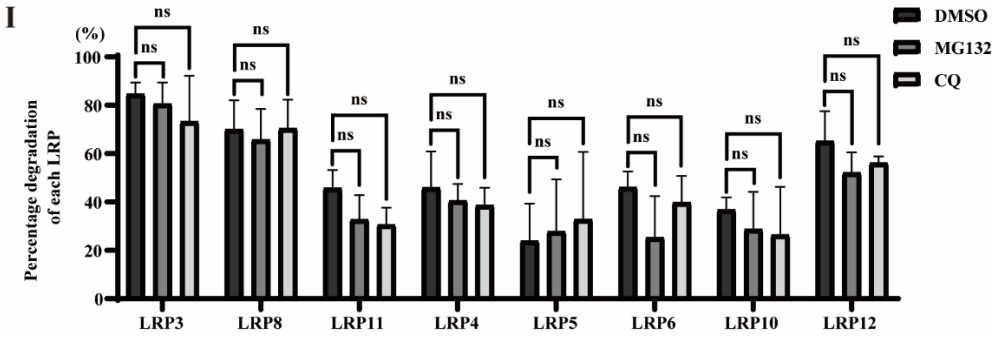

Figure 3. 3. (Continued)

Figure 3. 3. Effects of proteasome inhibitor (MG132) and lysosome inhibitor (chloroquine) on MT1-MMP-mediated degradation of LDLR family members. (**A** to **H**) **Each LRP with overexpressed MT1-MMP and proteasome or lysosome inhibition.** Huh7 cells were transfected with different C-terminal DDK-tagged LRP plasmids, LRP3 (**A**) or LRP8 (**B**) or LRP11 (**C**) or LRP 4 (**D**) or LRP5 (**E**) or LRP6 (**F**) or LRP10 (**G**) or LRP12 (**H**), and either empty vector (**Con**) or HA-tagged wild-type MT1-MMP (**WT**). 48 hours after transfection, cells were then treated with DMSO vehicle only or 10 μM MG132 or 10 μM chloroquine (**CQ**) for 8 hours. The whole-cell lysate was then isolated from collected cells and subjected to immunoblotting. Proteins on immunoblots were detected by rabbit anti-DDK (OriGene), rabbit anti-MT1-MMP (Abcam), mouse anti-TFR (BD Biosciences), rabbit anti-LDLR (Abcam) and rabbit anti-ubiquitin (Proteintech) antibodies. On the representative immunoblot image, * indicated the mature form of LRP and # indicated its immature form. (**H**) **Quantification of the degradation of each LRP under treatments.** The percentage degradation of each LRP is calculated from the ratio of the densitometry of each LRP with wild-type MT1-MMP to the LRP with empty vector under the same treatment. Values of all data were mean with S. D.. Student's *t*-test was used to analyze and determine the statistical significance between groups. n = 3 for each condition; ns = not significant.

3.2.4 Effect of γ-secretase on MT1-MMP-mediated degradation of LRPs

After ectodomain shedding, transmembrane proteins often undergo γ-secretase-mediated second cleavage, which releases the C-terminal cytoplasmic fragment that is rapidly cleared by cells. γ-secretase is the proteinase reported to generate intracellular domains of several LDLR family members, including LDLR, LRP1 and LRP8 [301-303], and we observed the presence of cleaved intracellular C-terminal fragments of LRP3 and 11 in the presence of MT1-MMP (**Fig. 3.1**). To investigate the possible connection between MT1-MMP-mediated LDLR family member degradation and γ-secretase-mediated receptor degradation, we treated cells with DAPT, a γ-secretase inhibitor (**Fig. 3.4**). In LRP8, inhibition of γ-secretase increased the level of a membrane-anchored CTF at ~20 kDa in the absence and presence of MT1-MMP (**Fig. 3.4A** and **3.4D**). Overexpression of MT1-MMP showed a mild increasing trend of CTF-LPR8, but the difference did not reach to statistical significance. LRP3 and LRP11 showed clear membrane-associated CTFs, which were not affected by DAPT treatment (**Fig. 3.4B**, **3.4C**, **3.4E** and **3.4F**). All other LDLR family members did not display any CTFs even under γ-secretase inhibition (**Fig. 3.4G-K**). These results suggested that γ-secretase plays a role in the further cleavage of membrane-anchored CTF of LRP8. However, its role in cleavage of other LRPs after MT1-MMP-mediated shedding needs to be further studied.

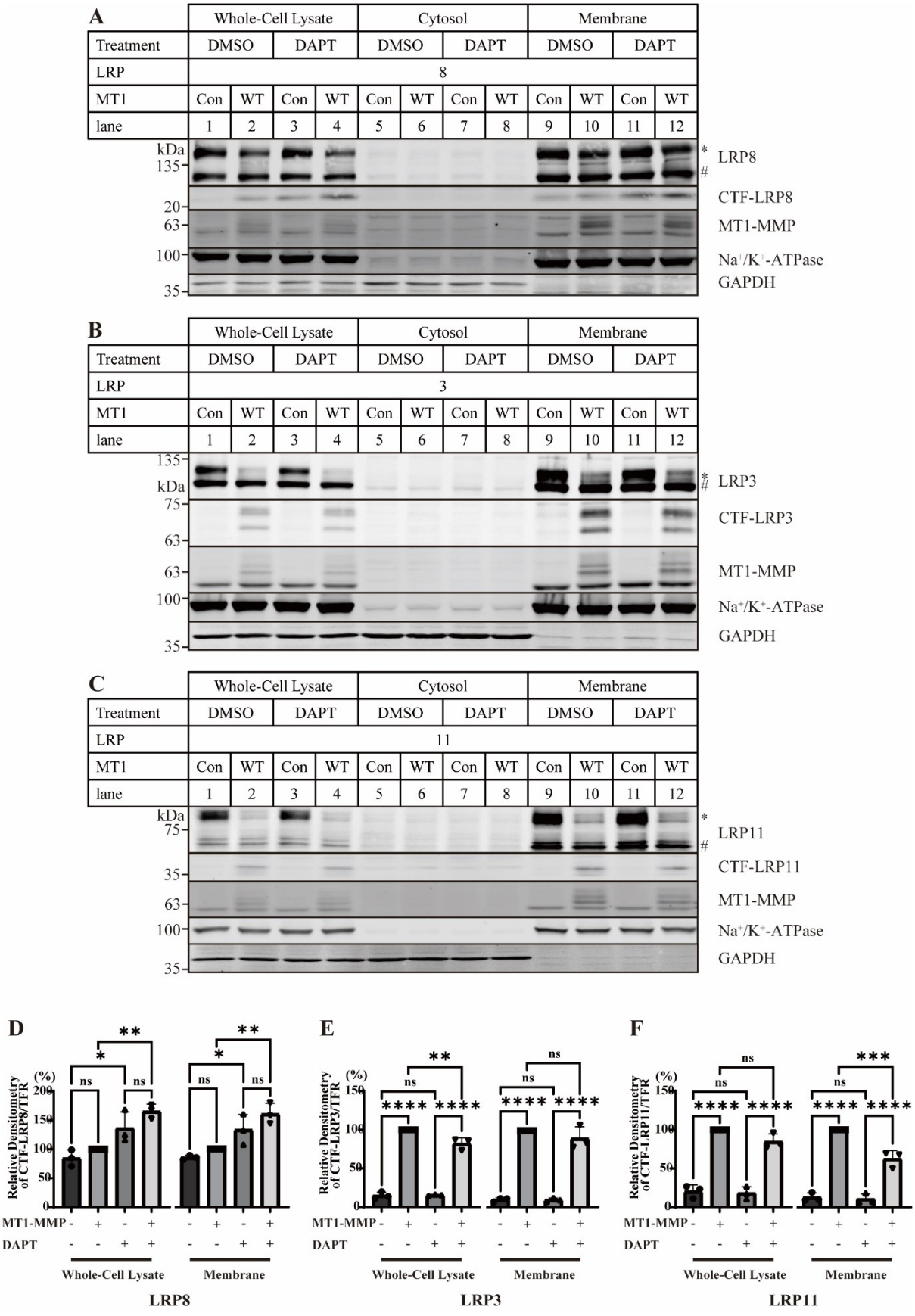
A
Whole-Cell Lysate
Cytosol
Membrane
Treatment
DMSO
DAPT
LRP
8
MT1
Con
WT
lane
kDa
135
20
63
100
35
LRP8
CTF-LRP8
MT1-MMP
Na+/K+-ATPase
GAPDH
B
3
75
LRP3
CTF-LRP3
C
11
LRP11
CTF-LRP11
D
E
F
Relative Densitometry of CTF-LRP8/TFR
Relative Densitometry of CTF-LRP3/TFR
Relative Densitometry of CTF-LRP11/TFR
MT1-MMP
DAPT
Whole-Cell Lysate
Membrane
LRP8
LRP3
LRP11

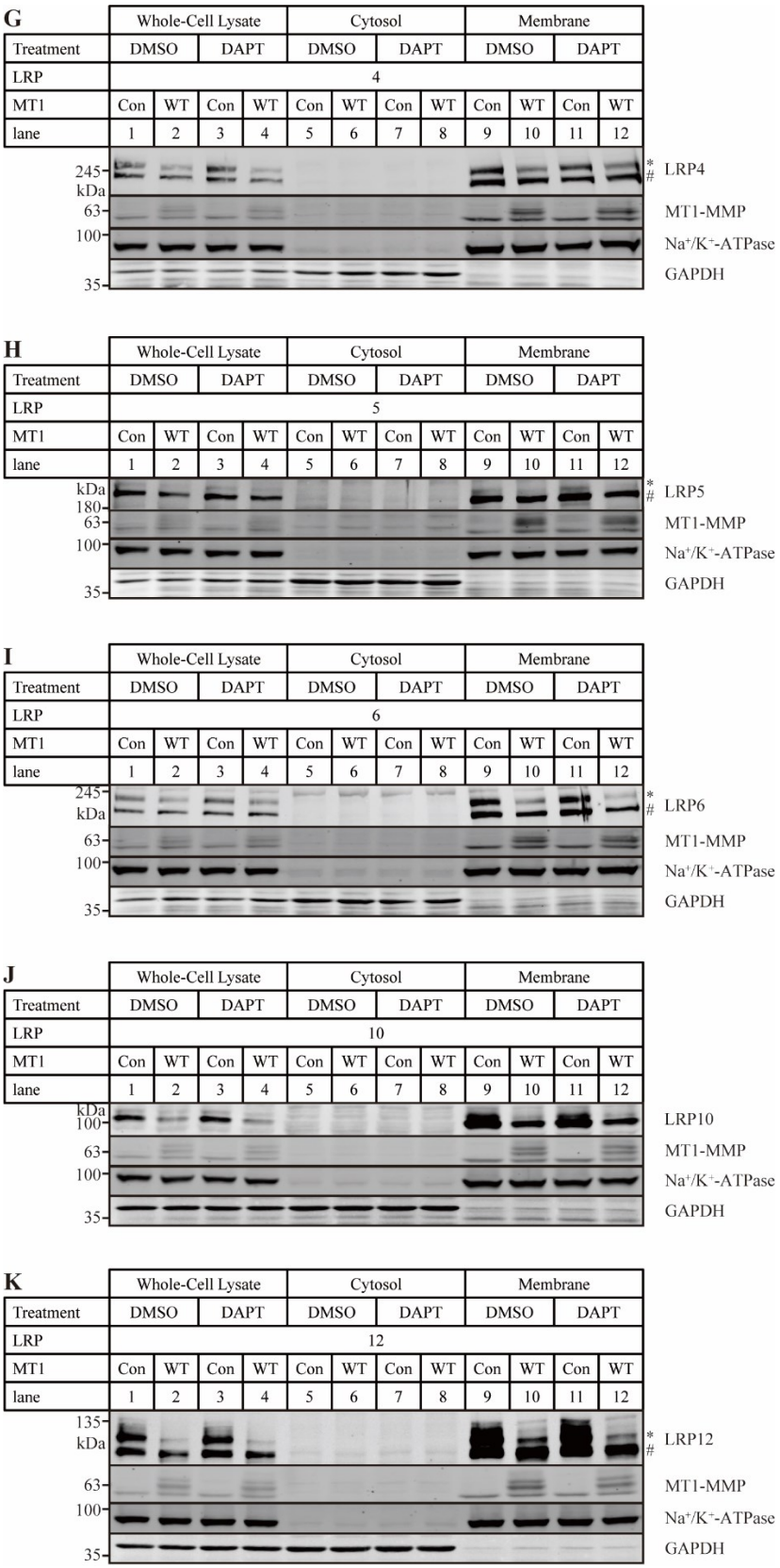

Figure 3. 4. (Continued)

Figure 3. 4. Effects of γ-secretase inhibitor (DAPT) on MT1-MMP-mediated degradation of LDLR family members. (**A, B and C**) **Subcellular distribution of LRP8 (A), 3 (B) and 11 (C) under γ-secretase inhibition and MT1-MMP-mediated degradation.** Huh7 cells were transiently transfected with C-terminal DDK-tagged LRP plasmids (LRP8 or LRP3 or LRP11) and empty vector (**Con**) or HA-tagged wild-type MT1-MMP (**WT**), respectively. 24 hours after transfection, cells were then treated with 10 μM DAPT dissolved in DMSO or DMSO vehicle only for 16 hours. Cells were then harvested to generate whole-cell lysate, cytosol fraction and membrane fraction. 10 ug of total proteins of each fraction were separated by a 4-20% SDS-PAGE gel and subjected to immunoblotting. Proteins on immunoblots were detected by rabbit anti-DDK (OriGene), rabbit anti-MT1-MMP (Abcam), rabbit anti-Na^+/K^+-ATPase and mouse anti-GAPDH antibodies. On the representative immunoblot image, * indicated the mature form of LRP and # indicated its immature form. CTF, C-terminal fragment. (**D**, **E** and **F**) **Quantifications of C-terminal fragments of LRP8, 3 and 11.** The relative densitometry was the ratio of the densitometry of CTF-LRP to TFR in the same condition. The relative densitometries of CTF-LPR with MT1-MMP and DMSO treatments were defined as 100%. Values of all data were mean with S. D.. Student's *t*-test was used to analyze and determine the statistical significance between groups. n = 3 for each condition; ns = not significant; *, $p < 0.05$; **, $p < 0.01$; ***, $p < 0.001$; ****, $p < 0.0001$. (**G** to **K**) **Subcellular distribution of LRP4 (G), 5 (H), 6 (I), 10 (J) and 12 (K) under γ-secretase inhibition and MT1-MMP-mediated degradation.** The experiments were performed as described in **panels A**, **B** and **C** above except using C-terminal DDK-tagged LRP4, 5, 6, 10 and 12 plasmids inside for transfection and no apparent C-terminal fragments were observed.

3.2.5 Interactions between MT1-MMP and LRP3/LRP11

Unlike other LDLR family members, the C-terminal domain of LRP3 and LRP11 appeared not to be rapidly cleared by cells. To understand the underlying mechanism, we investigated the interaction between MT1-MMP and LRP3 or LRP11 by co-immunoprecipitation (**Fig. 3.5**). Wild-type MT1-MMP and catalytically inactive E240A were both applied since the proteolytic activity of MT1-MMP might interfere with the pulling down between MT1-MMP and its substrates. Wild-type MT1-MMP and MT1-MMP E240A were immunoprecipitated from whole-cell lysate of wild-type or mutant MT1-MMP and LRP3 or LRP11 co-overexpressing Huh7 cells using an anti-HA antibody since MT1-MMP contains an HA-tag in its HPX domain. Immature LRP3 and LRP11 were present in both wild-type MT1-MMP and MT1-MMP-E240A lanes (**Fig. 3.5A and 3.5C**). The mature LRP3 and LPR11 were only clearly observed under the conditions with the catalytically inactive E240A. Surprisingly, the CTFs-LRP3 but not CTF-LRP11 were also co-immunoprecipitated by wild-type MT1-MMP. Next, LRP3 and LRP11 were reciprocally immunoprecipitated from the same whole-cell lysate by an anti-DDK antibody. In this situation, both wild-type MT1-MMP and MT1-MMP-E240A were pulled down by LRP3 and LRP11 but MT1-MMP-E240A signal was stronger than that of wild-type MT1-MMP (**Fig. 3.5B and 3.5D**). These findings suggest that MT1-MMP associates with LRP3 and LRP11.

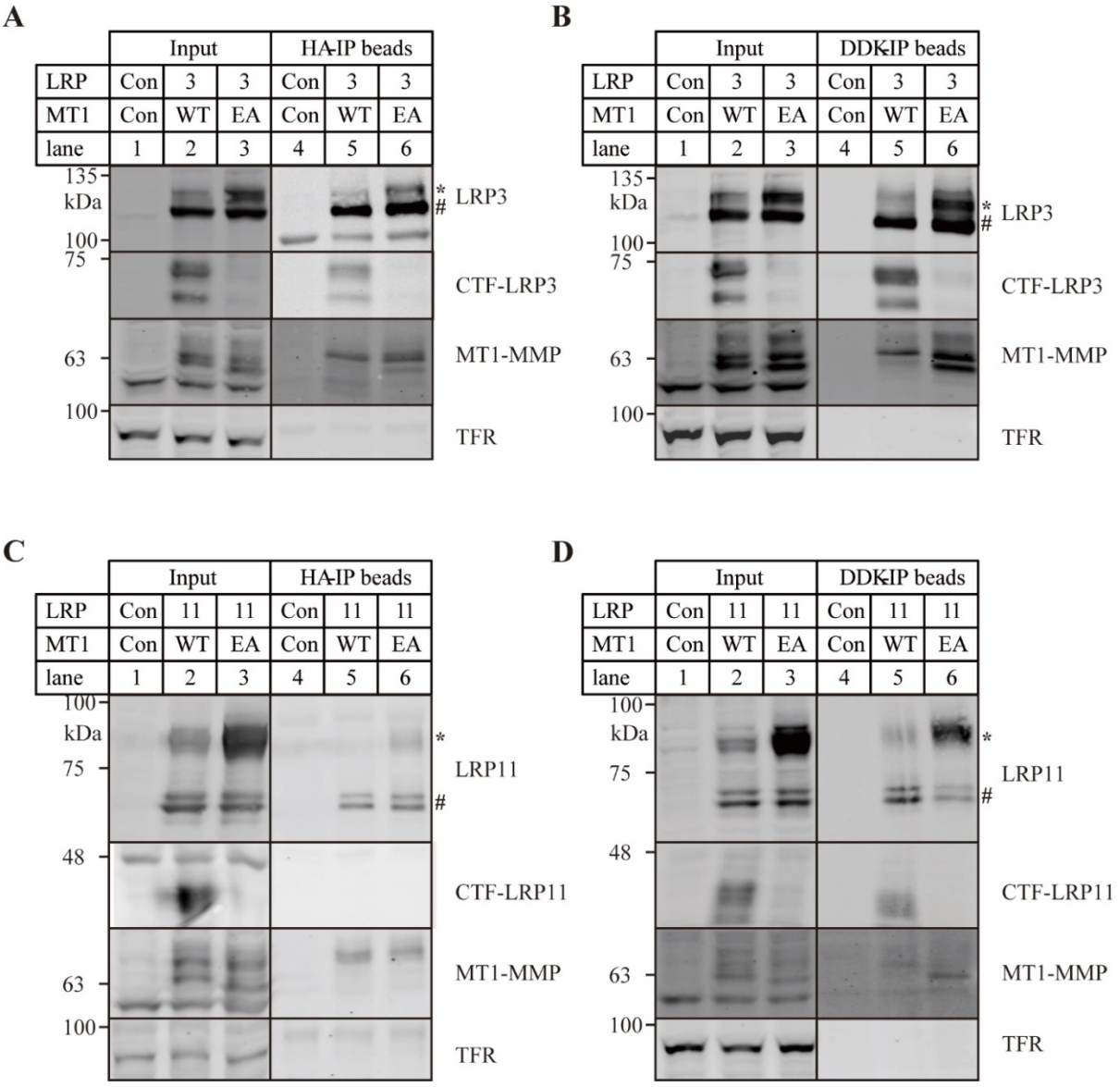

Figure 3. 5. Co-immunoprecipitation of MT1-MMP and selected LDLR family members. (**A** and **B**) **Immunoprecipitation of MT1-MMP (A) and LRP3 (B).** C-terminal DDK-tagged LRP3 and empty vector pcDNA (**Con**) or HA-tagged wild-type MT1-MMP (**WT**) or catalytically inactive MT1-MMP (**EA**) were transfected to Huh7 cells, respectively. 48 hours later, cells were harvested and whole-cell lysate was prepared. Whole-cell lysate with the same amount of total proteins was subjected to immunoprecipitation using protein G beads incubated with either mouse anti-HA (Proteintech; **panel A**) or mouse anti-DDK (Proteintech; **panel B**) antibodies at 4 ℃ overnight. The immunoprecipitated proteins (**HA-IP beads** or **DDK-IP beads**) were eluted and subjected to immunoblotting with whole-cell lysate (**Input**) as controls. Proteins on immunoblots were detected by rabbit anti-DDK (OriGene), rabbit anti-MT1-MMP (Abcam) and mouse anti-TFR (BD Biosciences) antibodies. On the representative immunoblot image, * indicated the mature form of LRP and # indicated its immature form. CTF, C-terminal fragment. (**C** and **D**) **Immunoprecipitation of MT1-MMP (A) and LRP11 (B).** The experiments were performed as described in **panels A** and **B** above except using C-terminal DDK-tagged LRP11 plasmid inside of LRP3 plasmid for transfection.

3.2.6 Colocalization of MT1-MMP and LRP3/LRP11

To further confirm the interaction between MT1-MMP and LRP3/LRP11, we performed immunofluorescence using confocal microscopy to assess the colocalization of MT1-MMP and LRP3 or LRP11. Both Wild-type MT1-MMP and catalytically inactive E240A mutant were applied in the immunofluorescence because wild-type MT1-MMP might disturb the colocalization (**Fig. 3.6** and **Fig. 3.7**). LRP3 or LRP11 was displayed in green and MT1-MMP was displayed in red. LRP3 was distributed on the cell periphery in the presence or absence of MT1-MMP-WT or E240A (**Fig. 3.6**). Wild-type MT1 and E240A mutant appeared in a similar pattern as LRP3, and the two proteins were overlapped and shown in yellow color when merged. Unlike LRP3, LRP11 only showed a spatial overlap with the catalytically inactive MT1-MMP E240A (**Fig. 3.7**). When co-expressed, LRP11 and wild-type MT1-MMP were still primarily distributed on the cell periphery but they were barely overlapped (**Fig. 3.7B**). The LRP11 signal also appeared in a tentacle and fuzz pattern pointing out of the cell which was distinct from the smooth circular signals observed in cells expressing LRP11 alone or with MT1-MMP E240A (**Fig. 3.7B *vs* Fig. 3.7A** and **3.7C**). Nevertheless, these findings further confirmed the association between MT1-MMP and LR3/LRP11 spatially.

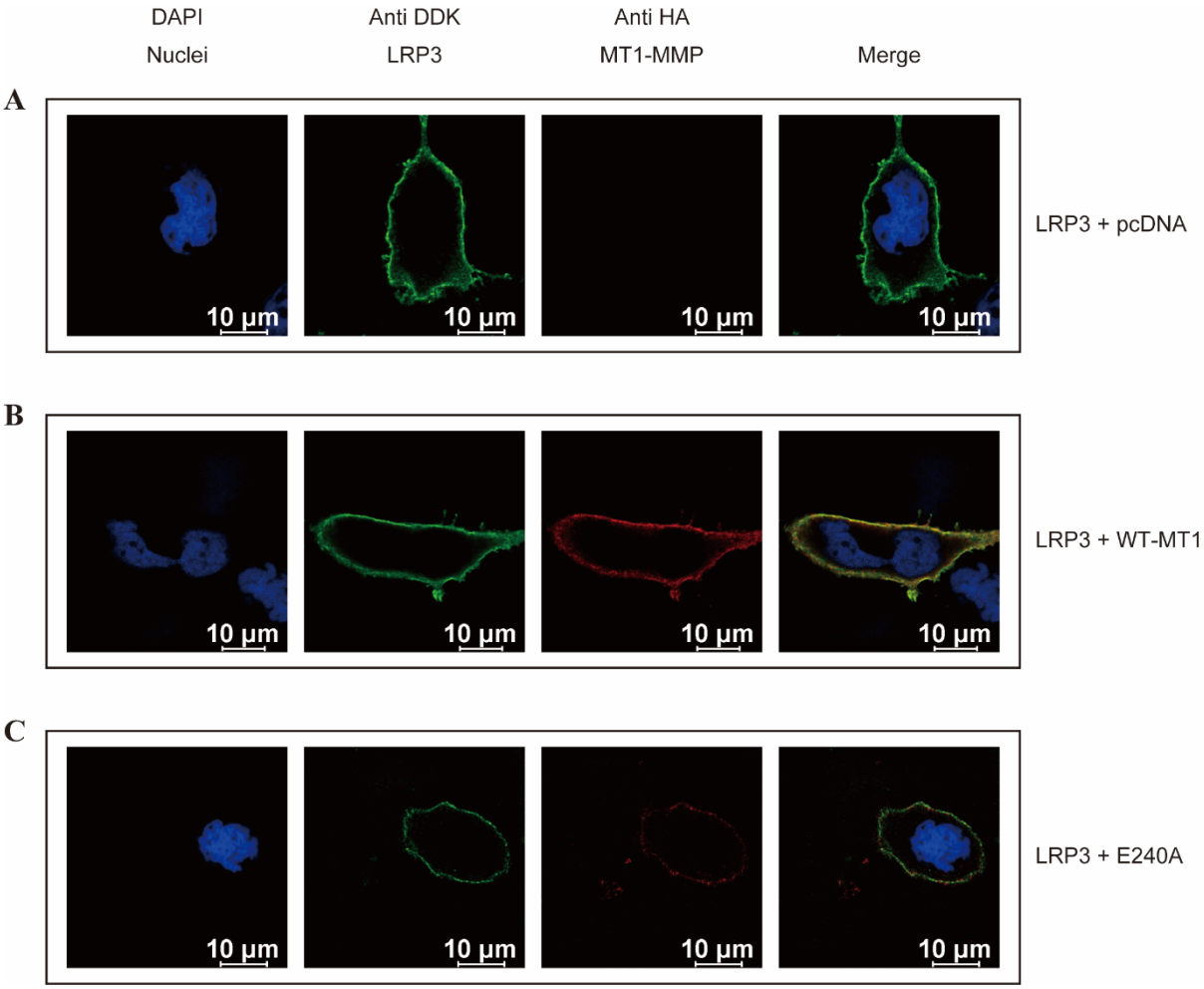

Figure 3. 6. Immunofluorescent images of LRP3 and MT1-MMP distributions. Huh7 cells were transiently transfected with C-terminal DDK-tagged LRP3 and either empty vector (**A**), or HA-tagged wild-type MT1-MMP (**B**), or HA-tagged catalytically inactive MT1-MMP mutant (**C**). Transfected cells were allowed to grow for 48 hours, followed by fixation and permeabilization. After that cells were stained with rabbit anti-DDK (OriGene; shown as green) and mouse anti-HA (Proteintech; shown as red) antibodies, and co-labelled with DAPI (shown as blue). Representative images were shown and generated by confocal microscopy. An x-y optical section of the cells illustrates the cellular distribution of proteins (magnification: 300X or 325X).

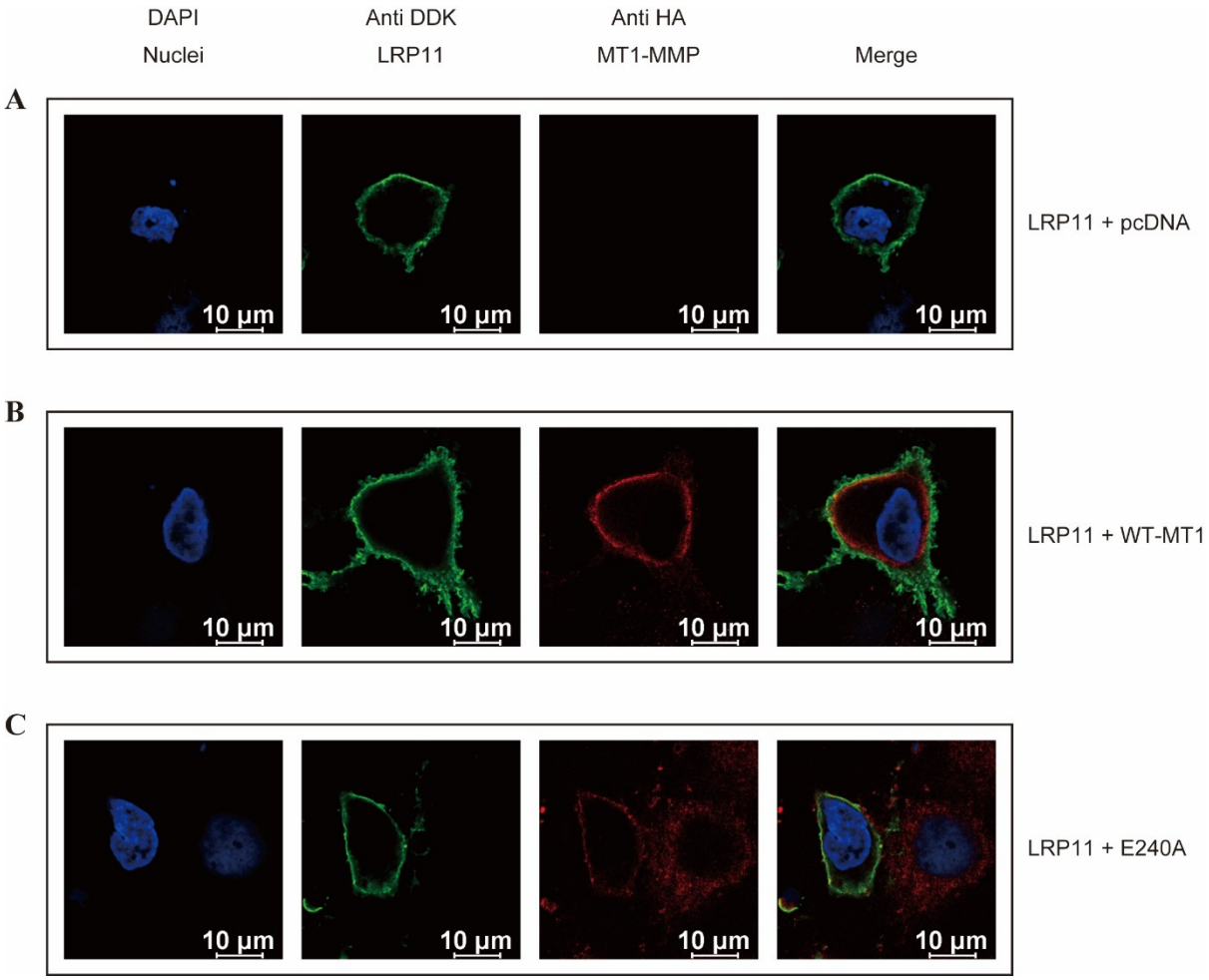

Figure 3. 7. Immunofluorescent images of LRP11 and MT1-MMP distributions. Huh7 cells were transiently transfected with C-terminal DDK-tagged LRP11 and either empty vector (**A**), or HA-tagged wild-type MT1-MMP (**B**), or HA-tagged catalytically inactive MT1-MMP mutant (**C**). Transfected cells were allowed to grow for 48 hours, followed by fixation and permeabilization. After that cells were stained with rabbit anti-DDK (OriGene; shown as green) and mouse anti-HA (Proteintech; shown as red) antibodies, and co-labelled with DAPI (shown as blue). Representative images were shown and generated by confocal microscopy. An x-y optical section of the cells illustrates the cellular distribution of proteins (magnification: 325X).

3.3 Discussion

The LDLR family is a group of versatile membrane receptors which play irreplaceable roles in lipoprotein metabolism [3], nervous system development and maintenance [94,282], bone homeostasis [275], and cancer progression [276]. The soluble form of LDLR family members has been frequently observed in extracellular fluids [75,179,304-307]. It is generally believed that the proteolytic activities of metalloproteinases are responsible for the ectodomain shedding of LDLR family members and the release of soluble LDLR family members [185]. Here, we focused on MT1-MMP which is a member of the matrix metalloproteinases family and functions mainly in extracellular matrix remodelling [186]. Recent studies have shown that LDLR, LRP1 and LRP4 were shed by MT1-MMP on the cell surface [174,176,277]. In this study, we found that all the LDLR family members we tested were degraded by MT1-MMP.

The screening of eight LDLR family members shown that MT1-MMP could mediate the degradation of their mature forms (**Fig. 3.1**). No apparent reductions were observed in immature forms of LDLR family members in the presence of overexpressed MT1-MMP. Our finding provided additional evidence that metalloproteinases, at least MT1-MMP, can promote the degradation of LDLR family observed elsewhere [185]. One limitation of other studies reported previously on metalloproteinases-mediated shedding of LDLR family members is the incapability of identifying which specific metalloproteinase was involved in [175,177,181,308]. In these studies, broad-spectrum matrix metalloproteinases inhibitors were applied to prove that metalloproteinase activities were responsible for the LDLR family shedding thus detailed information on metalloproteinases was absent. The general metalloproteinases inhibitors (e.g.

GM6001 and TAPI) inhibit most members in the MMP family and ADAM family which have nearly 50 members and both belong to the metzincin superfamily [309-311]. Hence, knowing which metalloproteinases mediate the shedding of the LDLR family is critical for further research.

The physiological role of MT1-MMP mainly relies on its proteolytic activity, especially in the cases of MT1-MMP-mediated degradation of proteins [225]. For this reason, the proteolytic inactive MT1-MMP E240A mutant was also applied in the screening of LDLR family members (**Fig. 3.1**). The results generally matched our hypothesis that the proteolytic activity is essential for MT1-MMP-mediated degradation of the LDLR family with the exception of LRP10. Both wild-type and proteolytic inactive forms of MT1-MMP can induce the same degree degradation on LRP10 (**Fig. 3.1E** and **F**). Meanwhile, the degradations of LRP8 and LRP12 were reduced but not eliminated under the proteolytic inactive MT1-MMP E240A treatment (**Fig. 3.1B** and **F**). These results implied that there might be a non-proteolytic mechanism of MT1-MMP which caused the degradation of LRP10 and partially of LRP8 and LRP12. The non-proteolytic roles of MT1-MMP were less studied which involves the other structural domains instead of the catalytic domain [312]. For example, the C-terminal cytoplasmic tail of MT1-MMP has a signaling function independent of enzyme activity [313]. The hemopexin domain regulates the association of MT1-MMP and other proteins by heterodimerization which may affect the cellular distribution of MT1-MMP and associated proteins [202,204].

To better understand the mechanisms in MT1-MMP-mediated degradation of the LDLR family, we tested the effects of domain deletion in MT1-MMP on LDLR family degradation (**Fig. 3.2**). Catalytic domain deletion (ΔCAT) gave identical results as the proteolytic inactive mutant (E240A) that only LRP10 degradation was not affected (**Fig. 3.2M**). Although both ΔCAT and

E240A are proteolytic inactive, the catalytic domain also serves as a binding interface with other proteins [314]. Thus, its deletion clarified the role of the catalytic domain in protein association was not required in LRP10 degradation. Surprisingly, the MT-loop deletion did not abolish the degradation that happened on LDLR family members. In the previous study, the MT-loop of MT1-MMP was essential for the MT1-MMP-mediated shedding of LDLR whose deletion results in a complete abolishment of LDLR shedding [201]. Hemopexin domain deletion and cytoplasmic tail deletion were both indistinguishable from the wild-type MT1-MMP in its ability to promote LDLR family degradation. Thus, the dimerization and signaling transduction of MT1-MMP were not involved in the MT1-MMP-mediated degradation of LDLR family members. The domain-deleted MT1-MMP further confirmed the role of the proteolytic activity of MT1-MMP in the degradation of LDLR family members which did not rely much on other structures of MT1-MMP. Meanwhile, it also demonstrated that the MT1-MMP proteolysis-independent degradation of LRP10 did not rely on the domains we tested.

MT1-MMP mediated degradation of LDLR family members was proteasome and lysosome independent (**Fig. 3.3**). It is consistent with the general understanding of the metalloproteinases-mediate shedding of LDLR family members that the metalloproteinases directly cleave their substrates [185]. However, LRP10 did not undergo MT1-MMP-mediated ectodomain shedding. Interestingly, the MT1-MMP mediated degradation of LRP10 was also not affected when either the proteasome or lysosome pathways was inhibited (**Fig. 3.3G**). It is of note that MG132 and chloroquine do not completely inhibit proteasome and lysosome-mediated protein degradation, respectively. The remaining activity may be sufficient for MT1-MMP-mediated degradation of LRP10. Alternatively, both pathway may be involved in this

process. Inhibition of one pathway can be compensated by the other one. Unlike other LDLR family members, the subcellular distribution of LRP10 is mostly between the *trans*-Golgi network (TGN) and early endosomes where LRP10 keeps its cycling [133,135]. The deficiency of LRP10 on the cell surface may explain why LRP10 did not undergo shedding by MT1-MMP. Chloroquine was applied to block the lysosomal degradation pathway by impairing the acidification of endosomes [315]. The pH in early endosomes resembles the extracellular environmental pH which is barely affected by chloroquine. One speculated role of LRP10 is trafficking unwanted proteins accumulated in the Golgi apparatus to endosomes for further degradation [135]. Transiently overexpressed MT1-MMP and its mutants are heavily accumulated in the *trans*-Golgi network which may trigger LRP10-mediated sorting to endosomes. And in the process, some LRP10 may be degraded due to the complex environment in endosomes which contain proteases functioning at neutral pH [316]. Further studies are required to test this hypothesis and figure out the mechanism of LRP10 degradation.

Transmembrane protein undergoes shedding would generate a soluble ectodomain and a C-terminal fragment which may be further processed by γ-secretase to generate a soluble intracellular domain (ICD) [317]. ICDs of LDLR family members are generally believed to have signal transduction roles [318,319]. In the screening, the CTFs of LRP3 and LRP11 were observed in the presence of MT1-MMP (**Fig. 3.1A**). Levels of CTF-LRP3 and CTF-LRP11 were not increased when γ-secretase activity was inhibited (**Fig. 3.4B** and **3.4C**) which implied that proteinases other than γ-secretase play an essential role in this process but generate ICD at a lower rate. Interestingly, after degradation, CTF-LRP3 but not CTF-LRP11 was associated with MT1-MMP (**Fig. 3.5**). This suggested that CTF-LRP3 and CTF-LRP11 may have undiscovered

but distinct functions. Two articles published by Ao's group have reported two different molecular masses of rat LRP3 (i.e. ~120 kDa in chondrocytes [73] and ~80 kDa in bone marrow-derived stem cells [72]) which are close to the molecular masses of full-length and CTF-LRP3 we observed here. It suggested that 1) CTF-LRP3 may exist and be detectable at physiological levels of LRP3 and MT1-MMP, and 2) Full-length and CTF of LRP3 levels may be associated with bone marrow-derived stem cell differentiation which is controlled by MT1-MMP [320]. It was reported that LRP11 could facilitate cancer cells immune evasion through β-catenin induced PD-L1 expression [144]. LRP5/6 mutants that lack the extracellular domain constitutively activate the canonical Wnt signaling, resulting in increased β-catenin levels [321]. The CTF-LRP11 without the extracellular domain may also have a signaling function. Further research to figure out the exact biological roles of CTF-LRP3 and CTF-LRP11.

We are aware of three major limitations of this study. The first is the utilization of transient overexpression to study the effects of MT1-MMP on different LDLR family members. Overexpressed MT1-MMP and LDLR family members could have abnormal subcellular distributions which might not reflect physiological protein statuses and functions. The non-physiological protein levels might exaggerate the effect and could be physiologically irrelevant. It also held us back from studying the large LDLR family members (i.e. LRP1, LRP1B and LRP2 with molecular masses ~600 kDa). Second, domain-deleted MT1-MMP mutants could have distorted structures distinct from wild-type MT1-MMP which might indirectly affect MT1-MMP degrading LDLR family members. The third is the lack of detection of the soluble ectodomains of LDLR family members which could be key to proving the mechanism of MT1-MMP-mediated degradation of LDLR family members.

In conclusion, this study has shown that MT1-MMP could promote the degradation of mature LDLR family members in proteolytic activity-dependent and -independent ways. CTFs of LRP3 and LRP11 were generated during the degradation and prolongedly existed in cells. Further studies are required on the biological importance of MT1-MMP-mediated degradation of each LDLR family member.

Chapter 4

Combinative effect of MT1-MMP knockdown and statin treatment on increasing LDLR levels

4.1 Introduction

Globally, the number one cause of death is cardiovascular diseases (CVDs) which count for almost one-third of total deaths annually [260]. Prevalence cases of CVD worldwide were estimated at 621 million in 2021 which counts for ~8% of the global population at that time [260]. In the United States, nearly 1 in every 10 adults ≥20 years of age have been diagnosed with CVDs [322]. Thus, people have been looking for possibilities to reduce the incidence of CVDs for decades. LDL-cholesterol is considered to be a leading modifiable risk factor for the mortality of CVDs. It was estimated that 18.6% of total cardiovascular deaths in 2021 were attributed to high circulating LDL-cholesterol levels [323]. Hence, lowering LDL-cholesterol in the blood is a key strategy to reduce substantially elevated cardiovascular risk in current society. As the catabolism of LDL particles largely relies on the hepatic LDLR activity, increasing the hepatic LDLR activity or expression levels is an effective way to reduce LDL-cholesterol levels and subsequently CVD risks.

Statins are the most common medications that are prescribed to patients for reducing LDL-cholesterol levels and preventing the development of CVDs [267]. Since September 1987 when the U.S. FDA approved the first commercial statin – "lovastatin", there have been a total of 6 statin medications introduced to the market and extended millions of lives [324]. Statins is a class of drugs which act as HMG-CoA reductase inhibitors to block the rate-limiting step of intracellular *de novo* cholesterol synthesis [267]. Impaired cholesterol synthesis leads to reduced levels of intracellular cholesterol levels which activate sterol regulatory element-binding protein 2 (SREBP2) to upregulate LDLR expression and enhance LDL-cholesterol clearance.

The risk of CVDs can be reduced by 40-50% for every 2-3 mmol/L reduction in LDL-cholesterol by statin treatments [269].

High-intensity statin is capable of lowering LDL-cholesterol by 50% [278]. However, a 50% reduction is not always sufficient for hypercholesterolemia patients who have a high baseline of LDL-cholesterol levels [270]. Besides the maximum dose of statin intake, those patients have to take extra combined medications to facilitate a further decrease in LDL-cholesterol levels. Common medications combined with statins are PCSK9 inhibitors (inhibit PCSK9-driven LDLR degradation), ezetimibe (reduce diet cholesterol absorption), MTP inhibitors (impair VLDLR and chylomicron production) and bile acid sequestrants (reduce bile acids reabsorption) [278]. However, PCSK9 inhibitors are not financially viable [325]; MTP inhibitors and bile acid sequestrants commonly develop severe gastrointestinal symptoms [274,326]; and the efficacy of ezetimibe is low [278].

Although statins are generally well tolerated, there are still some potential adverse effects that should be paid attention to [267]. The most common one is statin-associated muscle symptoms (SAMS) including myalgia, cramps and weakness [327]. Meanwhile, there is no particular treatment for SAMS except for withdrawing statin medication. Besides SAMS, long-term taking statins will dose-dependently increase the onset risk of diabetes and exacerbate existing type 2 diabetes mellitus [279]. As a life-long medication, combined statin-based therapies are recommended to minimize adverse metabolic consequences [328].

Hence, in order to enhance the LDL-cholesterol lowering results and/or avoid intolerance for statins, additional combined therapy with statin for reducing LDL-cholesterol levels is needed.

Transcriptionally upregulated LDLR through statin-driven activation of SREBP2 cannot avoid post-translational downregulation [37]. Preventing post-translational downregulation of LDLR is essential to fully liberate statin therapy efficacy. PCSK9 inhibitors act to block LDLR lysosomal degradation which doubles the statin efficacy on lowering LDL-cholesterol levels in combination therapy [278]. Besides the intracellular lysosomal degradation of LDLR, ectodomain shedding by sheddases also reduces the LDLR levels. Membrane type 1-matrix metalloproteinase (MT1-MMP) was recently discovered to mediate the ectodomain shedding of LDLR, and knockdown of hepatic MT1-MMP is able to reduce the LDL-cholesterol levels in mice [174]. Here, we studied if statin combined with the depletion of hepatic MT1-MMP is a new potential therapy to enhance statin therapy efficacy and minimize statin-related adverse events.

4.2 Results

4.2.1 Dose-dependent effects of lovastatin on LDLR expression

To determine an appropriate dose of lovastatin applied in live cells, a dose-dependent experiment was conducted in HepG2 (**Fig. 4.1A** and **4.1B**). Whole-cell lysate of HepG2 cells treated with different amounts of lovastatin was subjected to immunoblotting to assess LDLR level. As shown in **Fig. 4.1**, when lovastatin concentration reached 1 μM, LDLR level in HepG2 cells was significantly increased compared to the control. The peak of the increase in LDLR level was reached when 10 μM of lovastatin was applied to cells. While for 50 μM statin treatment, LDLR level started to decrease. We also observed a clear decrease in the level of transferrin receptor when the same volume of whole-cell lysate was subjected to immunoblotting, suggested a loss of cell viability (**Fig. 4.1A lane 6**). Indeed, we observed obvious changes in cell morphology and a decrease in attached cells after 24 h treatment with 50 μM of lovastatin (**Fig. 4.1C**), which was further decreased in cells treated with 100 μM of lovastatin for 24 h. Therefore, 1μM of statin was used in the following experiments to avoid cytotoxicity.

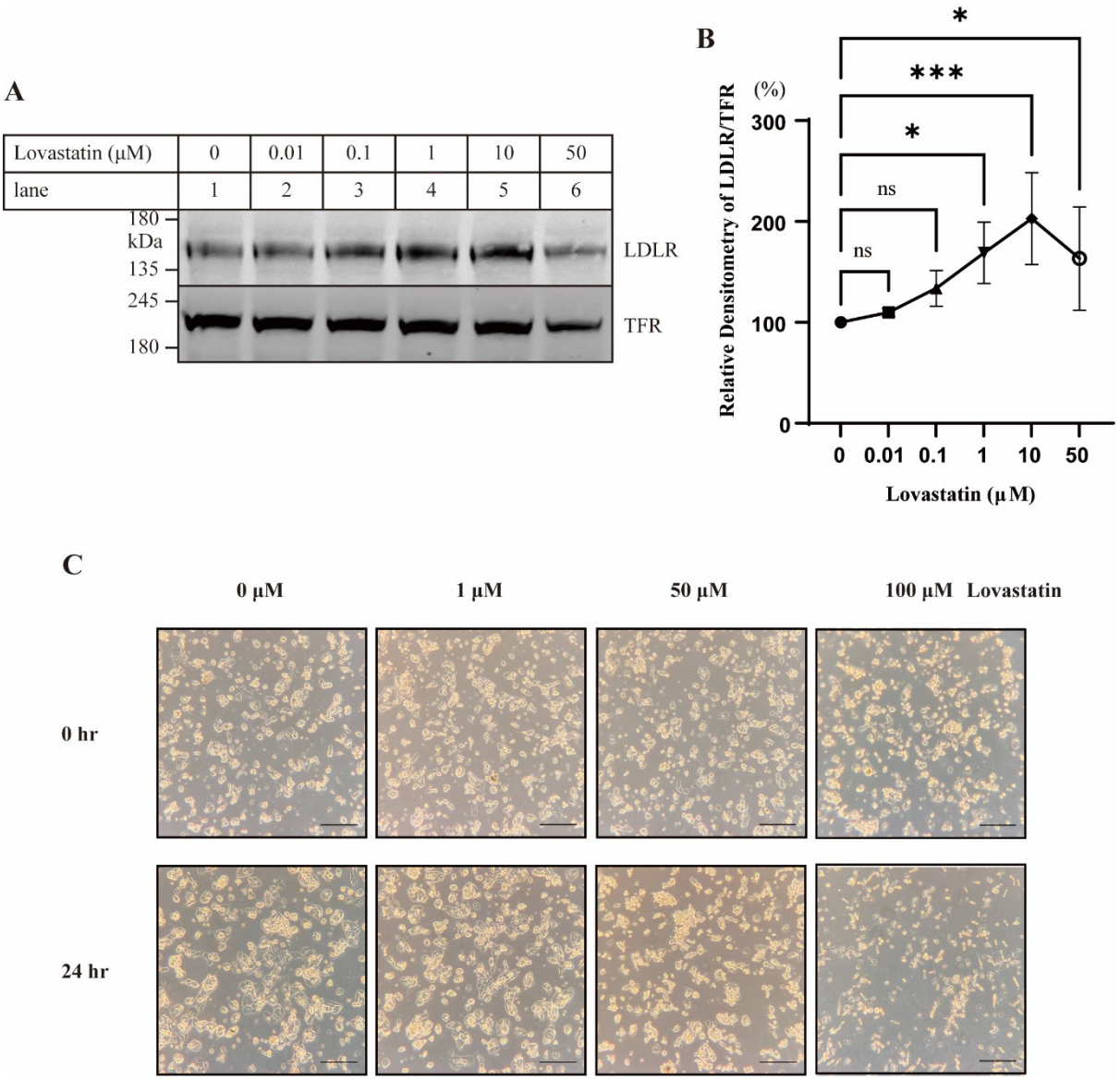

Figure 4. 1. The effects of lovastatin on HepG2 cells. (A and B) Lovastatin dose titration. 48 hours after cell-seeding, HepG2 cells were treated with different doses of lovastatin dissolved in DMSO and supplemented with 5 μg/mL mevalonate for 24 hours. Cells were then collected and lysed in the same conditions. The same volume of whole-cell lysate was subjected to immunoblotting. Proteins on the immunoblots were then detected by rabbit anti-LDLR (Abcam) and mouse anti-TFR (BD Biosciences) antibodies. For quantifications, the relative densitometry was the ratio of the densitometry of LDLR to TFR in the same condition. The relative densitometries of LDLR in HepG2 cells treated with DMSO, e.g. 0 μM lovastatin, were set as 100%. Values of all data were mean with S. D.. One-way ANOVA followed by multiple comparisons was used to analyze and determine the statistical significance between groups. n = 4 for each condition; ns = not significant; *, $p < 0.05$; **, $p < 0.01$; ***, $p < 0.001$; ****, $p < 0.0001$. (**C**) **Representative images of HepG2 cells before and after lovastatin treatments.** Images were taken from the inverted microscope at time 0-hour and 24-hour of the lovastatin treatment of different concentrations (magnification: 40X, Scale bar: 50 μm).

4.2.2 Additive effect of MT1-MMP knockdown and statin on LDLR expression

Statin therapy is the most common and effective strategy to increase hepatic LDLR expression and lower circulating LDL cholesterol. Since MT1-MMP and statin regulate LDLR through distinct mechanisms, we tested the combined effect of MT1-MMP knockdown and statin treatment on LDLR levels. HepG2 cells were transiently transfected with siRNA to knock down MT1-MMP and then treated with or without 1 μM of lovastatin for 24 hours. As expected, MT1-MMP knockdown and statin treatment alone significantly increased LDLR levels (**Fig. 4.2A** and **4.2B**). Combination of MT1-MMP knockdown and statin treatment significantly increased LDLR levels compared to either treatment alone. qRT-PCR data showed that knockdown of MT1-MMP had no significant effect on mRNA levels of *LDLR*, whereas statin treatment significantly increased mRNA levels of *SREBP2* and *LDLR* (**Fig. 4.2C**). Thus, MT1-MMP silencing and statin treatment have an additive effect on the increased in LDLR levels.

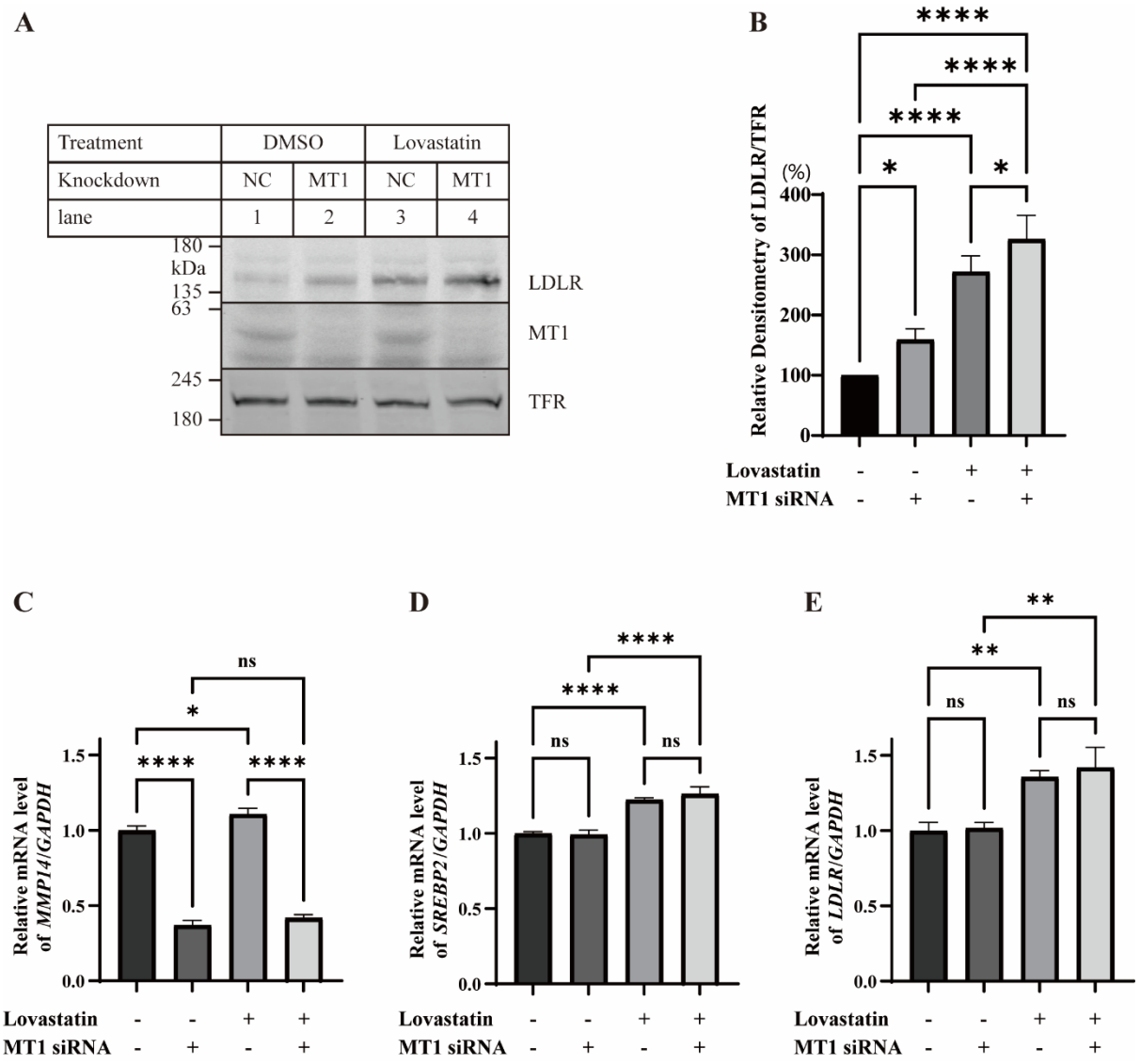
A
Treatment
DMSO
Lovastatin
Knockdown
NC
MT1
NC
MT1
lane
1
2
3
4
180
kDa
135
63
245
180
LDLR
MT1
TFR
B
Relative Densitometry of LDLR/TFR
(%)
400
300
200
100
0
****
****
****
*
*
Lovastatin - - + +
MT1 siRNA - + - +
C
Relative mRNA level of MMP14/GAPDH
1.5
1.0
0.5
0.0
ns
*
****
****
Lovastatin - - + +
MT1 siRNA - + - +
D
Relative mRNA level of SREBP2/GAPDH
1.5
1.0
0.5
0.0
****
****
ns
ns
Lovastatin - - + +
MT1 siRNA - + - +
E
Relative mRNA level of LDLR/GAPDH
1.5
1.0
0.5
0.0
**
**
ns
ns
Lovastatin - - + +
MT1 siRNA - + - +

Figure 4. 2. The effects of lovastatin and MT1-MMP knockdown on LDLR. (**A** and **B**) **Immunoblotting and quantification of LDLR levels.** HepG2 cells were seeded and transfected with negative control (**NC**) or MT1-MMP (**MT1**) siRNAs for 48 hours. After that, cells were treated with DMSO vehicle only or 1 μM of lovastatin dissolved in DMSO supplemented with 5 μg/mL mevalonate. 24 hours later, cells were collected and lysed. The same amounts of whole-cell lysate were subjected to immunoblotting. Proteins on the immunoblots were then detected by rabbit anti-LDLR (Abcam), rabbit anti-MT1-MMP (Abcam) and mouse anti-TFR (BD Biosciences) antibodies. For quantifications, the relative densitometry was the ratio of the densitometry of LDLR to TFR in the same condition. The relative densitometries of LDLR in HepG2 cells transfected with **NC** siRNA and treated with DMSO were set as 100%. Values of all data were mean with S. D.. Two-way ANOVA followed by multiple comparisons was used to analyze and determine the statistical significance between groups. n = 4 for each condition; ns = not significant; *, $p < 0.05$; **, $p < 0.01$; ***, $p < 0.001$; ****, $p < 0.0001$. (**C** to **E**) **mRNA levels of targeted genes.** HepG2 cells were treated the same as immunoblotting (**panels A** and **B**) except that total RNA was collected by PureLink^{TM} RNA Mini Kit (Invitrogen) and cDNA was synthesized by High-Capacity cDNA Reverse Transcription Kit (Applied Biosystems). mRNA levels of each targeted gene were measured by qRT-PCR. The relative mRNA levels were the ratios of the target gene mRNA levels to the *GAPDH* mRNA level. The average relative mRNA level of each target gene in HepG2 cells transfected with **NC** siRNA and treated with DMSO were set as 1. Values of all data were mean with S. D. of one technical triplicate. Two-way ANOVA followed by multiple comparisons was used to analyze and determine the statistical significance between groups. ns = not significant; *, $p < 0.05$; **, $p < 0.01$; ***, $p < 0.001$; ****, $p < 0.0001$.

4.2.3 MMP14Flox/LKO mice fed by western diet + 0.2% lovastatin

Next, we tested the effects of combined treatment of hepatic MT1-MMP knockdown and statin in mice. To mimic diet-induced hypercholesterolemia, MMP14Flox and MMP14LKO mice were first fed by a powered western diet for 10 days, followed by additional 10 days of western diet supplemented with or without 0.2% lovastatin. Unexpectedly, LDLR levels in the liver of statin-fed mice were apparently lower than that of non-statin-fed mice (**Fig. 4.3A**, **4.3B** and **4.3C**). We observed that mice supplied with statin had a significant loss of body weight, indicating that these mice had health issues (**Fig. 4.3D**). The liver of statin-fed mice trended to have stiff and white plagues, suggesting liver damage (**Fig. 4.3F**). To confirm this, we measured plasma alanine transaminase (ALT) levels (**Fig. 4.3E**) and found that ALT levels of statin-fed mice were significantly higher than those non-statin-fed mice. Therefore, western diet supplemented with 0.2% statin led to liver damage in mice.

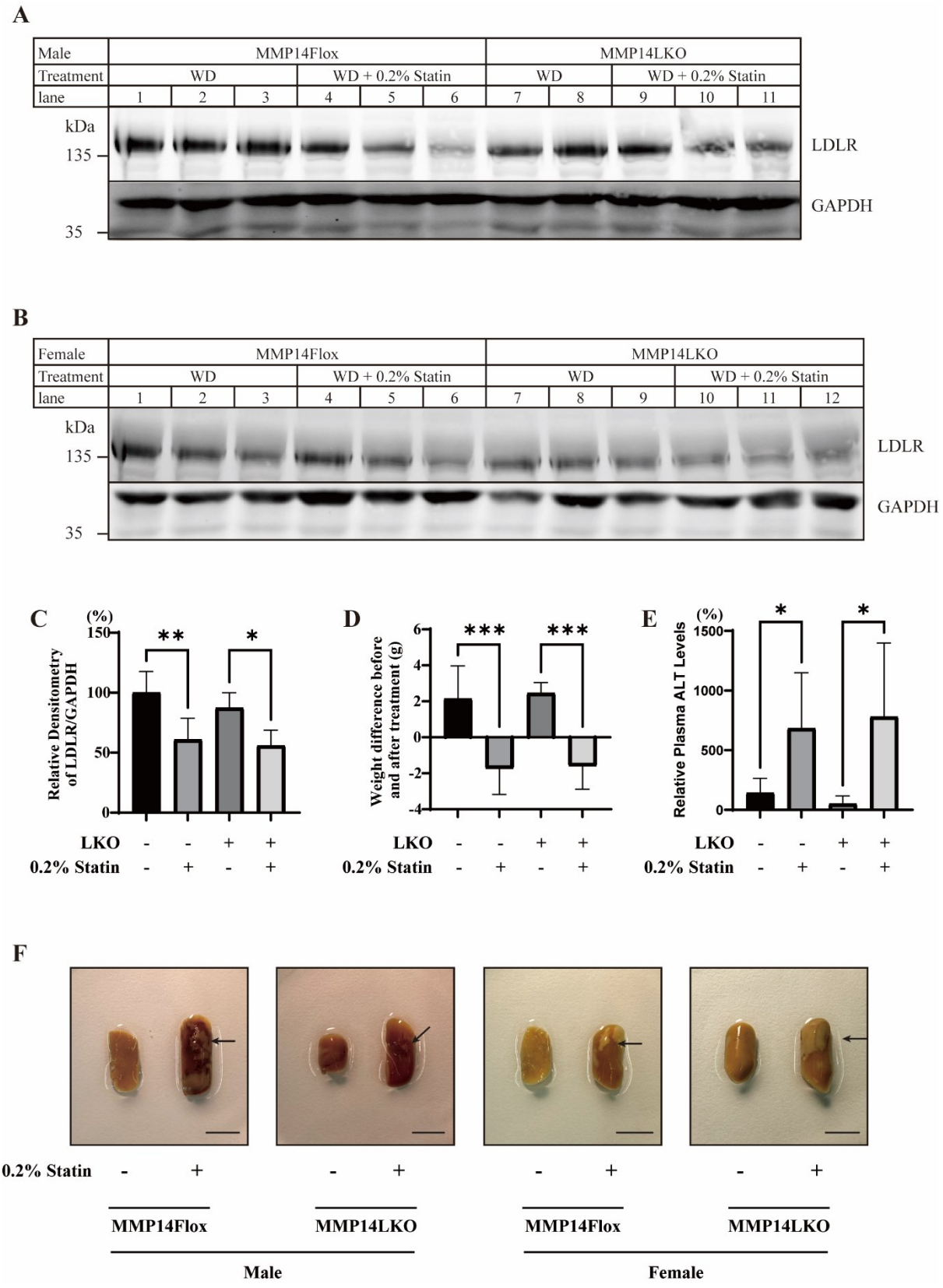
A
Male
MMP14Flox
MMP14LKO
Treatment
WD
WD + 0.2% Statin
WD
WD + 0.2% Statin
lane
1 2 3 4 5 6 7 8 9 10 11
kDa
135
35
LDLR
GAPDH
B
Female
MMP14Flox
MMP14LKO
Treatment
WD
WD + 0.2% Statin
WD
WD + 0.2% Statin
lane
1 2 3 4 5 6 7 8 9 10 11 12
kDa
135
35
LDLR
GAPDH
C
Relative Densitometry of LDLR/GAPDH
(%)
150
100
50
0
**
*
LKO - - + +
0.2% Statin - + - +
D
Weight difference before and after treatment (g)
6
4
2
0
-2
-4
***
***
LKO - - + +
0.2% Statin - + - +
E
Relative Plasma ALT Levels
(%)
1500
1000
500
0
*
*
LKO - - + +
0.2% Statin - + - +
F
0.2% Statin - + - + - + - +
MMP14Flox
MMP14LKO
MMP14Flox
MMP14LKO
Male
Female

Figure 4. 3. The effects of 0.2% lovastatin in the western diet on MMP14Flox and MMP14LKO mice. MMP14Flox and MMP14LKO mice were first fed by a powered western diet for 10 days and then fed by a powered western diet supplemented with or without 0.2% lovastatin *ad libitum* for additional 10 days. After that mice were euthanized after a 12-hour fasting, and tissues were collected. (**A** and **B**) **Effects of 0.2% lovastatin on the hepatic LDLR.** Liver samples were homogenized and subjected to immunoblotting. 50 ug of each sample was loaded and separated by SDS-PAGE. Proteins on the immunoblots were then detected by rabbit anti-mouse LDLR and mouse anti-GAPDH antibodies. (**C**) **Quantification of hepatic LDLR levels.** The relative densitometry was the ratio of the densitometry of LDLR to GAPDH in the same condition. The average relative densitometries of LDLR of MMP14Flox mice in each blot were set as 100% and used to normalize all the LDLR bands in the same blot. (**D**) **Weight change after lovastatin treatment.** Weight changes were calculated from the weight of mice on day 20 subtracting the weight of mice on day 10. (**E**) **Plasma alanine aminotransferase (ALT) activities.** The ALT levels of mouse plasma on day 20 were measured by using Alanine Transaminase Colorimetric Activity Assay Kit (Cayman Chemical) or Micro Alanine Aminotransferase (ALT/GPT) Activity Assay Kit (Abbkine) according to the manufacturer's instructions. The plasma ALT levels were normalized by the average plasma ALT levels of mice fed by Western diet only. (**F**) **Representative images of mouse livers.** Left lobes of mouse livers were collected and preserved in 10% formalin solution. Images were taken after the left lobes were formalin-fixed. The scale bar represents 1 cm in length. Values of all data were mean with S. D.. Two-way ANOVA followed by multiple comparisons was used to analyze and determine the statistical significance between groups in (**C** and **D**). Student's *t*-test was used to analyze and determine the statistical significance between groups in (**E**). n = 6 (3 males and 3 females) for each group except for MMP14LKO mice fed by western diet n = 5 (2 males and 3 females); ns = not significant; *, $p < 0.05$; **, $p < 0.01$; ***, $p < 0.001$; ****, $p < 0.0001$.

4.3 Discussion

Stains is a class of efficient and widespread LDL-cholesterol lowering medication that has been applied on hypercholesterolemia patients for decades to reduce the incidence of major CVDs and slow down the progression of existing CVDs [267]. Even though statins are the guideline-directed primary medications for the prevention of CVDs and statins are considered to be safe and well-tolerated in most adults, there are still some concerns regarding statin-induced adverse events and over-prescription of statins [329]. The major reason for over-prescription is due to the insufficient LDL-cholesterol reduction by statin monotherapy in certain patients [270]. Recently, Alabi et al. reported that MT1-MMP is able to shed the cell surface LDLR and knockdown of MT1-MMP can significantly increase hepatic LDLR levels as well as reduce plasma LDL-cholesterol levels [174]. Here, we investigated the effects of MT1-MMP knockdown in the absence or presence of statin treatments through *in vitro* and *in vivo* studies. Our *in vitro* study showed that by using MT1-MMP knockdown and statin treatment together, the LDLR levels can be increased by almost 3-fold.

We found that MT1-MMP knockdown has an additive effect on the increase of cellular LDLR levels in the presence of statin treatment (**Fig. 4.2**). However, high doses of lovastatin showed cytotoxicity. Consistently, Bridgeman et al. reported dose-dependent decreases of cell viability in four different statins [330]. To avoid the cell mortality induced by both lovastatin and transfection reagent, 1 μM of lovastatin was used in the study. Sole treatments of MT1-MMP knockdown or 1 μM of lovastatin increased LDLR protein levels by ~60% and ~170%, respectively (**Fig. 4.2A** and **4.2B**). As expected, combing MT1-MMP knockdown and 1 μM of

lovastatin treatments showed an enhanced LDLR increase effect which produced an ~230% increase. This agreed with our hypothesis that MT1-MMP knockdown has an additive effect on increasing LDLR levels combed with statin treatment. MT1-MMP knockdown reduces the post-translational shedding of LDLR and statins activate the transcription of LDLR [174,267]. Thus, mechanisms of MT1-MMP knockdown and statin in regulating LDLR levels are independent and additive. The results on mRNA levels also supported the independence that MT1-MMP knockdown and statin treatment did not significantly affected the transcriptions of related genes of each other (**Fig. 4.2C** to **E**). These results corroborate the finding of Alabi et al.'s work regarding the potential of MT1-MMP as a new therapeutic target in treating hypercholesteremia [174].

Next, we shifted our research to focus on the effect of hepatic MT1-MMP knockdown in the presence of statin treatments. 0.2% (w/w) of lovastatin was supplemented into the food fed to mice for 10 days which is a common strategy for lovastatin administration in mice model [331,332]. Unlike other research carried out in this area, mice fed with lovastatin experienced decreases in body weight (**Fig. 4.3D**) and a few cases of death. The amount of lovastatin administrated to mice was initially estimated as 400 mg/kg/day based on the assumption of 4 g of food intake daily and 20 g of body weight. The minimal toxic dose of lovastatin to mice was reported as 500 mg/kg/day [333]. The reason for applying a high dose of lovastatin was to better study the additive effect of hepatic MT1-MMP knockdown on LDLR levels. Unfortunately, mice fed with 0.2% lovastatin suffered from liver damage which was proved by elevated plasma ALT levels (**Fig. 4.3E**). A possible explanation for this might be that our mice were fed with western diet instead of chow diet which might increase the daily food intake or impose an additional

burden on liver function [334]. It might push the liver across the safety boundary when a 400 mg/kg/day dose of lovastatin had already stressed the liver. This is an important issue for future research that reduced lovastatin dosage should be applied when mice were fed with western diet. Unexpected liver injury in mice caused by high-dose statin also alerted us to the danger of statin overdose and statin-induced liver injury [335]. Lowering statin dosage by combing another cholesterol lowering strategy to achieve the same effect is a possible method of prevention of statin-induced liver injury, which is the purpose of this study.

Statins as the gold-standard treatment for the reduction of high LDL-cholesterol levels in the blood and subsequently prevention of CVDs seem would not be changed in the next few decades. Hence, finding a way to reduce statin-related adverse events and enhance statin efficacy in lowering LDL-cholesterol is an urgent request. Statin combination therapies are the most potential approach to reach the goal that two or more medications act together to facilitate the lowering of LDL-cholesterol [278]. Here we test the possibility of utilizing MT1-MMP as a target and combining it with normal statin treatment as a new statin combination therapy. Our *in vitro* study showed promising results in increasing the hepatic LDLR levels through two independent pathways. However, the *in vivo* study in mice was not successful in proving the efficacy of MT1-MMP knockdown and statin combined treatment which was largely due to statin intolerance. Yet, this negative result further emphasizes the importance of the prevention of statin intolerance and the necessity of new statin combination therapies.

Chapter 5

Conclusion and Future Directions

5.1 Conclusion

The purpose of the current study was to determine the effects of MT1-MMP on the LDLR family. The LDLR family is a group of versatile transmembrane receptors regulating lipid metabolism [3], nervous system development [336], cancer progression [276] and so on. The LDLR family members have been widely believed to be shed and regulated by metalloproteinases [185]. Independent studies have shown that a few metalloproteinase members are responsible for the shedding of different individual LDLR family members [179,337]. However, it was unclear whether a specific metalloproteinase can shed the entire LDLR family. MT1-MMP is a key member of matrix metalloproteinases that play critical roles in extracellular matrix remodelling [186]. MT1-MMP regulates the extracellular matrix homeostasis involving embryogenesis [210], angiogenesis [292] and cancer progression [229]. It has been reported that MT1-MMP mediates the ectodomain shedding of LDLR, LRP1 and LRP4 [174,176,277]. In this study, we provide new evidence that MT1-MMP also mediates the degradation of other LDLR family members. Meanwhile, due to the importance of MT1-MMP-mediated hepatic LDLR shedding in cholesterol homeostasis, we investigated the possibility of targeting hepatic MT1-MMP as an additional treatment combined with the traditional statin therapy.

MT1-MMP was able to mediate the degradation of all screened mature forms of LDLR family members. The proteolytic activity of MT1-MMP was responsible for the degradation of LDLR family members except for LRP10. The mechanism of LRP10 degradation induced by MT1-MMP was unknown but at least it was proteasome- and lysosome-independent. During the degradation of LRP3 and LRP11 by MT1-MMP, it also generated prolonged C-terminal

fragments of LRP3 and LRP11 retaining in the cell. The exact functions of CTF-LRP3 and CTF-LRP11 were unknown. Yet, CTF-LRP3 interacted and colocalized with MT1-MMP but LRP11 did not. Further research should be undertaken to investigate the degradation mechanism of LRP10 and the biological roles of CTF-LRP3 and CTF-LRP11.

Statin monotherapy has limited effect on reducing LDL-cholesterol by maximal ~50% and it is accompanied by dose-dependent adverse effects [278,279]. MT1-MMP knockdown has shown an additive effect together with lovastatin treatment on increasing the LDLR levels in HepG2 cells. LDLR levels are regulated by MT1-MMP through post-translational shedding and by statin through LDLR transcriptional activation [174,267]. Mice fed with a Western diet supplemented with high-dose lovastatin have shown statin-induced liver damage and were unfortunately unable to demonstrate the additive effect of MT1-MMP knockdown. The study should be repeated using a low dose of lovastatin.

Our work has led to the conclusion that MT1-MMP regulates the cellular levels of LDLR family members. It suggests that MT1-MMP should be considered as a potential target when studying the LDLR family member related biological processes.

5.2 Future Directions

- **Confirm the presence of ectodomain fragments of each LDLR family member**

In current study, the LDLR family members we expressed in cells were C-terminal tagged so only the C-terminal fragments could be detected. Metalloproteinases-mediated degradation of

LDLR family members is generally believed through cell surface ectodomain shedding [185]. Thus, the presence of soluble ectodomain fragments of LDLR family members would help us understand the mechanism of MT1-MMP-mediated degradation of LDLR family members. After shedding, the soluble ectodomain of LDLR family members are still partially functional. For example, the ectodomain of LRP4 is proven to inhibit canonical Wnt/β-catenin signaling as the full-length LRP4 [182]. Studying the ectodomain fragments can help us understand the physiological role of LDLR family member shedding.

- **Investigate the mechanisms of MT1-MMP-mediated degradation of LPR10**

In our study, the mechanism of MT1-MMP-mediated degradation of LRP10 was unclear. It did not rely on the proteolytic activity of MT1-MMP or each major structural domain of MT1-MMP. The degradation was also independent of the proteasomal or lysosomal pathway. Based on the unique subcellular distribution of LRP10 cycling between the *trans*-Golgi network and early endosomes [133], it suggests that early endosomes may play a role in the degradation of LRP10.

- **Investigate the roles of CTF-LRP3 and CTF-LRP11**

We observed prolonged CTF-LRP3 and CTF-LRP11 retaining in the cell in the presence of MT1-MMP. Both LRP3 and LRP11 are poorly studied and it is the first time reporting the existence of their C-terminal fragments generated by MT1-MMP. Two molecular masses of LRP3 have been reported elsewhere[70,72,73] which implies that full-length and CTF of LRP3 are both noteworthy. LRP3 levels were detectable in multiple mouse tissues, and its expression in

certain tissues (e.g. the skin) were affected in inducible MT1-MMP whole-body conditional knockout mice (**Fig. 5.1**). CTF-LRP11 has never been observed before and the potential role of full-length LRP11 and CTF-LRP11 requires further research.

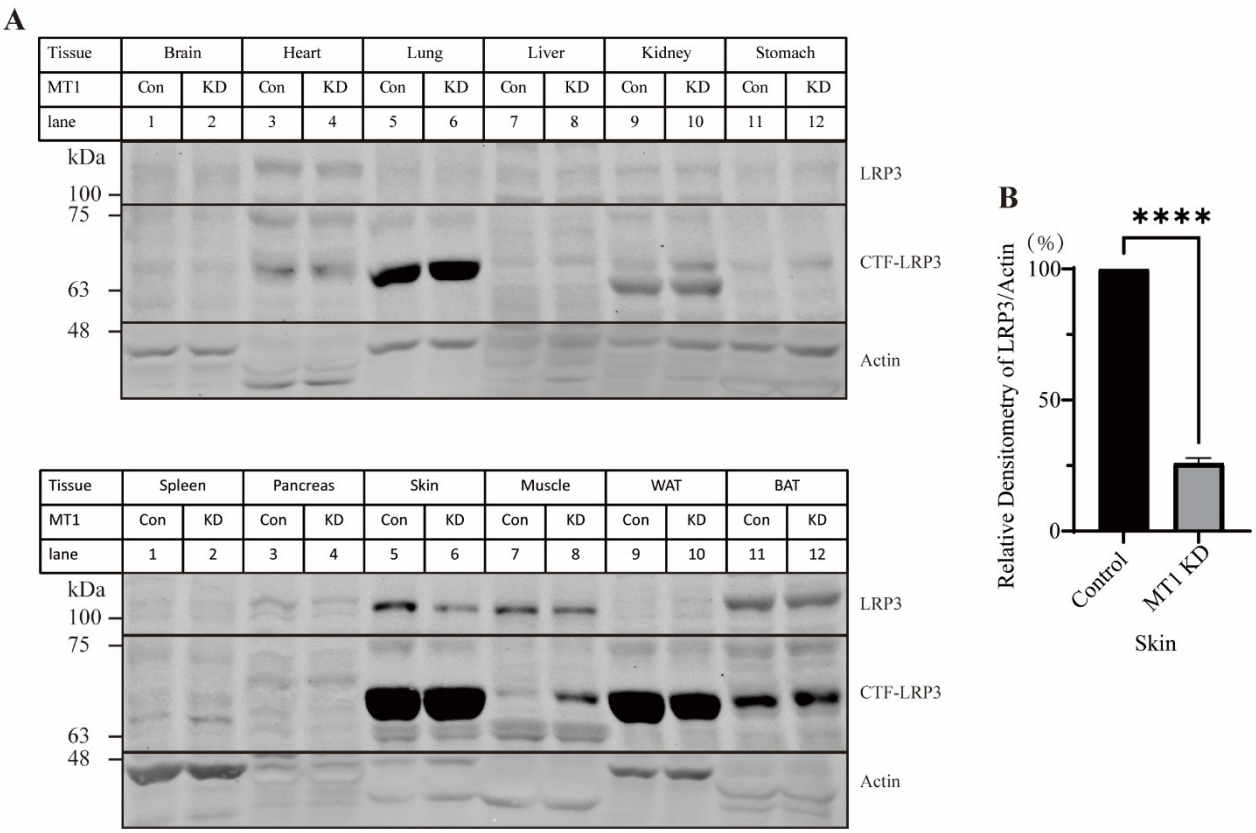

Figure 5. 1. The effects of MT1-MMP knockdown on mouse tissues. (**A**) **Screening the LRP3 levels in tissues of whole-body knockdown mouse.** ROSA26Cre-*Mmp14*^{Flox} mice were either injected with olive oil (n = 3) or tamoxifen (n = 3) dissolved in olive oil (75 mg/kg) to induce MT1-MMP knockdown. The tissues listed above were collected after 3 weeks of injection. Tissues were then homogenized in RIPA buffer supplemented with proteinase inhibitors. 50 μg of total proteins of each tissue homogenate were then subjected to immunoblotting. Proteins on immunoblots were detected by rabbit anti-LRP3 (Proteintech) and mouse anti-Actin antibodies. (**B**) **Quantifications of full-length LRP3 in the skin.** The relative densitometry was the ratio of the densitometry of LRP3 to Actin in the same condition. The relative densitometries of LRP3 with olive oil injection were defined as 100%. Values of all data were mean with S. D.. Student *t*-test was used to analyze and determine the statistical significance between groups. n = 3 for each condition; ns = not significant; *, $p < 0.05$; **, $p < 0.01$; ***, $p < 0.001$; ****, $p < 0.0001$.

- **Research the combinative effects of MT1-MMP knockdown and statin treatment**

In our study, a Western diet supplemented with 0.2% lovastatin caused liver damage in mice. These mice did not provide us with a suitable model to study the combinative effects of MT1-MMP knockdown. Hence, a low dosage of lovastatin should be applied to future research.

Bibliography

1. Herz, J. & Willnow, T.E. Functions of the LDL receptor gene family. *Ann N Y Acad Sci* **737**, 14-19 (1994).
2. Reading, B.J.*, et al.* Lrp13 is a novel vertebrate lipoprotein receptor that binds vitellogenins in teleost fishes. *J Lipid Res* **55**, 2287-2295 (2014).
3. Go, G.W. & Mani, A. Low-density lipoprotein receptor (LDLR) family orchestrates cholesterol homeostasis. *Yale J Biol Med* **85**, 19-28 (2012).
4. Esser, V., Limbird, L.E., Brown, M.S., Goldstein, J.L. & Russell, D.W. Mutational analysis of the ligand binding domain of the low density lipoprotein receptor. *J Biol Chem* **263**, 13282-13290 (1988).
5. Nogi, T. How multi-scale structural biology elucidated context-dependent variability in ectodomain conformation along with the ligand capture and release cycle for LDLR family members. *Biophys Rev* **10**, 481-492 (2018).
6. Chen, W.J., Goldstein, J.L. & Brown, M.S. NPXY, a sequence often found in cytoplasmic tails, is required for coated pit-mediated internalization of the low density lipoprotein receptor. *J Biol Chem* **265**, 3116-3123 (1990).
7. May, P. & Herz, J. LDL receptor-related proteins in neurodevelopment. *Traffic* **4**, 291-301 (2003).
8. Principe, C., Dionisio de Sousa, I.J., Prazeres, H., Soares, P. & Lima, R.T. LRP1B: A Giant Lost in Cancer Translation. *Pharmaceuticals (Basel)* **14**(2021).
9. Guo, J.*, et al.* MANSC: a seven-cysteine-containing domain present in animal membrane and extracellular proteins. *Trends Biochem Sci* **29**, 172-174 (2004).
10. Calvier, L., Herz, J. & Hansmann, G. Interplay of Low-Density Lipoprotein Receptors, LRPs, and Lipoproteins in Pulmonary Hypertension. *JACC Basic Transl Sci* **7**, 164-180 (2022).
11. Goldstein, J.L. & Brown, M.S. Familial hypercholesterolemia: identification of a defect in the regulation of 3-hydroxy-3-methylglutaryl coenzyme A reductase activity associated with overproduction of cholesterol. *Proc Natl Acad Sci U S A* **70**, 2804-2808 (1973).
12. Goldstein, J.L. & Brown, M.S. The LDL receptor. *Arterioscler Thromb Vasc Biol* **29**, 431-438 (2009).
13. Tolleshaug, H., Goldstein, J.L., Schneider, W.J. & Brown, M.S. Posttranslational processing of the LDL receptor and its genetic disruption in familial hypercholesterolemia. *Cell* **30**, 715-724 (1982).
14. Filipovic, I. Effect of inhibiting N-glycosylation on the stability and binding activity of the low density lipoprotein receptor. *J Biol Chem* **264**, 8815-8820 (1989).
15. Wang, S.*, et al.* Site-specific O-glycosylation of members of the low-density lipoprotein receptor superfamily enhances ligand interactions. *J Biol Chem* **294**, 8349 (2019).
16. Gu, H.M. & Zhang, D.W. Hypercholesterolemia, low density lipoprotein receptor and proprotein convertase subtilisin/kexin-type 9. *J Biomed Res* **29**, 356-361 (2015).
17. Russell, D.W., Brown, M.S. & Goldstein, J.L. Different combinations of cysteine-rich

repeats mediate binding of low density lipoprotein receptor to two different proteins. *J Biol Chem* **264**, 21682-21688 (1989).
18. Martinez-Olivan, J., Arias-Moreno, X., Velazquez-Campoy, A., Millet, O. & Sancho, J. LDL receptor/lipoprotein recognition: endosomal weakening of ApoB and ApoE binding to the convex face of the LR5 repeat. *FEBS J* **281**, 1534-1546 (2014).
19. Anderson, R.G., Brown, M.S. & Goldstein, J.L. Role of the coated endocytic vesicle in the uptake of receptor-bound low density lipoprotein in human fibroblasts. *Cell* **10**, 351-364 (1977).
20. Pearse, B.M. Clathrin: a unique protein associated with intracellular transfer of membrane by coated vesicles. *Proc Natl Acad Sci U S A* **73**, 1255-1259 (1976).
21. Rudenko, G.*, et al.* Structure of the LDL receptor extracellular domain at endosomal pH. *Science* **298**, 2353-2358 (2002).
22. Brown, M.S., Anderson, R.G. & Goldstein, J.L. Recycling receptors: the round-trip itinerary of migrant membrane proteins. *Cell* **32**, 663-667 (1983).
23. Defesche, J.C.*, et al.* Familial hypercholesterolaemia. *Nat Rev Dis Primers* **3**, 17093 (2017).
24. McGowan, M.P., Hosseini Dehkordi, S.H., Moriarty, P.M. & Duell, P.B. Diagnosis and Treatment of Heterozygous Familial Hypercholesterolemia. *J Am Heart Assoc* **8**, e013225 (2019).
25. Cuchel, M.*, et al.* Homozygous familial hypercholesterolaemia: new insights and guidance for clinicians to improve detection and clinical management. A position paper from the Consensus Panel on Familial Hypercholesterolaemia of the European Atherosclerosis Society. *Eur Heart J* **35**, 2146-2157 (2014).
26. Herz, J.*, et al.* Surface location and high affinity for calcium of a 500-kd liver membrane protein closely related to the LDL-receptor suggest a physiological role as lipoprotein receptor. *EMBO J* **7**, 4119-4127 (1988).
27. Herz, J., Kowal, R.C., Goldstein, J.L. & Brown, M.S. Proteolytic processing of the 600 kd low density lipoprotein receptor-related protein (LRP) occurs in a trans-Golgi compartment. *EMBO J* **9**, 1769-1776 (1990).
28. Nichols, C.E.*, et al.* Lrp1 Regulation of Pulmonary Function. Follow-Up of Human GWAS in Mice. *Am J Respir Cell Mol Biol* **64**, 368-378 (2021).
29. Gonias, S.L. & Campana, W.M. LDL receptor-related protein-1: a regulator of inflammation in atherosclerosis, cancer, and injury to the nervous system. *Am J Pathol* **184**, 18-27 (2014).
30. Rohlmann, A., Gotthardt, M., Hammer, R.E. & Herz, J. Inducible inactivation of hepatic LRP gene by cre-mediated recombination confirms role of LRP in clearance of chylomicron remnants. *J Clin Invest* **101**, 689-695 (1998).
31. Kowal, R.C., Herz, J., Goldstein, J.L., Esser, V. & Brown, M.S. Low density lipoprotein receptor-related protein mediates uptake of cholesteryl esters derived from apoprotein E-enriched lipoproteins. *Proc Natl Acad Sci U S A* **86**, 5810-5814 (1989).
32. Herz, J., Clouthier, D.E. & Hammer, R.E. LDL receptor-related protein internalizes and degrades uPA-PAI-1 complexes and is essential for embryo implantation. *Cell* **71**, 411-421 (1992).
33. Mao, H., Xie, L. & Pi, X. Low-Density Lipoprotein Receptor-Related Protein-1

Signaling in Angiogenesis. *Front Cardiovasc Med* **4**, 34 (2017).
34. Ramanathan, A., Nelson, A.R., Sagare, A.P. & Zlokovic, B.V. Impaired vascular-mediated clearance of brain amyloid beta in Alzheimer's disease: the role, regulation and restoration of LRP1. *Front Aging Neurosci* **7**, 136 (2015).
35. Xing, P.*, et al.* Roles of low-density lipoprotein receptor-related protein 1 in tumors. *Chin J Cancer* **35**, 6 (2016).
36. Au, D.T., Arai, A.L., Fondrie, W.E., Muratoglu, S.C. & Strickland, D.K. Role of the LDL Receptor-Related Protein 1 in Regulating Protease Activity and Signaling Pathways in the Vasculature. *Curr Drug Targets* **19**, 1276-1288 (2018).
37. van de Sluis, B., Wijers, M. & Herz, J. News on the molecular regulation and function of hepatic low-density lipoprotein receptor and LDLR-related protein 1. *Curr Opin Lipidol* **28**, 241-247 (2017).
38. Potere, N., Del Buono, M.G., Mauro, A.G., Abbate, A. & Toldo, S. Low Density Lipoprotein Receptor-Related Protein-1 in Cardiac Inflammation and Infarct Healing. *Front Cardiovasc Med* **6**, 51 (2019).
39. Liu, C.X., Li, Y., Obermoeller-McCormick, L.M., Schwartz, A.L. & Bu, G. The putative tumor suppressor LRP1B, a novel member of the low density lipoprotein (LDL) receptor family, exhibits both overlapping and distinct properties with the LDL receptor-related protein. *J Biol Chem* **276**, 28889-28896 (2001).
40. Pastrana, D.V., Hanson, A.J., Knisely, J., Bu, G. & Fitzgerald, D.J. LRP 1 B functions as a receptor for Pseudomonas exotoxin. *Biochim Biophys Acta* **1741**, 234-239 (2005).
41. Wagner, T. & Pietrzik, C.U. The role of lipoprotein receptors on the physiological function of APP. *Exp Brain Res* **217**, 377-387 (2012).
42. Cam, J.A., Zerbinatti, C.V., Li, Y. & Bu, G. Rapid endocytosis of the low density lipoprotein receptor-related protein modulates cell surface distribution and processing of the beta-amyloid precursor protein. *J Biol Chem* **280**, 15464-15470 (2005).
43. Cam, J.A.*, et al.* The low density lipoprotein receptor-related protein 1B retains beta-amyloid precursor protein at the cell surface and reduces amyloid-beta peptide production. *J Biol Chem* **279**, 29639-29646 (2004).
44. Liu, C.X.*, et al.* LRP-DIT, a putative endocytic receptor gene, is frequently inactivated in non-small cell lung cancer cell lines. *Cancer Res* **60**, 1961-1967 (2000).
45. Yu, G.*, et al.* LRP1B mutation associates with increased tumor mutation burden and inferior prognosis in liver hepatocellular carcinoma. *Medicine (Baltimore)* **101**, e29763 (2022).
46. Langbein, S.*, et al.* Alteration of the LRP1B gene region is associated with high grade of urothelial cancer. *Lab Invest* **82**, 639-643 (2002).
47. Nakagawa, T.*, et al.* Genetic or epigenetic silencing of low density lipoprotein receptor-related protein 1B expression in oral squamous cell carcinoma. *Cancer Sci* **97**, 1070-1074 (2006).
48. Cowin, P.A.*, et al.* LRP1B deletion in high-grade serous ovarian cancers is associated with acquired chemotherapy resistance to liposomal doxorubicin. *Cancer Res* **72**, 4060-4073 (2012).
49. Ni, S.*, et al.* Down expression of LRP1B promotes cell migration via RhoA/Cdc42 pathway and actin cytoskeleton remodeling in renal cell cancer. *Cancer Sci* **104**, 817-

825 (2013).
50. Li, Y.*, et al.* Low density lipoprotein (LDL) receptor-related protein 1B impairs urokinase receptor regeneration on the cell surface and inhibits cell migration. *J Biol Chem* **277**, 42366-42371 (2002).
51. Wang, Z.*, et al.* Down-regulation of LRP1B in colon cancer promoted the growth and migration of cancer cells. *Exp Cell Res* **357**, 1-8 (2017).
52. Christensen, E.I. & Birn, H. Megalin and cubilin: multifunctional endocytic receptors. *Nat Rev Mol Cell Biol* **3**, 256-266 (2002).
53. Pieper-Furst, U. & Lammert, F. Low-density lipoprotein receptors in liver: old acquaintances and a newcomer. *Biochim Biophys Acta* **1831**, 1191-1198 (2013).
54. Christensen, E.I., Birn, H., Storm, T., Weyer, K. & Nielsen, R. Endocytic receptors in the renal proximal tubule. *Physiology (Bethesda)* **27**, 223-236 (2012).
55. Willnow, T.E.*, et al.* Defective forebrain development in mice lacking gp330/megalin. *Proc Natl Acad Sci U S A* **93**, 8460-8464 (1996).
56. Elsakka, E.G.E., Mokhtar, M.M., Hegazy, M., Ismail, A. & Doghish, A.S. Megalin, a multi-ligand endocytic receptor, and its participation in renal function and diseases: A review. *Life Sci* **308**, 120923 (2022).
57. Moestrup, S.K. & Verroust, P.J. Megalin- and cubilin-mediated endocytosis of protein-bound vitamins, lipids, and hormones in polarized epithelia. *Annu Rev Nutr* **21**, 407-428 (2001).
58. Nykjaer, A.*, et al.* An endocytic pathway essential for renal uptake and activation of the steroid 25-(OH) vitamin D3. *Cell* **96**, 507-515 (1999).
59. Leheste, J.R.*, et al.* Hypocalcemia and osteopathy in mice with kidney-specific megalin gene defect. *FASEB J* **17**, 247-249 (2003).
60. Nielsen, R., Christensen, E.I. & Birn, H. Megalin and cubilin in proximal tubule protein reabsorption: from experimental models to human disease. *Kidney Int* **89**, 58-67 (2016).
61. Hilpert, J.*, et al.* Megalin antagonizes activation of the parathyroid hormone receptor. *J Biol Chem* **274**, 5620-5625 (1999).
62. Hammes, A.*, et al.* Role of endocytosis in cellular uptake of sex steroids. *Cell* **122**, 751-762 (2005).
63. Kerjaschki, D. & Farquhar, M.G. The pathogenic antigen of Heymann nephritis is a membrane glycoprotein of the renal proximal tubule brush border. *Proc Natl Acad Sci U S A* **79**, 5557-5561 (1982).
64. Uhlen, M.*, et al.* Proteomics. Tissue-based map of the human proteome. *Science* **347**, 1260419 (2015).
65. Mahadevappa, R., Nielsen, R., Christensen, E.I. & Birn, H. Megalin in acute kidney injury: foe and friend. *Am J Physiol Renal Physiol* **306**, F147-154 (2014).
66. Mori, K.*, et al.* Endocytic delivery of lipocalin-siderophore-iron complex rescues the kidney from ischemia-reperfusion injury. *J Clin Invest* **115**, 610-621 (2005).
67. Jobst-Schwan, T.*, et al.* Renal uptake of the antiapoptotic protein survivin is mediated by megalin at the apical membrane of the proximal tubule. *Am J Physiol Renal Physiol* **305**, F734-744 (2013).
68. Quiros, Y., Vicente-Vicente, L., Morales, A.I., Lopez-Novoa, J.M. & Lopez-Hernandez, F.J. An integrative overview on the mechanisms underlying the renal tubular

cytotoxicity of gentamicin. *Toxicol Sci* **119**, 245-256 (2011).
69. Ishii, H.*, et al.* cDNA cloning of a new low-density lipoprotein receptor-related protein and mapping of its gene (LRP3) to chromosome bands 19q12-q13. 2. *Genomics* **51**, 132-135 (1998).
70. Cuchillo-Ibanez, I.*, et al.* The apolipoprotein receptor LRP3 compromises APP levels. *Alzheimers Res Ther* **13**, 181 (2021).
71. Elsafadi, M.*, et al.* MicroRNA-4739 regulates osteogenic and adipocytic differentiation of immortalized human bone marrow stromal cells via targeting LRP3. *Stem Cell Res* **20**, 94-104 (2017).
72. Shi, Y.*, et al.* Inhibition of LDL receptor-related protein 3 suppresses chondrogenesis of stem cells, inhibits proliferation, and promotes apoptosis. *Biochem Biophys Res Commun* **635**, 77-83 (2022).
73. Cao, C.*, et al.* Cholesterol-induced LRP3 downregulation promotes cartilage degeneration in osteoarthritis by targeting Syndecan-4. *Nat Commun* **13**, 7139 (2022).
74. May, P., Woldt, E., Matz, R.L. & Boucher, P. The LDL receptor-related protein (LRP) family: an old family of proteins with new physiological functions. *Ann Med* **39**, 219-228 (2007).
75. Wu, H.*, et al.* Distinct roles of muscle and motoneuron LRP4 in neuromuscular junction formation. *Neuron* **75**, 94-107 (2012).
76. Nakayama, M.*, et al.* Identification of high-molecular-weight proteins with multiple EGF-like motifs by motif-trap screening. *Genomics* **51**, 27-34 (1998).
77. Johnson, E.B., Hammer, R.E. & Herz, J. Abnormal development of the apical ectodermal ridge and polysyndactyly in Megf7-deficient mice. *Hum Mol Genet* **14**, 3523-3538 (2005).
78. Fliniaux, I., Mikkola, M.L., Lefebvre, S. & Thesleff, I. Identification of dkk4 as a target of Eda-A1/Edar pathway reveals an unexpected role of ectodysplasin as inhibitor of Wnt signalling in ectodermal placodes. *Dev Biol* **320**, 60-71 (2008).
79. Zhang, B.*, et al.* Wnt proteins regulate acetylcholine receptor clustering in muscle cells. *Mol Brain* **5**, 7 (2012).
80. Bullock, W.A.*, et al.* Lrp4 Mediates Bone Homeostasis and Mechanotransduction through Interaction with Sclerostin In Vivo. *iScience* **20**, 205-215 (2019).
81. Davidson, G. LRPs in WNT Signalling. *Handb Exp Pharmacol* **269**, 45-73 (2021).
82. Leupin, O.*, et al.* Bone overgrowth-associated mutations in the LRP4 gene impair sclerostin facilitator function. *J Biol Chem* **286**, 19489-19500 (2011).
83. Choi, H.Y., Dieckmann, M., Herz, J. & Niemeier, A. Lrp4, a novel receptor for Dickkopf 1 and sclerostin, is expressed by osteoblasts and regulates bone growth and turnover in vivo. *PLoS One* **4**, e7930 (2009).
84. Fish, L.A. & Fallon, J.R. Multiple MuSK signaling pathways and the aging neuromuscular junction. *Neurosci Lett* **731**, 135014 (2020).
85. Tian, Q.B., Nakayama, K., Okano, A. & Suzuki, T. Identification of mRNAs localizing in the postsynaptic region. *Brain Res Mol Brain Res* **72**, 147-157 (1999).
86. Tian, Q.B.*, et al.* Interaction of LDL receptor-related protein 4 (LRP4) with postsynaptic scaffold proteins via its C-terminal PDZ domain-binding motif, and its regulation by Ca/calmodulin-dependent protein kinase II. *Eur J Neurosci* **23**, 2864-

2876 (2006).
87. Weatherbee, S.D., Anderson, K.V. & Niswander, L.A. LDL-receptor-related protein 4 is crucial for formation of the neuromuscular junction. *Development* **133**, 4993-5000 (2006).
88. DeChiara, T.M.*, et al.* The receptor tyrosine kinase MuSK is required for neuromuscular junction formation in vivo. *Cell* **85**, 501-512 (1996).
89. Gautam, M.*, et al.* Defective neuromuscular synaptogenesis in agrin-deficient mutant mice. *Cell* **85**, 525-535 (1996).
90. Glass, D.J.*, et al.* Agrin acts via a MuSK receptor complex. *Cell* **85**, 513-523 (1996).
91. Zhang, W., Coldefy, A.S., Hubbard, S.R. & Burden, S.J. Agrin binds to the N-terminal region of Lrp4 protein and stimulates association between Lrp4 and the first immunoglobulin-like domain in muscle-specific kinase (MuSK). *J Biol Chem* **286**, 40624-40630 (2011).
92. Zhang, B.*, et al.* LRP4 serves as a coreceptor of agrin. *Neuron* **60**, 285-297 (2008).
93. Zong, Y.*, et al.* Structural basis of agrin-LRP4-MuSK signaling. *Genes Dev* **26**, 247-258 (2012).
94. DePew, A.T. & Mosca, T.J. Conservation and Innovation: Versatile Roles for LRP4 in Nervous System Development. *J Dev Biol* **9**(2021).
95. Badders, N.M.*, et al.* The Wnt receptor, Lrp5, is expressed by mouse mammary stem cells and is required to maintain the basal lineage. *PLoS One* **4**, e6594 (2009).
96. Kelly, O.G., Pinson, K.I. & Skarnes, W.C. The Wnt co-receptors Lrp5 and Lrp6 are essential for gastrulation in mice. *Development* **131**, 2803-2815 (2004).
97. Hey, P.J.*, et al.* Cloning of a novel member of the low-density lipoprotein receptor family. *Gene* **216**, 103-111 (1998).
98. Brown, S.D.*, et al.* Isolation and characterization of LRP6, a novel member of the low density lipoprotein receptor gene family. *Biochem Biophys Res Commun* **248**, 879-888 (1998).
99. Kim, D.H.*, et al.* A new low density lipoprotein receptor related protein, LRP5, is expressed in hepatocytes and adrenal cortex, and recognizes apolipoprotein E. *J Biochem* **124**, 1072-1076 (1998).
100. Ye, Z.J.*, et al.* LRP6 protein regulates low density lipoprotein (LDL) receptor-mediated LDL uptake. *J Biol Chem* **287**, 1335-1344 (2012).
101. Tamai, K.*, et al.* LDL-receptor-related proteins in Wnt signal transduction. *Nature* **407**, 530-535 (2000).
102. Steinhart, Z. & Angers, S. Wnt signaling in development and tissue homeostasis. *Development* **145**(2018).
103. Pinson, K.I., Brennan, J., Monkley, S., Avery, B.J. & Skarnes, W.C. An LDL-receptor-related protein mediates Wnt signalling in mice. *Nature* **407**, 535-538 (2000).
104. Mao, J.*, et al.* Low-density lipoprotein receptor-related protein-5 binds to Axin and regulates the canonical Wnt signaling pathway. *Mol Cell* **7**, 801-809 (2001).
105. Zhan, T., Rindtorff, N. & Boutros, M. Wnt signaling in cancer. *Oncogene* **36**, 1461-1473 (2017).
106. Zhang, Y. & Wang, X. Targeting the Wnt/beta-catenin signaling pathway in cancer. *J Hematol Oncol* **13**, 165 (2020).

107. Li, Y. & Bu, G. LRP5/6 in Wnt signaling and tumorigenesis. *Future Oncol* **1**, 673-681 (2005).
108. Gong, Y.*, et al.* LDL receptor-related protein 5 (LRP5) affects bone accrual and eye development. *Cell* **107**, 513-523 (2001).
109. Boyden, L.M.*, et al.* High bone density due to a mutation in LDL-receptor-related protein 5. *N Engl J Med* **346**, 1513-1521 (2002).
110. Brance, M.L.*, et al.* High bone mass from mutation of low-density lipoprotein receptor-related protein 6 (LRP6). *Bone* **141**, 115550 (2020).
111. Lim, S.Y. Romosozumab for the treatment of osteoporosis in women: Efficacy, safety, and cardiovascular risk. *Womens Health (Lond)* **18**, 17455057221125577 (2022).
112. Joiner, D.M., Ke, J., Zhong, Z., Xu, H.E. & Williams, B.O. LRP5 and LRP6 in development and disease. *Trends Endocrinol Metab* **24**, 31-39 (2013).
113. Zhong, Z., Baker, J.J., Zylstra-Diegel, C.R. & Williams, B.O. Lrp5 and Lrp6 play compensatory roles in mouse intestinal development. *J Cell Biochem* **113**, 31-38 (2012).
114. Kim, D.H.*, et al.* Human apolipoprotein E receptor 2. A novel lipoprotein receptor of the low density lipoprotein receptor family predominantly expressed in brain. *J Biol Chem* **271**, 8373-8380 (1996).
115. Ruiz, J.*, et al.* The apoE isoform binding properties of the VLDL receptor reveal marked differences from LRP and the LDL receptor. *J Lipid Res* **46**, 1721-1731 (2005).
116. D'Arcangelo, G.*, et al.* Reelin is a ligand for lipoprotein receptors. *Neuron* **24**, 471-479 (1999).
117. Jokinen, E.V.*, et al.* Regulation of the very low density lipoprotein receptor by thyroid hormone in rat skeletal muscle. *J Biol Chem* **269**, 26411-26418 (1994).
118. Frykman, P.K., Brown, M.S., Yamamoto, T., Goldstein, J.L. & Herz, J. Normal plasma lipoproteins and fertility in gene-targeted mice homozygous for a disruption in the gene encoding very low density lipoprotein receptor. *Proc Natl Acad Sci U S A* **92**, 8453-8457 (1995).
119. Ulrich, V.*, et al.* Genetic variants of ApoE and ApoER2 differentially modulate endothelial function. *Proc Natl Acad Sci U S A* **111**, 13493-13498 (2014).
120. Tacken, P.J.*, et al.* LDL receptor deficiency unmasks altered VLDL triglyceride metabolism in VLDL receptor transgenic and knockout mice. *J Lipid Res* **41**, 2055-2062 (2000).
121. Boyles, J.K.*, et al.* A role for apolipoprotein E, apolipoprotein A-I, and low density lipoprotein receptors in cholesterol transport during regeneration and remyelination of the rat sciatic nerve. *J Clin Invest* **83**, 1015-1031 (1989).
122. Duit, S., Mayer, H., Blake, S.M., Schneider, W.J. & Nimpf, J. Differential functions of ApoER2 and very low density lipoprotein receptor in Reelin signaling depend on differential sorting of the receptors. *J Biol Chem* **285**, 4896-4908 (2010).
123. Trommsdorff, M.*, et al.* Reeler/Disabled-like disruption of neuronal migration in knockout mice lacking the VLDL receptor and ApoE receptor 2. *Cell* **97**, 689-701 (1999).
124. Boycott, K.M.*, et al.* Homozygous deletion of the very low density lipoprotein receptor gene causes autosomal recessive cerebellar hypoplasia with cerebral gyral simplification. *Am J Hum Genet* **77**, 477-483 (2005).

125. Strittmatter, W.J. & Roses, A.D. Apolipoprotein E and Alzheimer's disease. *Annu Rev Neurosci* **19**, 53-77 (1996).
126. Blanchard, J.W.*, et al.* APOE4 impairs myelination via cholesterol dysregulation in oligodendrocytes. *Nature* **611**, 769-779 (2022).
127. Holtzman, D.M., Herz, J. & Bu, G. Apolipoprotein E and apolipoprotein E receptors: normal biology and roles in Alzheimer disease. *Cold Spring Harb Perspect Med* **2**, a006312 (2012).
128. Chen, Y., Durakoglugil, M.S., Xian, X. & Herz, J. ApoE4 reduces glutamate receptor function and synaptic plasticity by selectively impairing ApoE receptor recycling. *Proc Natl Acad Sci U S A* **107**, 12011-12016 (2010).
129. Hoe, H.S.*, et al.* F-spondin interaction with the apolipoprotein E receptor ApoEr2 affects processing of amyloid precursor protein. *Mol Cell Biol* **25**, 9259-9268 (2005).
130. Weeber, E.J.*, et al.* Reelin and ApoE receptors cooperate to enhance hippocampal synaptic plasticity and learning. *J Biol Chem* **277**, 39944-39952 (2002).
131. Herring, A.*, et al.* Reelin depletion is an early phenomenon of Alzheimer's pathology. *J Alzheimers Dis* **30**, 963-979 (2012).
132. Sugiyama, T.*, et al.* A novel low-density lipoprotein receptor-related protein mediating cellular uptake of apolipoprotein E-enriched beta-VLDL in vitro. *Biochemistry* **39**, 15817-15825 (2000).
133. Boucher, R.*, et al.* Intracellular trafficking of LRP9 is dependent on two acidic cluster/dileucine motifs. *Histochem Cell Biol* **130**, 315-327 (2008).
134. Brodeur, J.*, et al.* Calnuc binds to LRP9 and affects its endosomal sorting. *Traffic* **10**, 1098-1114 (2009).
135. Brodeur, J.*, et al.* LDLR-related protein 10 (LRP10) regulates amyloid precursor protein (APP) trafficking and processing: evidence for a role in Alzheimer's disease. *Mol Neurodegener* **7**, 31 (2012).
136. Guo, L.*, et al.* Sex specific molecular networks and key drivers of Alzheimer's disease. *Mol Neurodegener* **18**, 39 (2023).
137. Quadri, M.*, et al.* LRP10 genetic variants in familial Parkinson's disease and dementia with Lewy bodies: a genome-wide linkage and sequencing study. *Lancet Neurol* **17**, 597-608 (2018).
138. Zhao, Y.*, et al.* The role of genetics in Parkinson's disease: a large cohort study in Chinese mainland population. *Brain* **143**, 2220-2234 (2020).
139. Chen, Y.*, et al.* LRP10 in autosomal-dominant Parkinson's disease. *Mov Disord* **34**, 912-916 (2019).
140. Daida, K.*, et al.* Mutation analysis of LRP10 in Japanese patients with familial Parkinson's disease, progressive supranuclear palsy, and frontotemporal dementia. *Neurobiol Aging* **84**, 235 e211-235 e216 (2019).
141. Grochowska, M.M.*, et al.* LRP10 interacts with SORL1 in the intracellular vesicle trafficking pathway in non-neuronal brain cells and localises to Lewy bodies in Parkinson's disease and dementia with Lewy bodies. *Acta Neuropathol* **142**, 117-137 (2021).
142. Gabrielsson, B.G.*, et al.* Evaluation of reference genes for studies of gene expression in human adipose tissue. *Obes Res* **13**, 649-652 (2005).

143. Wang, Y.*, et al.* The role of low density lipoprotein receptor-related protein 11 as a tumor promoter in cervical cancer. *Cancer Manag Res* **11**, 8081-8093 (2019).
144. Gan, S.*, et al.* LRP11 activates beta-catenin to induce PD-L1 expression in prostate cancer. *J Drug Target* **28**, 508-515 (2020).
145. Ye, H. & Zhang, N. Identification of the Upregulation of MRPL13 as a Novel Prognostic Marker Associated with Overall Survival Time and Immunotherapy Response in Breast Cancer. *Comput Math Methods Med* **2021**, 1498924 (2021).
146. Gu, F.*, et al.* An integrative pan-cancer analysis illustrating the key role of LRP11 in cervical cancer. *Medicine (Baltimore)* **102**, e33201 (2023).
147. Zhu, C.*, et al.* A Novel Gene Prognostic Signature Based on Differential DNA Methylation in Breast Cancer. *Front Genet* **12**, 742578 (2021).
148. Yang, X.*, et al.* Transcriptome analysis provides new insights into cold adaptation of corsac fox (Vulpes Corsac). *Ecol Evol* **12**, e8866 (2022).
149. Zhang, D.*, et al.* Min pig skeletal muscle response to cold stress. *PLoS One* **17**, e0274184 (2022).
150. Xu, J.*, et al.* Genetic regulatory network analysis reveals that low density lipoprotein receptor-related protein 11 is involved in stress responses in mice. *Psychiatry Res* **220**, 1131-1137 (2014).
151. Battle, M.A., Maher, V.M. & McCormick, J.J. ST7 is a novel low-density lipoprotein receptor-related protein (LRP) with a cytoplasmic tail that interacts with proteins related to signal transduction pathways. *Biochemistry* **42**, 7270-7282 (2003).
152. Qing, J., Wei, D., Maher, V.M. & McCormick, J.J. Cloning and characterization of a novel gene encoding a putative transmembrane protein with altered expression in some human transformed and tumor-derived cell lines. *Oncogene* **18**, 335-342 (1999).
153. Bethge, N.*, et al.* A gene panel, including LRP12, is frequently hypermethylated in major types of B-cell lymphoma. *PLoS One* **9**, e104249 (2014).
154. Grasse, S.*, et al.* Epigenomic profiling of non-small cell lung cancer xenografts uncover LRP12 DNA methylation as predictive biomarker for carboplatin resistance. *Genome Med* **10**, 55 (2018).
155. Huang, M.*, et al.* LRP12 is an endogenous transmembrane inactivator of alpha4 integrins. *Cell Rep* **42**, 112667 (2023).
156. Grote, A.*, et al.* LRP12 silencing during brain development results in cortical dyslamination and seizure sensitization. *Neurobiol Dis* **86**, 170-176 (2016).
157. Schneider, S., Gulacsi, A. & Hatten, M.E. Lrp12/Mig13a reveals changing patterns of preplate neuronal polarity during corticogenesis that are absent in reeler mutant mice. *Cereb Cortex* **21**, 134-144 (2011).
158. Gibbons, A.S., Thomas, E.A., Scarr, E. & Dean, B. Low Density Lipoprotein Receptor-Related Protein and Apolipoprotein E Expression is Altered in Schizophrenia. *Front Psychiatry* **1**, 19 (2010).
159. Ishiura, H.*, et al.* Noncoding CGG repeat expansions in neuronal intranuclear inclusion disease, oculopharyngodistal myopathy and an overlapping disease. *Nat Genet* **51**, 1222-1232 (2019).
160. Kumutpongpanich, T.*, et al.* Clinicopathologic Features of Oculopharyngodistal Myopathy With LRP12 CGG Repeat Expansions Compared With Other

Oculopharyngodistal Myopathy Subtypes. *JAMA Neurol* **78**, 853-863 (2021).
161. Davis, C.G.*, et al.* Acid-dependent ligand dissociation and recycling of LDL receptor mediated by growth factor homology region. *Nature* **326**, 760-765 (1987).
162. Lagace, T.A. PCSK9 and LDLR degradation: regulatory mechanisms in circulation and in cells. *Curr Opin Lipidol* **25**, 387-393 (2014).
163. Zelcer, N., Hong, C., Boyadjian, R. & Tontonoz, P. LXR regulates cholesterol uptake through Idol-dependent ubiquitination of the LDL receptor. *Science* **325**, 100-104 (2009).
164. Herz, J. & Strickland, D.K. LRP: a multifunctional scavenger and signaling receptor. *J Clin Invest* **108**, 779-784 (2001).
165. Melman, L.*, et al.* Proteasome regulates the delivery of LDL receptor-related protein into the degradation pathway. *Mol Biol Cell* **13**, 3325-3335 (2002).
166. Rondon-Ortiz, A.N.*, et al.* High Concentrations of Rosiglitazone Reduce mRNA and Protein Levels of LRP1 in HepG2 Cells. *Front Pharmacol* **8**, 772 (2017).
167. Canuel, M.*, et al.* Proprotein convertase subtilisin/kexin type 9 (PCSK9) can mediate degradation of the low density lipoprotein receptor-related protein 1 (LRP-1). *PLoS One* **8**, e64145 (2013).
168. Sandoval, L., Fuentealba, L.M. & Marzolo, M.P. Participation of OCRL1, and APPL1, in the expression, proteolysis, phosphorylation and endosomal trafficking of megalin: Implications for Lowe Syndrome. *Front Cell Dev Biol* **10**, 911664 (2022).
169. Poirier, S.*, et al.* The proprotein convertase PCSK9 induces the degradation of low density lipoprotein receptor (LDLR) and its closest family members VLDLR and ApoER2. *J Biol Chem* **283**, 2363-2372 (2008).
170. Liu, F.*, et al.* Suppression of Membranous LRP5 Recycling, Wnt/beta-Catenin Signaling, and Colon Carcinogenesis by 15-LOX-1 Peroxidation of Linoleic Acid in PI3P. *Cell Rep* **32**, 108049 (2020).
171. Kirsch, N.*, et al.* Angiopoietin-like 4 Is a Wnt Signaling Antagonist that Promotes LRP6 Turnover. *Dev Cell* **43**, 71-82 e76 (2017).
172. Clark, P. Protease-mediated ectodomain shedding. *Thorax* **69**, 682-684 (2014).
173. Hemming, M.L., Elias, J.E., Gygi, S.P. & Selkoe, D.J. Proteomic profiling of gamma-secretase substrates and mapping of substrate requirements. *PLoS Biol* **6**, e257 (2008).
174. Alabi, A.*, et al.* Membrane type 1 matrix metalloproteinase promotes LDL receptor shedding and accelerates the development of atherosclerosis. *Nat Commun* **12**, 1889 (2021).
175. Chen, Q., Takahashi, Y., Oka, K. & Ma, J.X. Functional Differences of Very-Low-Density Lipoprotein Receptor Splice Variants in Regulating Wnt Signaling. *Mol Cell Biol* **36**, 2645-2654 (2016).
176. Rozanov, D.V., Hahn-Dantona, E., Strickland, D.K. & Strongin, A.Y. The low density lipoprotein receptor-related protein LRP is regulated by membrane type-1 matrix metalloproteinase (MT1-MMP) proteolysis in malignant cells. *J Biol Chem* **279**, 4260-4268 (2004).
177. Zou, Z.*, et al.* Linking receptor-mediated endocytosis and cell signaling: evidence for regulated intramembrane proteolysis of megalin in proximal tubule. *J Biol Chem* **279**, 34302-34310 (2004).

178. Roubtsova, A.*, et al.* PCSK9 deficiency results in a specific shedding of excess LDLR in female mice only: Role of hepatic cholesterol. *Biochim Biophys Acta Mol Cell Biol Lipids* **1867**, 159217 (2022).
179. Ma, X.*, et al.* ADAM17 mediates ectodomain shedding of the soluble VLDL receptor fragment in the retinal epithelium. *J Biol Chem* **297**, 101185 (2021).
180. Liu, Q.*, et al.* LRP1 shedding in human brain: roles of ADAM10 and ADAM17. *Mol Neurodegener* **4**, 17 (2009).
181. Liu, C.X., Ranganathan, S., Robinson, S. & Strickland, D.K. gamma-Secretase-mediated release of the low density lipoprotein receptor-related protein 1B intracellular domain suppresses anchorage-independent growth of neuroglioma cells. *J Biol Chem* **282**, 7504-7511 (2007).
182. Dietrich, M.F.*, et al.* Ectodomains of the LDL receptor-related proteins LRP1b and LRP4 have anchorage independent functions in vivo. *PLoS One* **5**, e9960 (2010).
183. Seo, T.*, et al.* Haemorrhagic snake venom metalloproteases and human ADAMs cleave LRP5/6, which disrupts cell-cell adhesions in vitro and induces haemorrhage in vivo. *FEBS J* **284**, 1657-1671 (2017).
184. Hoe, H.S.*, et al.* The metalloprotease inhibitor TIMP-3 regulates amyloid precursor protein and apolipoprotein E receptor proteolysis. *J Neurosci* **27**, 10895-10905 (2007).
185. Emonard, H. & Marbaix, E. Low-density lipoprotein receptor-related protein in metalloproteinase-mediated pathologies: recent insights. *Metalloproteinases In Medicine* **2**, 9-18 (2015).
186. Itoh, Y. Membrane-type matrix metalloproteinases: Their functions and regulations. *Matrix Biol* **44-46**, 207-223 (2015).
187. Sato, H. & Seiki, M. Membrane-type matrix metalloproteinases (MT-MMPs) in tumor metastasis. *J Biochem* **119**, 209-215 (1996).
188. Nagase, H. Activation mechanisms of matrix metalloproteinases. *Biol Chem* **378**, 151-160 (1997).
189. Sato, H., Kinoshita, T., Takino, T., Nakayama, K. & Seiki, M. Activation of a recombinant membrane type 1-matrix metalloproteinase (MT1-MMP) by furin and its interaction with tissue inhibitor of metalloproteinases (TIMP)-2. *FEBS Lett* **393**, 101-104 (1996).
190. Yana, I. & Weiss, S.J. Regulation of membrane type-1 matrix metalloproteinase activation by proprotein convertases. *Mol Biol Cell* **11**, 2387-2401 (2000).
191. Golubkov, V.S.*, et al.* Membrane type-1 matrix metalloproteinase (MT1-MMP) exhibits an important intracellular cleavage function and causes chromosome instability. *J Biol Chem* **280**, 25079-25086 (2005).
192. Maybee, D.V., Ink, N.L. & Ali, M.A.M. Novel Roles of MT1-MMP and MMP-2: Beyond the Extracellular Milieu. *Int J Mol Sci* **23**(2022).
193. Xia, X.D.*, et al.* Membrane-type I matrix metalloproteinase (MT1-MMP), lipid metabolism, and therapeutic implications. *J Mol Cell Biol* **13**, 513-526 (2021).
194. Somerville, R.P., Oblander, S.A. & Apte, S.S. Matrix metalloproteinases: old dogs with new tricks. *Genome Biol* **4**, 216 (2003).
195. Golubkov, V.S.*, et al.* Internal cleavages of the autoinhibitory prodomain are required for membrane type 1 matrix metalloproteinase activation, although furin cleavage alone

generates inactive proteinase. *J Biol Chem* **285**, 27726-27736 (2010).
196. Georgiadis, D. & Yiotakis, A. Specific targeting of metzincin family members with small-molecule inhibitors: progress toward a multifarious challenge. *Bioorg Med Chem* **16**, 8781-8794 (2008).
197. Rozanov, D.V.*, et al.* Mutation analysis of membrane type-1 matrix metalloproteinase (MT1-MMP). The role of the cytoplasmic tail Cys(574), the active site Glu(240), and furin cleavage motifs in oligomerization, processing, and self-proteolysis of MT1-MMP expressed in breast carcinoma cells. *J Biol Chem* **276**, 25705-25714 (2001).
198. Cao, J.*, et al.* Distinct roles for the catalytic and hemopexin domains of membrane type 1-matrix metalloproteinase in substrate degradation and cell migration. *J Biol Chem* **279**, 14129-14139 (2004).
199. English, W.R., Holtz, B., Vogt, G., Knauper, V. & Murphy, G. Characterization of the role of the "MT-loop": an eight-amino acid insertion specific to progelatinase A (MMP2) activating membrane-type matrix metalloproteinases. *J Biol Chem* **276**, 42018-42026 (2001).
200. Woskowicz, A.M., Weaver, S.A., Shitomi, Y., Ito, N. & Itoh, Y. MT-LOOP-dependent localization of membrane type I matrix metalloproteinase (MT1-MMP) to the cell adhesion complexes promotes cancer cell invasion. *J Biol Chem* **288**, 35126-35137 (2013).
201. Wang, M.*, et al.* Identification of amino acid residues in the MT-loop of MT1-MMP critical for its ability to cleave low-density lipoprotein receptor. *Front Cardiovasc Med* **9**, 917238 (2022).
202. Itoh, Y.*, et al.* Cell surface collagenolysis requires homodimerization of the membrane-bound collagenase MT1-MMP. *Mol Biol Cell* **17**, 5390-5399 (2006).
203. Kajita, M.*, et al.* Membrane-type 1 matrix metalloproteinase cleaves CD44 and promotes cell migration. *J Cell Biol* **153**, 893-904 (2001).
204. Mori, H.*, et al.* CD44 directs membrane-type 1 matrix metalloproteinase to lamellipodia by associating with its hemopexin-like domain. *EMBO J* **21**, 3949-3959 (2002).
205. Wu, Y.I.*, et al.* Glycosylation broadens the substrate profile of membrane type 1 matrix metalloproteinase. *J Biol Chem* **279**, 8278-8289 (2004).
206. Itoh, Y., Ito, N., Nagase, H. & Seiki, M. The second dimer interface of MT1-MMP, the transmembrane domain, is essential for ProMMP-2 activation on the cell surface. *J Biol Chem* **283**, 13053-13062 (2008).
207. Jiang, A.*, et al.* Regulation of membrane-type matrix metalloproteinase 1 activity by dynamin-mediated endocytosis. *Proc Natl Acad Sci U S A* **98**, 13693-13698 (2001).
208. Uekita, T., Itoh, Y., Yana, I., Ohno, H. & Seiki, M. Cytoplasmic tail-dependent internalization of membrane-type 1 matrix metalloproteinase is important for its invasion-promoting activity. *J Cell Biol* **155**, 1345-1356 (2001).
209. Rozanov, D.V., Deryugina, E.I., Monosov, E.Z., Marchenko, N.D. & Strongin, A.Y. Aberrant, persistent inclusion into lipid rafts limits the tumorigenic function of membrane type-1 matrix metalloproteinase in malignant cells. *Exp Cell Res* **293**, 81-95 (2004).
210. Holmbeck, K.*, et al.* MT1-MMP-deficient mice develop dwarfism, osteopenia, arthritis,

and connective tissue disease due to inadequate collagen turnover. *Cell* **99**, 81-92 (1999).
211. Zhou, Z.*, et al.* Impaired endochondral ossification and angiogenesis in mice deficient in membrane-type matrix metalloproteinase I. *Proc Natl Acad Sci U S A* **97**, 4052-4057 (2000).
212. Oblander, S.A.*, et al.* Distinctive functions of membrane type 1 matrix-metalloprotease (MT1-MMP or MMP-14) in lung and submandibular gland development are independent of its role in pro-MMP-2 activation. *Dev Biol* **277**, 255-269 (2005).
213. Munoz-Saez, E., Moracho, N., Learte, A.I.R., Arroyo, A.G. & Sanchez-Camacho, C. Dynamic Expression of Membrane Type 1-Matrix Metalloproteinase (Mt1-mmp/Mmp14) in the Mouse Embryo. *Cells* **10**(2021).
214. Caley, M.P., Martins, V.L. & O'Toole, E.A. Metalloproteinases and Wound Healing. *Adv Wound Care (New Rochelle)* **4**, 225-234 (2015).
215. Atkinson, J.J., Toennies, H.M., Holmbeck, K. & Senior, R.M. Membrane type 1 matrix metalloproteinase is necessary for distal airway epithelial repair and keratinocyte growth factor receptor expression after acute injury. *Am J Physiol Lung Cell Mol Physiol* **293**, L600-610 (2007).
216. Murphy, G.*, et al.* Mechanisms for pro matrix metalloproteinase activation. *APMIS* **107**, 38-44 (1999).
217. Koshikawa, N., Giannelli, G., Cirulli, V., Miyazaki, K. & Quaranta, V. Role of cell surface metalloprotease MT1-MMP in epithelial cell migration over laminin-5. *J Cell Biol* **148**, 615-624 (2000).
218. Schenk, S.*, et al.* Binding to EGF receptor of a laminin-5 EGF-like fragment liberated during MMP-dependent mammary gland involution. *J Cell Biol* **161**, 197-209 (2003).
219. Kadono, Y.*, et al.* Membrane type 1-matrix metalloproteinase is involved in the formation of hepatocyte growth factor/scatter factor-induced branching tubules in madin-darby canine kidney epithelial cells. *Biochem Biophys Res Commun* **251**, 681-687 (1998).
220. Jacob, A. & Prekeris, R. The regulation of MMP targeting to invadopodia during cancer metastasis. *Front Cell Dev Biol* **3**, 4 (2015).
221. Shimizu-Hirota, R.*, et al.* MT1-MMP regulates the PI3Kdelta.Mi-2/NuRD-dependent control of macrophage immune function. *Genes Dev* **26**, 395-413 (2012).
222. Rajavashisth, T.B.*, et al.* Membrane type 1 matrix metalloproteinase expression in human atherosclerotic plaques: evidence for activation by proinflammatory mediators. *Circulation* **99**, 3103-3109 (1999).
223. Schneider, F.*, et al.* Matrix-metalloproteinase-14 deficiency in bone-marrow-derived cells promotes collagen accumulation in mouse atherosclerotic plaques. *Circulation* **117**, 931-939 (2008).
224. Lee, H.S. & Kim, W.J. The Role of Matrix Metalloproteinase in Inflammation with a Focus on Infectious Diseases. *Int J Mol Sci* **23**(2022).
225. Gifford, V. & Itoh, Y. MT1-MMP-dependent cell migration: proteolytic and non-proteolytic mechanisms. *Biochem Soc Trans* **47**, 811-826 (2019).
226. Silvestro, M.*, et al.* The Nonproteolytic Intracellular Domain of Membrane-Type 1 Matrix Metalloproteinase Coordinately Modulates Abdominal Aortic Aneurysm and

Atherosclerosis in Mice-Brief Report. *Arterioscler Thromb Vasc Biol* **42**, 1244-1253 (2022).
227. Attur, M.*, et al.* Membrane-type 1 Matrix Metalloproteinase Modulates Tissue Homeostasis by a Non-proteolytic Mechanism. *iScience* **23**, 101789 (2020).
228. Bassiouni, W., Ali, M.A.M. & Schulz, R. Multifunctional intracellular matrix metalloproteinases: implications in disease. *FEBS J* **288**, 7162-7182 (2021).
229. Knapinska, A.M. & Fields, G.B. The Expanding Role of MT1-MMP in Cancer Progression. *Pharmaceuticals (Basel)* **12**(2019).
230. Li, Y.*, et al.* The overexpression membrane type 1 matrix metalloproteinase is associated with the progression and prognosis in breast cancer. *Am J Transl Res* **7**, 120-127 (2015).
231. Wang, Y.Z.*, et al.* MMP-14 overexpression correlates with poor prognosis in non-small cell lung cancer. *Tumour Biol* **35**, 9815-9821 (2014).
232. He, L.*, et al.* Matrix metalloproteinase-14 is a negative prognostic marker for patients with gastric cancer. *Dig Dis Sci* **58**, 1264-1270 (2013).
233. Kamat, A.A.*, et al.* The clinical relevance of stromal matrix metalloproteinase expression in ovarian cancer. *Clin Cancer Res* **12**, 1707-1714 (2006).
234. Cho, S.J.*, et al.* STAT3 mediates RCP-induced cancer cell invasion through the NF-kappaB/Slug/MT1-MMP signaling cascade. *Arch Pharm Res* **45**, 460-474 (2022).
235. Brasher, M.I.*, et al.* Syntaxin4-Munc18c Interaction Promotes Breast Tumor Invasion and Metastasis by Regulating MT1-MMP Trafficking. *Mol Cancer Res* **20**, 434-445 (2022).
236. Ikeda, K., Kaneko, R., Tsukamoto, E., Funahashi, N. & Koshikawa, N. Proteolytic cleavage of membrane proteins by membrane type-1 MMP regulates cancer malignant progression. *Cancer Sci* (2022).
237. Koshikawa, N.*, et al.* Proteolysis of EphA2 Converts It from a Tumor Suppressor to an Oncoprotein. *Cancer Res* **75**, 3327-3339 (2015).
238. Liu, G., Atteridge, C.L., Wang, X., Lundgren, A.D. & Wu, J.D. The membrane type matrix metalloproteinase MMP14 mediates constitutive shedding of MHC class I chain-related molecule A independent of A disintegrin and metalloproteinases. *J Immunol* **184**, 3346-3350 (2010).
239. Guo, X.*, et al.* Control of SARS-CoV-2 infection by MT1-MMP-mediated shedding of ACE2. *Nat Commun* **13**, 7907 (2022).
240. da Silva-Neto, P.V.*, et al.* Matrix Metalloproteinases on Severe COVID-19 Lung Disease Pathogenesis: Cooperative Actions of MMP-8/MMP-2 Axis on Immune Response through HLA-G Shedding and Oxidative Stress. *Biomolecules* **12**(2022).
241. Gutman, H.*, et al.* Matrix Metalloproteinases Expression Is Associated with SARS-CoV-2-Induced Lung Pathology and Extracellular-Matrix Remodeling in K18-hACE2 Mice. *Viruses* **14**(2022).
242. Guo, X.*, et al.* Regulation of age-associated insulin resistance by MT1-MMP-mediated cleavage of insulin receptor. *Nat Commun* **13**, 3749 (2022).
243. Chow, C.F.W.*, et al.* Body weight regulation via MT1-MMP-mediated cleavage of GFRAL. *Nat Metab* **4**, 203-212 (2022).
244. Li, X.*, et al.* Critical Role of Matrix Metalloproteinase 14 in Adipose Tissue

Remodeling during Obesity. *Mol Cell Biol* **40**(2020).
245. Asthana, P., Guo, X. & Wong, H.L.X. MT1-MMP - A potential drug target for the management of the obesity. *Expert Opin Ther Targets* **26**, 761-765 (2022).
246. Higashi, S. & Miyazaki, K. Novel processing of beta-amyloid precursor protein catalyzed by membrane type 1 matrix metalloproteinase releases a fragment lacking the inhibitor domain against gelatinase A. *Biochemistry* **42**, 6514-6526 (2003).
247. Liao, M.C. & Van Nostrand, W.E. Degradation of soluble and fibrillar amyloid beta-protein by matrix metalloproteinase (MT1-MMP) in vitro. *Biochemistry* **49**, 1127-1136 (2010).
248. Garcia-Gonzalez, L., Pilat, D., Baranger, K. & Rivera, S. Emerging Alternative Proteinases in APP Metabolism and Alzheimer's Disease Pathogenesis: A Focus on MT1-MMP and MT5-MMP. *Front Aging Neurosci* **11**, 244 (2019).
249. Miller, M.C.*, et al.* Membrane type 1 matrix metalloproteinase is a crucial promoter of synovial invasion in human rheumatoid arthritis. *Arthritis Rheum* **60**, 686-697 (2009).
250. Kaneko, K.*, et al.* Selective Inhibition of Membrane Type 1 Matrix Metalloproteinase Abrogates Progression of Experimental Inflammatory Arthritis: Synergy With Tumor Necrosis Factor Blockade. *Arthritis Rheumatol* **68**, 521-531 (2016).
251. Itoh, Y. Metalloproteinases in Rheumatoid Arthritis: Potential Therapeutic Targets to Improve Current Therapies. *Prog Mol Biol Transl Sci* **148**, 327-338 (2017).
252. Gilardoni, M.B.*, et al.* Decreased expression of the low-density lipoprotein receptor-related protein-1 (LRP-1) in rats with prostate cancer. *J Histochem Cytochem* **51**, 1575-1580 (2003).
253. Lehti, K., Rose, N.F., Valavaara, S., Weiss, S.J. & Keski-Oja, J. MT1-MMP promotes vascular smooth muscle dedifferentiation through LRP1 processing. *J Cell Sci* **122**, 126-135 (2009).
254. Yamamoto, K.*, et al.* Inhibition of Shedding of Low-Density Lipoprotein Receptor-Related Protein 1 Reverses Cartilage Matrix Degradation in Osteoarthritis. *Arthritis Rheumatol* **69**, 1246-1256 (2017).
255. Pratt, J., Haidara, K. & Annabi, B. MT1-MMP Expression Levels and Catalytic Functions Dictate LDL Receptor-Related Protein-1 Ligand Internalization Capacity in U87 Glioblastoma Cells. *Int J Mol Sci* **23**(2022).
256. Etique, N., Verzeaux, L., Dedieu, S. & Emonard, H. LRP-1: a checkpoint for the extracellular matrix proteolysis. *Biomed Res Int* **2013**, 152163 (2013).
257. Van den Steen, P.E.*, et al.* The hemopexin and O-glycosylated domains tune gelatinase B/MMP-9 bioavailability via inhibition and binding to cargo receptors. *J Biol Chem* **281**, 18626-18637 (2006).
258. Guo, Y.*, et al.* Blocking Wnt/LRP5 signaling by a soluble receptor modulates the epithelial to mesenchymal transition and suppresses met and metalloproteinases in osteosarcoma Saos-2 cells. *J Orthop Res* **25**, 964-971 (2007).
259. Zhang, J., Li, Y., Liu, Q., Lu, W. & Bu, G. Wnt signaling activation and mammary gland hyperplasia in MMTV-LRP6 transgenic mice: implication for breast cancer tumorigenesis. *Oncogene* **29**, 539-549 (2010).
260. Collaborators, G.B.D.C.o.D. Global, regional, and national age-sex-specific mortality for 282 causes of death in 195 countries and territories, 1980-2017: a systematic

analysis for the Global Burden of Disease Study 2017. *Lancet* **392**, 1736-1788 (2018).
261. Roth, G.A.*, et al.* Global Burden of Cardiovascular Diseases and Risk Factors, 1990-2019: Update From the GBD 2019 Study. *J Am Coll Cardiol* **76**, 2982-3021 (2020).
262. Soler, E.P. & Ruiz, V.C. Epidemiology and risk factors of cerebral ischemia and ischemic heart diseases: similarities and differences. *Curr Cardiol Rev* **6**, 138-149 (2010).
263. Jung, E., Kong, S.Y., Ro, Y.S., Ryu, H.H. & Shin, S.D. Serum Cholesterol Levels and Risk of Cardiovascular Death: A Systematic Review and a Dose-Response Meta-Analysis of Prospective Cohort Studies. *Int J Environ Res Public Health* **19**(2022).
264. Anderson, K.M., Castelli, W.P. & Levy, D. Cholesterol and mortality. 30 years of follow-up from the Framingham study. *JAMA* **257**, 2176-2180 (1987).
265. Linton, M.F.*, et al.* The Role of Lipids and Lipoproteins in Atherosclerosis. in *Endotext* (eds. Feingold, K.R.*, et al.*) (South Dartmouth (MA), 2000).
266. Huff, T., Boyd, B. & Jialal, I. Physiology, Cholesterol. in *StatPearls* (Treasure Island (FL), 2023).
267. Sizar, O., Khare, S., Jamil, R.T. & Talati, R. Statin Medications. in *StatPearls* (Treasure Island (FL), 2023).
268. Kriaa, A.*, et al.* Microbial impact on cholesterol and bile acid metabolism: current status and future prospects. *J Lipid Res* **60**, 323-332 (2019).
269. Cholesterol Treatment Trialists, C.*, et al.* Efficacy and safety of more intensive lowering of LDL cholesterol: a meta-analysis of data from 170,000 participants in 26 randomised trials. *Lancet* **376**, 1670-1681 (2010).
270. Nohara, A.*, et al.* Homozygous Familial Hypercholesterolemia. *J Atheroscler Thromb* **28**, 665-678 (2021).
271. Gallego-Colon, E., Daum, A. & Yosefy, C. Statins and PCSK9 inhibitors: A new lipid-lowering therapy. *Eur J Pharmacol* **878**, 173114 (2020).
272. Sizar, O., Nassereddin, A. & Talati, R. Ezetimibe. in *StatPearls* (Treasure Island (FL), 2023).
273. Yu, M., Liang, C., Kong, Q., Wang, Y. & Li, M. Efficacy of combination therapy with ezetimibe and statins versus a double dose of statin monotherapy in participants with hypercholesterolemia: a meta-analysis of literature. *Lipids Health Dis* **19**, 1 (2020).
274. Rayan, R.A. & Sharma, S. Lomitapide. in *StatPearls* (Treasure Island (FL), 2023).
275. Lara-Castillo, N. & Johnson, M.L. LRP receptor family member associated bone disease. *Rev Endocr Metab Disord* **16**, 141-148 (2015).
276. Campion, O.*, et al.* Contribution of the Low-Density Lipoprotein Receptor Family to Breast Cancer Progression. *Front Oncol* **10**, 882 (2020).
277. Oentaryo, M.J., Tse, A.C. & Lee, C.W. Neuronal MT1-MMP mediates ECM clearance and Lrp4 cleavage for agrin deposition and signaling in presynaptic development. *J Cell Sci* **133**(2020).
278. Masana, L., Ibarretxe, D. & Plana, N. Reasons Why Combination Therapy Should Be the New Standard of Care to Achieve the LDL-Cholesterol Targets : Lipid-lowering combination therapy. *Curr Cardiol Rep* **22**, 66 (2020).
279. Galicia-Garcia, U.*, et al.* Statin Treatment-Induced Development of Type 2 Diabetes: From Clinical Evidence to Mechanistic Insights. *Int J Mol Sci* **21**(2020).

280. Seal, R.L.*, et al.* Genenames.org: the HGNC resources in 2023. *Nucleic Acids Res* **51**, D1003-D1009 (2023).
281. Dieckmann, M., Dietrich, M.F. & Herz, J. Lipoprotein receptors--an evolutionarily ancient multifunctional receptor family. *Biol Chem* **391**, 1341-1363 (2010).
282. Herz, J. The LDL Receptor Gene Family. *Neuron* **29**, 571-581 (2001).
283. Lu, Y., Tian, Q.B., Endo, S. & Suzuki, T. A role for LRP4 in neuronal cell viability is related to apoE-binding. *Brain Res* **1177**, 19-28 (2007).
284. Mahley, R.W., Weisgraber, K.H. & Huang, Y. Apolipoprotein E: structure determines function, from atherosclerosis to Alzheimer's disease to AIDS. *J Lipid Res* **50 Suppl**, S183-188 (2009).
285. Marais, A.D. Apolipoprotein E in lipoprotein metabolism, health and cardiovascular disease. *Pathology* **51**, 165-176 (2019).
286. Liu, J.*, et al.* Wnt/beta-catenin signalling: function, biological mechanisms, and therapeutic opportunities. *Signal Transduct Target Ther* **7**, 3 (2022).
287. Li, J., Liu, Z., Ren, Y., Shao, H. & Li, S. LRP5-/6 gene polymorphisms and its association with risk of abnormal bone mass in postmenopausal women. *J Orthop Surg Res* **18**, 369 (2023).
288. Sturznickel, J.*, et al.* Clinical Phenotype and Relevance of LRP5 and LRP6 Variants in Patients With Early-Onset Osteoporosis (EOOP). *J Bone Miner Res* **36**, 271-282 (2021).
289. Dlugosz, P. & Nimpf, J. The Reelin Receptors Apolipoprotein E receptor 2 (ApoER2) and VLDL Receptor. *Int J Mol Sci* **19**(2018).
290. Roslan, Z., Muhamad, M., Selvaratnam, L. & Ab-Rahim, S. The Roles of Low-Density Lipoprotein Receptor-Related Proteins 5, 6, and 8 in Cancer: A Review. *J Oncol* **2019**, 4536302 (2019).
291. Lee, H., Ibrahimi, L., Azar, D.T. & Han, K.Y. The Role of Membrane-Type 1 Matrix Metalloproteinase-Substrate Interactions in Pathogenesis. *Int J Mol Sci* **24**(2023).
292. Sounni, N.E., Paye, A., Host, L. & Noel, A. MT-MMPS as Regulators of Vessel Stability Associated with Angiogenesis. *Front Pharmacol* **2**, 111 (2011).
293. Pahwa, S., Stawikowski, M.J. & Fields, G.B. Monitoring and Inhibiting MT1-MMP during Cancer Initiation and Progression. *Cancers (Basel)* **6**, 416-435 (2014).
294. Niland, S., Riscanevo, A.X. & Eble, J.A. Matrix Metalloproteinases Shape the Tumor Microenvironment in Cancer Progression. *Int J Mol Sci* **23**(2021).
295. Page-McCaw, A., Ewald, A.J. & Werb, Z. Matrix metalloproteinases and the regulation of tissue remodelling. *Nat Rev Mol Cell Biol* **8**, 221-233 (2007).
296. Osenkowski, P., Toth, M. & Fridman, R. Processing, shedding, and endocytosis of membrane type 1-matrix metalloproteinase (MT1-MMP). *J Cell Physiol* **200**, 2-10 (2004).
297. Werny, L.*, et al.* MT1-MMP and ADAM10/17 exhibit a remarkable overlap of shedding properties. *FEBS J* **290**, 93-111 (2023).
298. Xu, R.*, et al.* N-Glycosylation of LRP6 by B3GnT2 Promotes Wnt/beta-Catenin Signalling. *Cells* **12**(2023).
299. Pahwa, S.*, et al.* Characterization and regulation of MT1-MMP cell surface-associated activity. *Chem Biol Drug Des* **93**, 1251-1264 (2019).
300. Wang, P., Nie, J. & Pei, D. The hemopexin domain of membrane-type matrix

metalloproteinase-1 (MT1-MMP) Is not required for its activation of proMMP2 on cell surface but is essential for MT1-MMP-mediated invasion in three-dimensional type I collagen. *J Biol Chem* **279**, 51148-51155 (2004).
301. Kim, K.*, et al.* gamma-Secretase Inhibition Lowers Plasma Triglyceride-Rich Lipoproteins by Stabilizing the LDL Receptor. *Cell Metab* **27**, 816-827 e814 (2018).
302. Zurhove, K., Nakajima, C., Herz, J., Bock, H.H. & May, P. Gamma-secretase limits the inflammatory response through the processing of LRP1. *Sci Signal* **1**, ra15 (2008).
303. Balmaceda, V.*, et al.* ApoER2 processing by presenilin-1 modulates reelin expression. *FASEB J* **28**, 1543-1554 (2014).
304. Wygrecka, M.*, et al.* Shedding of low-density lipoprotein receptor-related protein-1 in acute respiratory distress syndrome. *Am J Respir Crit Care Med* **184**, 438-448 (2011).
305. Mi, K. & Johnson, G.V. Regulated proteolytic processing of LRP6 results in release of its intracellular domain. *J Neurochem* **101**, 517-529 (2007).
306. Kounnas, M.Z., Chappell, D.A., Strickland, D.K. & Argraves, W.S. Glycoprotein 330, a member of the low density lipoprotein receptor family, binds lipoprotein lipase in vitro. *J Biol Chem* **268**, 14176-14181 (1993).
307. Fischer, D.G., Tal, N., Novick, D., Barak, S. & Rubinstein, M. An antiviral soluble form of the LDL receptor induced by interferon. *Science* **262**, 250-253 (1993).
308. Hoe, H.S. & Rebeck, G.W. Regulation of ApoE receptor proteolysis by ligand binding. *Brain Res Mol Brain Res* **137**, 31-39 (2005).
309. Malemud, C.J. Inhibition of MMPs and ADAM/ADAMTS. *Biochem Pharmacol* **165**, 33-40 (2019).
310. Pasternak, B. & Aspenberg, P. Metalloproteinases and their inhibitors-diagnostic and therapeutic opportunities in orthopedics. *Acta Orthop* **80**, 693-703 (2009).
311. Pluda, S., Mazzocato, Y. & Angelini, A. Peptide-Based Inhibitors of ADAM and ADAMTS Metalloproteinases. *Front Mol Biosci* **8**, 703715 (2021).
312. Strongin, A.Y. Proteolytic and non-proteolytic roles of membrane type-1 matrix metalloproteinase in malignancy. *Biochim Biophys Acta* **1803**, 133-141 (2010).
313. D'Alessio, S.*, et al.* Tissue inhibitor of metalloproteinases-2 binding to membrane-type 1 matrix metalloproteinase induces MAPK activation and cell growth by a non-proteolytic mechanism. *J Biol Chem* **283**, 87-99 (2008).
314. Fogarasi, M. & Dima, S. The Catalytic Domain Mediates Homomultimerization of MT1-MMP and the Prodomain Interferes with MT1-MMP Oligomeric Complex Assembly. *Biomolecules* **12**(2022).
315. Homewood, C.A., Warhurst, D.C., Peters, W. & Baggaley, V.C. Lysosomes, pH and the anti-malarial action of chloroquine. *Nature* **235**, 50-52 (1972).
316. Authier, F., Posner, B.I. & Bergeron, J.J. Endosomal proteolysis of internalized proteins. *FEBS Lett* **389**, 55-60 (1996).
317. Lichtenthaler, S.F., Lemberg, M.K. & Fluhrer, R. Proteolytic ectodomain shedding of membrane proteins in mammals-hardware, concepts, and recent developments. *EMBO J* **37**(2018).
318. Spuch, C., Ortolano, S. & Navarro, C. LRP-1 and LRP-2 receptors function in the membrane neuron. Trafficking mechanisms and proteolytic processing in Alzheimer's disease. *Front Physiol* **3**, 269 (2012).

319. Telese, F.*, et al.* LRP8-Reelin-Regulated Neuronal Enhancer Signature Underlying Learning and Memory Formation. *Neuron* **86**, 696-710 (2015).
320. Lu, C., Li, X.Y., Hu, Y., Rowe, R.G. & Weiss, S.J. MT1-MMP controls human mesenchymal stem cell trafficking and differentiation. *Blood* **115**, 221-229 (2010).
321. MacDonald, B.T. & He, X. Frizzled and LRP5/6 receptors for Wnt/beta-catenin signaling. *Cold Spring Harb Perspect Biol* **4**(2012).
322. Tsao, C.W.*, et al.* Heart Disease and Stroke Statistics-2022 Update: A Report From the American Heart Association. *Circulation* **145**, e153-e639 (2022).
323. Vaduganathan, M., Mensah, G.A., Turco, J.V., Fuster, V. & Roth, G.A. The Global Burden of Cardiovascular Diseases and Risk: A Compass for Future Health. *J Am Coll Cardiol* **80**, 2361-2371 (2022).
324. Endo, A. A historical perspective on the discovery of statins. *Proc Jpn Acad Ser B Phys Biol Sci* **86**, 484-493 (2010).
325. Arrieta, A., Page, T.F., Veledar, E. & Nasir, K. Economic Evaluation of PCSK9 Inhibitors in Reducing Cardiovascular Risk from Health System and Private Payer Perspectives. *PLoS One* **12**, e0169761 (2017).
326. Feingold, K.R. Cholesterol Lowering Drugs. in *Endotext* (eds. Feingold, K.R.*, et al.*) (South Dartmouth (MA), 2000).
327. Taylor, B.A. & Thompson, P.D. Statin-Associated Muscle Disease: Advances in Diagnosis and Management. *Neurotherapeutics* **15**, 1006-1017 (2018).
328. Koh, K.K., Sakuma, I., Shimada, K., Hayashi, T. & Quon, M.J. Combining Potent Statin Therapy with Other Drugs to Optimize Simultaneous Cardiovascular and Metabolic Benefits while Minimizing Adverse Events. *Korean Circ J* **47**, 432-439 (2017).
329. Ramkumar, S., Raghunath, A. & Raghunath, S. Statin Therapy: Review of Safety and Potential Side Effects. *Acta Cardiol Sin* **32**, 631-639 (2016).
330. Bridgeman, S.*, et al.* Statins Do Not Directly Inhibit the Activity of Major Epigenetic Modifying Enzymes. *Cancers (Basel)* **11**(2019).
331. Rashid, S.*, et al.* Decreased plasma cholesterol and hypersensitivity to statins in mice lacking Pcsk9. *Proc Natl Acad Sci U S A* **102**, 5374-5379 (2005).
332. Tang, W., Ma, Y. & Yu, L. Plasma cholesterol is hyperresponsive to statin in ABCG5/ABCG8 transgenic mice. *Hepatology* **44**, 1259-1266 (2006).
333. MacDonald, J.S.*, et al.* Preclinical evaluation of lovastatin. *Am J Cardiol* **62**, 16J-27J (1988).
334. Kim, J.Y., He, F. & Karin, M. From Liver Fat to Cancer: Perils of the Western Diet. *Cancers (Basel)* **13**(2021).
335. Bjornsson, E.S. Hepatotoxicity of statins and other lipid-lowering agents. *Liver Int* **37**, 173-178 (2017).
336. Pohlkamp, T., Wasser, C.R. & Herz, J. Functional Roles of the Interaction of APP and Lipoprotein Receptors. *Front Mol Neurosci* **10**, 54 (2017).
337. Selvais, C.*, et al.* Metalloproteinase-dependent shedding of low-density lipoprotein receptor-related protein-1 ectodomain decreases endocytic clearance of endometrial matrix metalloproteinase-2 and -9 at menstruation. *Endocrinology* **150**, 3792-3799 (2009).